5-2003

Characteristics, Evolution, and Lateral Variation of Lower Cretaceous Supradetachment Basins in the Daqing Shan, Inner Mongolia, China

Adrian K. Berry
Utah State University

CHARACTERISTICS, EVOLUTION, AND LATERAL VARIATION OF LOWER CRETACEOUS SUPRADETACHMENT BASINS IN THE DAQING SHAN, INNER MONGOLIA, CHINA

by

Adrian K. Berry

A thesis submitted in partial fulfillment
of the requirements of the degree

of

MASTER OF SCIENCE

in

Geology

Approved:

UTAH STATE UNIVERSITY
Logan, Utah

2003

ABSTRACT

Characteristics, Evolution, and Lateral Variation of Lower Cretaceous Supradetachment Basins in the Daqing Shan, Inner Mongolia, China

by

Adrian K. Berry, Master of Science

Utah State University, 2003

Major Professor: Dr. Bradley D. Ritts
Department: Geology

Lower Cretaceous basins associated with the Hohhot detachment in the Daqing Shan of Inner Mongolia, China, allow us to better understand the tectonic evolution of extensional basins formed in association with detachment faulting and metamorphic core complex formation. The six basins, informally named N1, N2, S1, S2, S3, and S4, are located in different structural settings, or depozones, throughout the detachment-metamorphic core complex setting, and although all basins are consistent with previously proposed models for supradetachment basin sedimentation, second-order variability in sedimentary style is exerted by these distinct structural settings. The basins are composed of coarse, predominantly footwall derived, conglomerate deposited by mass-wasting and alluvial fan processes. Paleocurrent direction is generally southerly, indicating transverse transport away from the bounding detachment fault.

Two of the basins, N2 and S3, provide us with an understanding of the temporal evolution of supradetachment basins in the upper plate of a metamorphic core complex. These basins were joined in their early stages, but were later separated as extensional unroofing exhumed the lower plate of the core complex and folded the master detachment fault, causing it to propagate a new splay to the surface. Continued extension was accommodated on this new splay, allowing for continued deposition of Lower Cretaceous strata above the detachment fault on the southern flank of the Daqing Shan antiform. Another basin, S2, displays the same stratigraphy and records a similar evolution, but we speculate that it formed separately in a primary corrugation of the master detachment fault. The only unit exposed in basin S4, located near the eastern end of the detachment, is the uppermost unit. Paleocurrent and provenance data are similar to other basins. Thus, it strongly resembles the other basins in spite of the magnitude of extension. Basin S1 is located in an intra-hanging wall setting and resembles the other basins with the exception of a centrally located fine-grained interval. Basin N1 was filled by similar depositional processes, but the proportions of fill that these processes are responsible for is variable in comparison to the other Lower Cretaceous basins in the Daqing Shan. This study establishes that the basins described are all of similar geometry and depositional style, and that supradetachment basins of this style may occur in various positions within a detachment-metamorphic core complex setting, regardless of proximity to the exhumed metamorphic core and magnitude of extension.

(173 pages)

ACKNOWLEDGMENTS

Acknowledgment is made to the Donors of the American Chemical Society Petroleum Research Fund (PRF # 35596-GB8 and PRF # 38900-B8 to Ritts), AAPG Grants-in-Aid program, Anadarko Petroleum Company, and Utah State University for providing financial support of this research. I would also like to thank Wang Jianmin of the Nei Mongol Bureau of Geology for logistical support. We thank Brian Darby, Cari Johnson, Greg Davis, Zheng Yadong, and Yaming Davis for their assistance and advice in the field. I would like to give special thanks to Lynde Nanson for her assistance in the field and for being a good cohort through a long field season. I would like to thank faculty and fellow graduate students at Utah State University, as well as my family and friends for supporting me as I worked on this project. Lastly, I would like to thank Carey Wicks for putting up with me on a daily basis and supporting me through this effort.

Adrian K. Berry

LIST OF TABLES

LIST OF FIGURES

CHAPTER I

INTRODUCTION

Supradetachment basins are an important type of extensional sedimentary basin related to movement on low-angle normal faults (detachment faults) and, sometimes, uplift of mid-crustal domes in metamorphic core complexes (Friedmann and Burbank, 1995; Lister and Davis, 1989). Because this type of basin has only recently been recognized, its classification, genetic stratigraphy, and tectonic significance remain incompletely understood. Many examples of supradetachment basins have been described, especially from the western United States; however, incomplete exposure and structural dismemberment hinder a holistic understanding of the geology and evolution of these systems (Beratan, 1991; Beratan and Nielson, 1996; Dickinson, 1991; Dorsey and Becker, 1995; Dorsey and Roberts, 1996; Fedo and Miller, 1992; Fillmore and Walker, 1996; Fillmore et al., 1994; Forshee and Yin, 1995; Friedmann and Burbank, 1995; Friedmann et al., 1996; Janecke et al., 1999, in press; Miller and John, 1988, 1999; Nielson and Beratan, 1995; Yarnold, 1994).

A series of newly documented syn-extensional supradetachment basins associated with the recently discovered Early Cretaceous Hohhot metamorphic core complex presents the opportunity to better understand the coupled structural and stratigraphic evolution of such systems (Davis et al., 2002). The well-documented structural geology and evolution of the Hohhot metamorphic core complex and associated detachment fault (Davis et al., 2002), make the Hohhot extensional system an unparalleled natural laboratory for studying the sedimentary geology of such systems. Depositional facies, detrital provenance and paleodrainage patterns in this evolving basin

system record initial movement on the detachment, breakup of the upper plate, and ultimately uplift of a metamorphic dome. Description of this sedimentary geology and basin evolution can provide new insights into general models of the formation of supradetachment basins.

Previous research concerning supradetachment basins provides conceptual models for supradetachment basins (Fillmore and Walker, 1994; Friedmann and Burbank, 1995). However, the general applicability of these models has been disputed (Janecke et al, 1999), largely due to variability of sedimentary styles in various structural settings. This research was undertaken to document a newly discovered series of basins above low-angle normal faults, as well as to provide a case study for comparison with previously studied supradetachment basins and related conceptual models. The preservation of the Daqing Shan basins in a variety of structural settings allow us to examine changes in basin geometry in response to variability of the controlling structures

CHAPTER II

CHARACTERISTICS AND EVOLUTION OF SUPRADETACHMENT BASINS ADJACENT TO THE HOHHOT METAMORPHIC CORE COMPLEX, INNER MONGOLIA, CHINA

Abstract

Lower Cretaceous basins associated with the Hohhot metamorphic core complex in the Daqing Shan of Inner Mongolia, China, allow us to understand the tectonic evolution of extensional basins formed coincident with detachment faulting and metamorphic core complex formation. The three-part stratigraphy in the basins records debris flow, mass-wasting, and waterlain deposition in an alluvial fan setting. These sedimentary rocks provide evidence of extensional break-up and reworking of these units early in the basin history, followed by sedimentation of coarse, transversely transported subaqueous channelized and sheetflood deposits of an alluvial fan system. The basins adjacent to the exhumed metamorphic core also record the structural evolution of the Hohhot metamorphic core complex. Extensional unroofing exhumed the metamorphic core and folded the master detachment fault, causing it to propagate a new splay to the surface and separate the previously contiguous basins. This new splay accommodated continued extension and allowed continued deposition of Lower Cretaceous strata above the detachment fault on the southern flank of the Daqing Shan antiform. The strata in these basins strongly resemble the proposed end-member model for supradetachment

basins (Friedmann and Burbank, 1995), and support the relevancy of models for supradetachment basin systems in research concerning highly extended regions.

Introduction

Supradetachment basins are an important type of extensional sedimentary basin related to movement on low-angle normal faults (detachment faults) and, sometimes, uplift of mid-crustal domes in metamorphic core complexes (Friedmann and Burbank, 1995; Lister and Davis, 1989). Because this type of basin has only recently been recognized, its classification, genetic stratigraphy, and tectonic significance remain incompletely understood. Many examples of supradetachment basins have been described, especially from the western United States; however, incomplete exposure and structural dismemberment hinder a holistic understanding of the geology and evolution of these systems (Beratan, 1991; Beratan and Nielson, 1996; Dickinson, 1991; Dorsey and Becker, 1995; Dorsey and Roberts, 1996; Fedo and Miller, 1992; Fillmore and Walker, 1996; Fillmore et al., 1994; Forshee and Yin, 1995; Friedmann and Burbank, 1995; Friedmann et al., 1996; Janecke et al., 1999, in press; Miller and John, 1988, 1999; Nielson and Beratan, 1995; Yarnold, 1994).

A series of newly documented syn-extensional supradetachment basins associated with the recently discovered Early Cretaceous Hohhot metamorphic core complex presents the opportunity to better understand the coupled structural and stratigraphic evolution of such systems (Davis et al., 2002). The well-documented structural geology and evolution of the Hohhot metamorphic core complex and associated detachment fault

(Davis et al., 2002), make the Hohhot extensional system an unparalleled natural laboratory for studying the sedimentary geology of such systems. Depositional facies, detrital provenance and paleodrainage patterns in this evolving basin system record initial movement on the detachment, breakup of the upper plate, and ultimately uplift of a metamorphic dome. Description of this sedimentary geology and basin evolution can provide new insights into general models of the formation of supradetachment basins.

Geologic Setting

The Hohhot metamorphic core complex is one of the most important structural features in the eastern Daqing Shan (Davis et al., 2002). It is located near the northern margin of the North China Block (Fig. 1), where it is superposed on a Late Jurassic through Early Cretaceous fold-thrust belt (Davis et al., 1998, 2001, 2002; Darby et al., 2001, 2002). The core complex, which was exhumed by a minimum of 40 km of extension on the Hohhot detachment fault, formed in response to rapid crustal extension that most likely occurred due to gravitational collapse following over-thickening of the crust in the Late Jurassic and earliest Cretaceous (Davis et al., 1998, 2002).

The Hohhot metamorphic core complex (as described by Davis et al., 2002), consists of the Daqing Shan antiform, a roughly east-west trending culmination of metamorphic and plutonic rocks, the Hohhot extensional detachment, and an upper plate of pre-Cretaceous crystalline and sedimentary units and Lower Cretaceous syn-extensional strata. South of the Daqing Shan antiform, the Hohhot detachment fault is a south-dipping low-angle (15-30°) normal fault system that is exposed along strike for

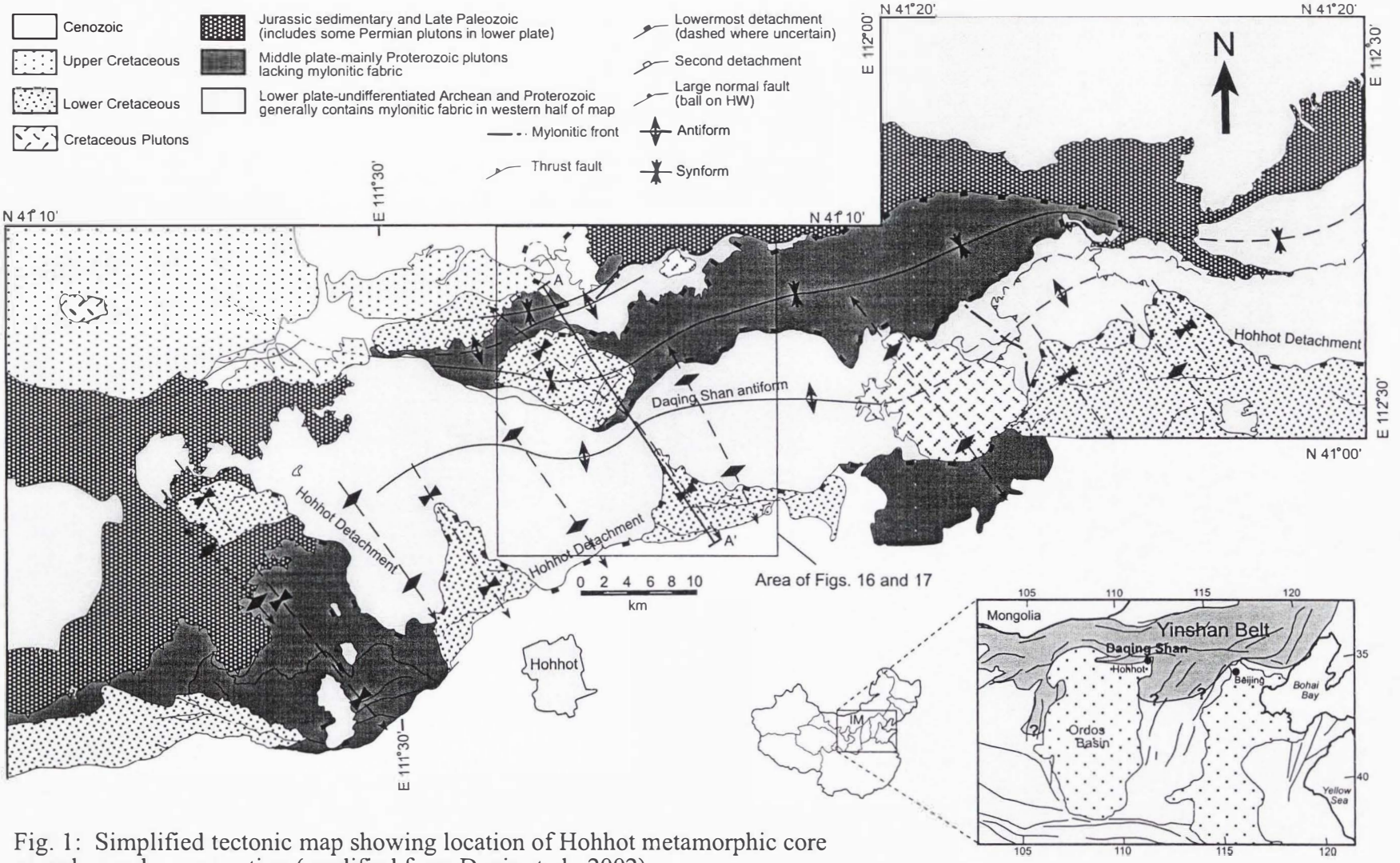

Fig. 1: Simplified tectonic map showing location of Hohhot metamorphic core complex and cross-section (modified form Davis et al., 2002).

>120 km (Fig. 1 and 2). This fault is the master detachment and is corrugated (Davis et al., 2002), with synforms in the detachment preserve numerous Lower Cretaceous nonmarine clastic basins. On the northern flank of the antiform, two detachment faults are stacked and synformally folded, with top-to-the south slip on both splays (Fig. 2) (Davis et al., 2002). The lower detachment separates mylonitic rocks from overlying non-mylonitic rocks, primarily Proterozoic crystalline rocks and Permian granitic gneisses. The upper detachment carries a succession of Cretaceous volcanic and sedimentary rocks in its upper plate (Fig. 2), that are highly deformed by normal faulting related to extension. The lower, oldest, detachment was the original detachment, but with extension, the footwall was progressively unloaded triggering isostatic uplift and bringing lower plate rocks to the surface. The resultant antiformally folded detachment was deactivated and a new splay propagated to the surface to accommodate further extension (Davis et al., 2002). The new splay, in turn, was also antiformally folded due to continued uplift with further unloading. The Hohhot detachment, on the southern flank of the Daqing Shan antiform, is the youngest fault splay and accommodated the remaining extension (Davis et al., 2002).

Characteristics of Lower Cretaceous Basins

Lower Cretaceous sedimentary basins are found discontinuously along the 120 km length of the Hohhot detachment. This study focuses on two of the Lower Cretaceous basins in the central part of the metamorphic core complex, one on the southern flank of the Daqing Shan antiform, the other on the northern flank, in a synformal keel (Fig. 1).

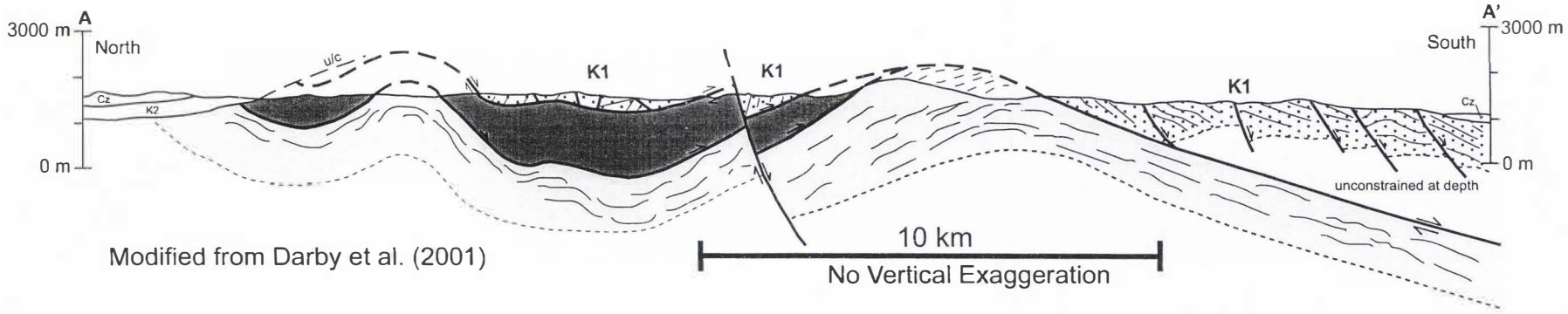

Fig. 2: Cross-section through Hohhot metamorphic core complex and Lower Cretaceous basins (modified from Davis et al, 2002). Cz - cenozoic, K2 - Late Cretaceous, K1 - Lower Cretaceous, u/c - unconformity.

These Lower Cretaceous sedimentary basins above the Hohhot detachment are interpreted to be syn-extensional for several reasons. First, Lower Cretaceous rocks are separated from older rocks by the Hohhot detachment, related normal faults, or unconformities, and occur only in the upper plate of the detachment. Second, these rocks are cut by low-and high-angle normal faults as a result of northwest southeast extension, consistent with movement on the detachment. Third, volcanic rocks in the base of the Lower Cretaceous succession have been dated at 125.2 ± 0.7 Ma, 125.7 ± 0.6 Ma, and 125.8 ± 0.6 Ma (sanidine single-crystal, weighted means $^{40}Ar/^{39}Ar$ age), coincident with the age of faulting determined by cooling ages and cross-cutting relationships in the footwall of the detachment (Davis et al., 2002). Fourth, these rocks consist predominantly of coarse conglomerate derived from sources that include footwall mylonite and other metamorphic rocks common in the lower plate of the detachment. Fifth, intraformational unconformities are present indicating rotation of strata due to continued upper plate faulting during deposition.

Stratigraphy and Sedimentology

The Hohhot basins comprise a dominantly clastic sedimentary section that is more than 1200 m thick (Fig. 3). We informally divide the basins into three lithostratigraphic members, K1a, K1b, and K1c, from bottom to top. These members are recognized in each basin, although their thickness and internal stratigraphy varies considerably throughout the study area.

The basal unit, K1a, is composed dominantly of unorganized, red, matrix-supported, pebble to cobble, conglomerate with interbedded bimodal volcanic rocks (Fig.

Fig. 3: Composite sections for the Hohhot basins tracking paleocurrent and provenance data.

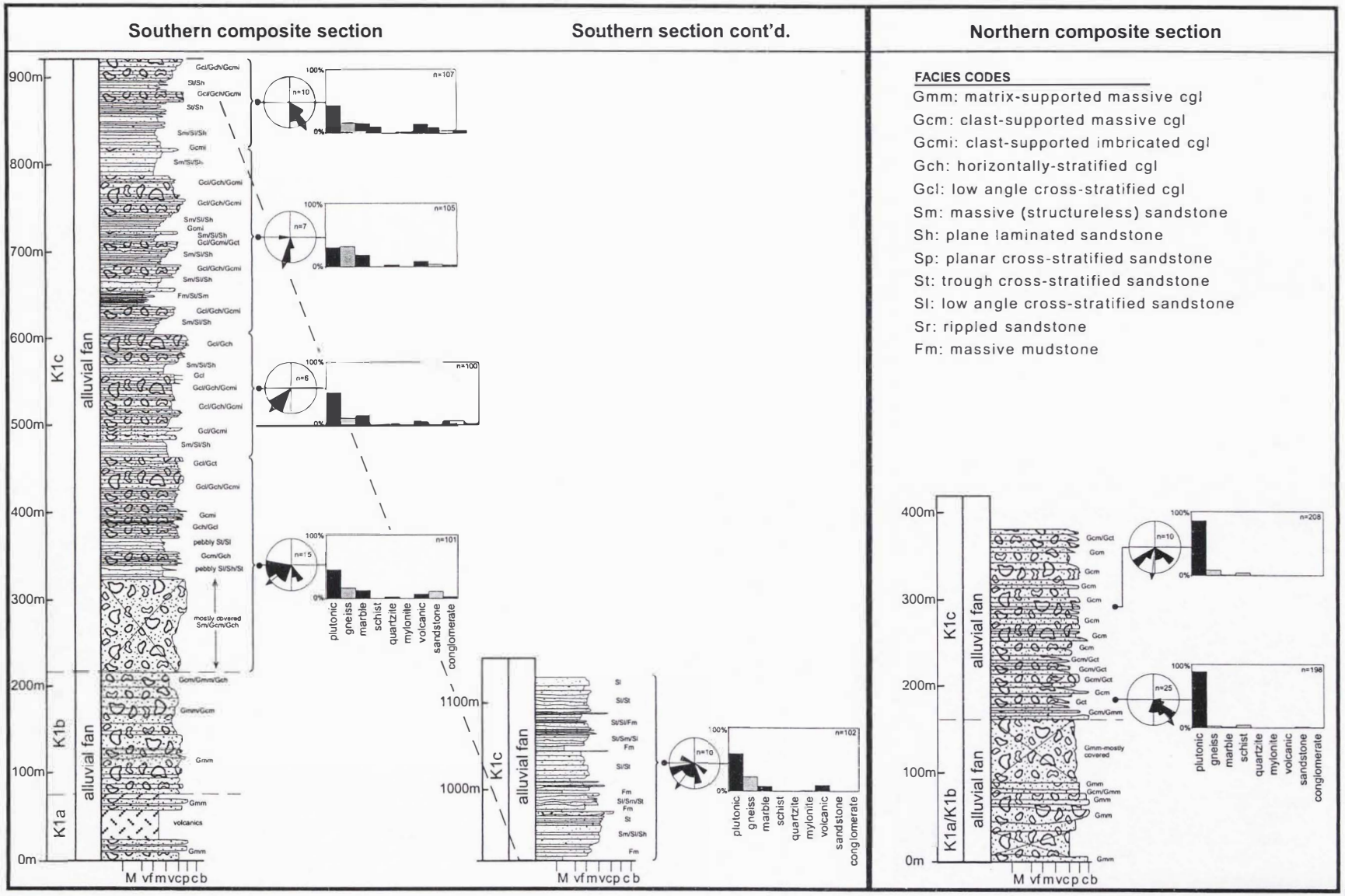
Southern composite section
Southern section cont'd.
Northern composite section
FACIES CODES
Gmm: matrix-supported massive cgl
Gcm: clast-supported massive cgl
Gcmi: clast-supported imbricated cgl
Gch: horizontally-stratified cgl
Gcl: low angle cross-stratified cgl
Sm: massive (structureless) sandstone
Sh: plane laminated sandstone
Sp: planar cross-stratified sandstone
St: trough cross-stratified sandstone
Sl: low angle cross-stratified sandstone
Sr: rippled sandstone
Fm: massive mudstone
900m
800m
700m
600m
500m
400m
300m
200m
100m
0m
1100m
1000m
K1c
K1b
K1a
K1a/K1b
alluvial fan
mostly covered
volcanics
plutonic
gneiss
marble
schist
quartzite
mylonite
volcanic
sandstone
conglomerate
M vf m vc p c b

4). The base of the section, depending on the location, is either a fault or an erosional unconformity over older rocks (Fig. 5). Member K1b, which overlies K1a, has similar red, matrix-supported conglomerate beds (Fig. 6) and lesser clast-supported, lenticular, pebble to cobble conglomerate. K1b lacks volcanic flows, but volcaniclastic grains are common in the matrix and minor sandstone beds. In addition, monolithologic blocks and megabreccia units are common in K1b (Fig. 7), and are most commonly composed of Proterozoic marble. The marble can be fairly intact, but is usually intensely fractured and brecciated and may be injected with the silty, red matrix that is common in K1b (Fig. 6).

K1a and K1b are interpreted as dominantly debris flow deposits based on the matrix-supported, disorganized nature of the conglomerate beds. Lesser streamflow and sheetflood deposits are marked by the better organized, clast-supported, lenticular to tabular conglomerates. This combination of minor waterlain deposits and debris flow deposits is interpreted to represent a proximal alluvial fan environment (Blair and McPherson, 1994). Large blocks and megabreccia units are interpreted as slide blocks and rock avalanche deposits, because they are completely contained within Lower Cretaceous conglomerate and exhibit characteristics of being emplaced as coherent to semi-coherent units (Friedmann, 1997).

The thickest unit, K1c, dominantly consists of well-organized, clast-supported, pebble to cobble conglomerate (Fig. 8). Beds are lenticular with erosive bases, and are interbedded with coarse sandstone and rare mudstone. Individual beds are organized into relatively tabular units on the order of a few meters to 10 m thick and extend for at least hundreds of meters laterally. Imbrication is abundant, as is trough cross-stratification and

Fig. 4: Photograph of K1a. K1a is a red, unorganized, matrix-supported, pebble to cobble conglomerate.

Fig. 5: Photograph of unconformity separating Lower Cretaceous sedimentary rocks from older rhyolitic volcanic rocks. Red line denotes unconformity.

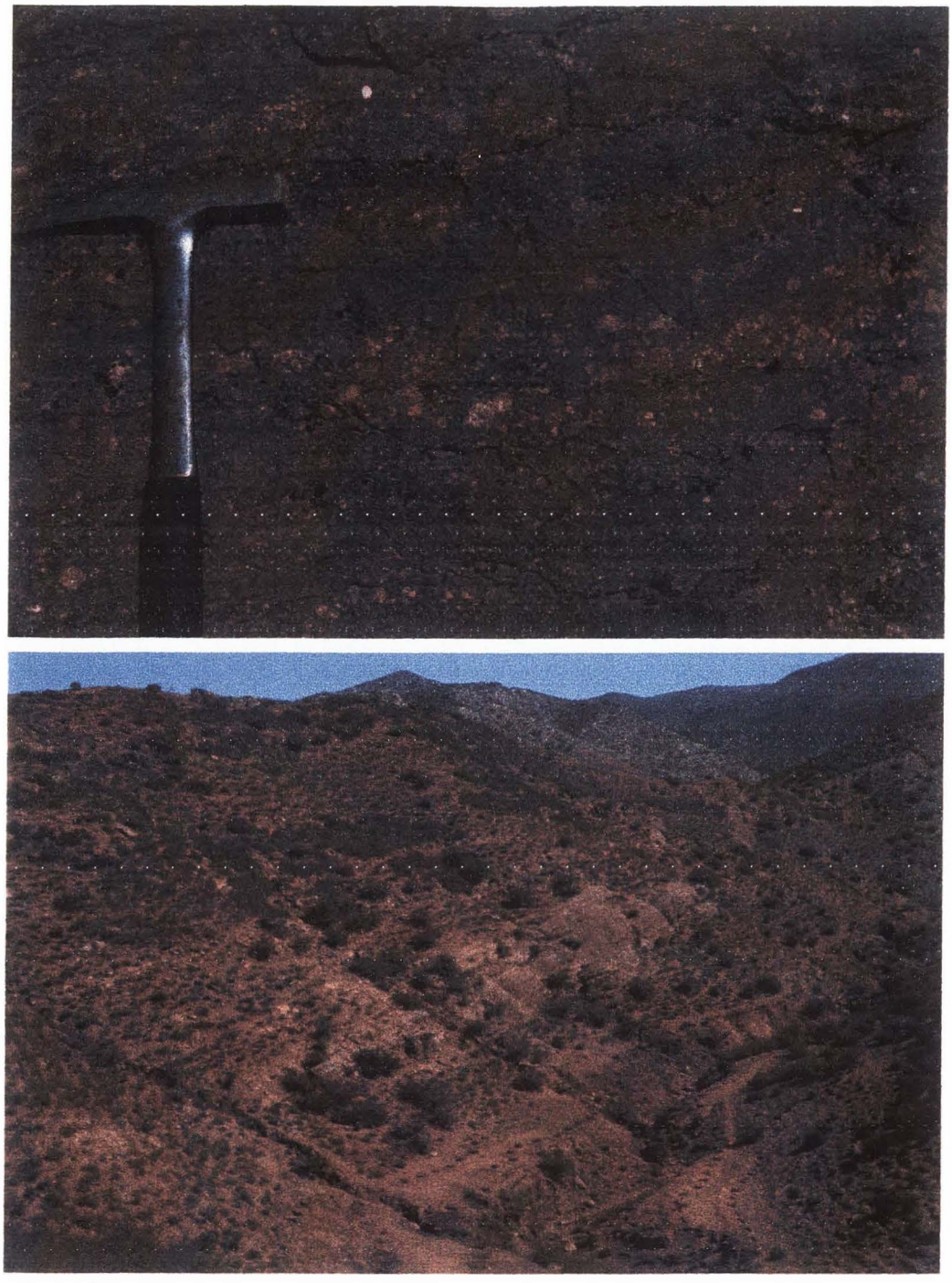

Fig. 6: Photographs of K1b. K1b is an unorganized, matrix-supported, pebble to cobble conglomerate (upper photo), with lesser organized, clast-supported, pebble to cobble, lenticular conglomerate beds (lower image).

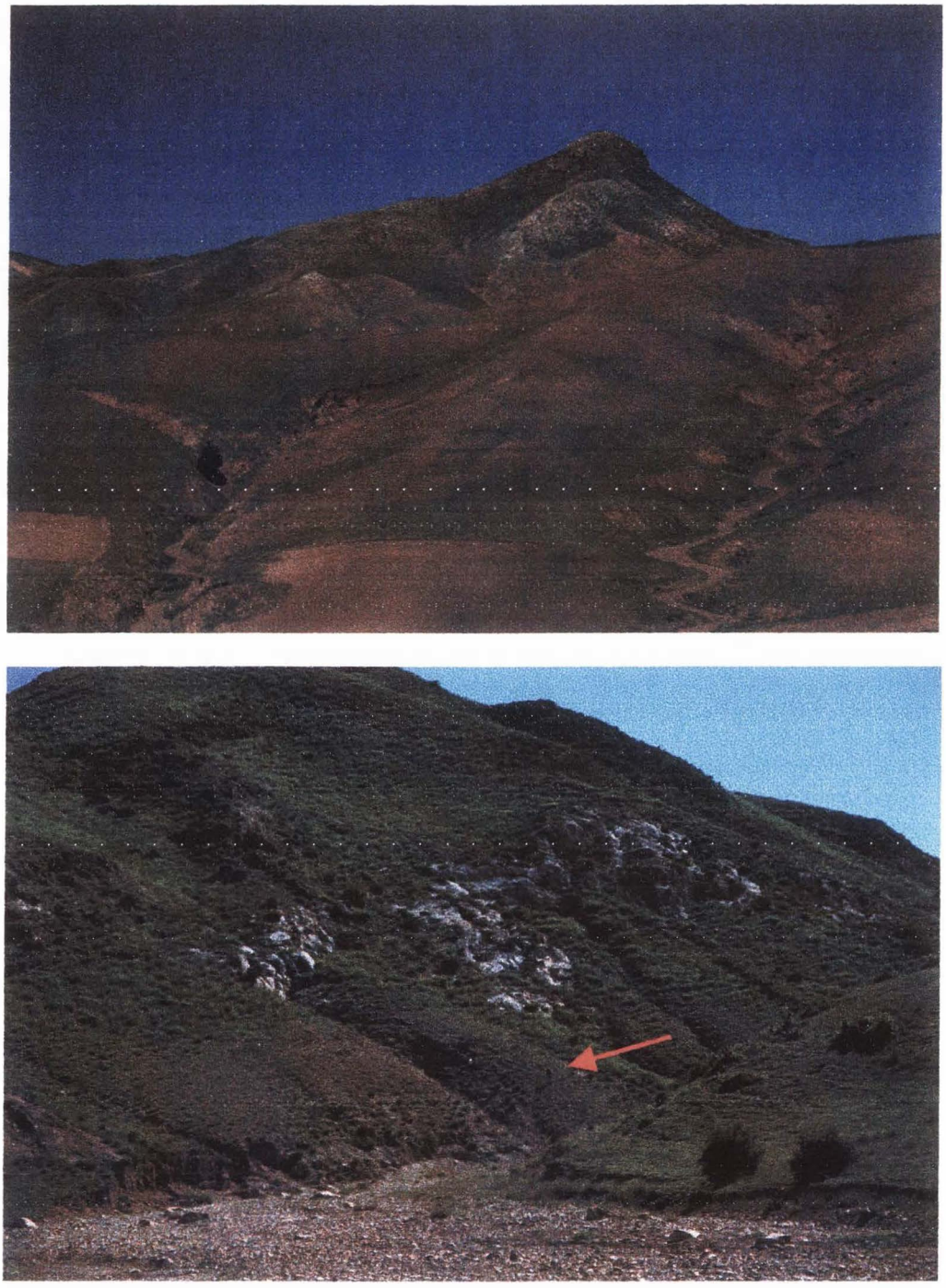

Fig. 7: Photographs of gravity-driven slide blocks within K1b. Slide blocks are white, Proterozoic marble, encased in red, K1b conglomerate. Arrow in lower photo points to a person for scale.

Fig. 8: Photographs of K1c. K1c is an organized, clast-supported, pebble to cobble conglomerate with abundant imbrication.

plane lamination in the sandstone. These conglomerates are interpreted as subaqueous channelized and sheetflood deposits based on their clast-supported, well-organized character. Large monolithologic, brecciated, gravity-driven slide blocks also occur in K1c. These blocks reach >2 km (long-axis) in size, and are typically composed of Proterozoic marble (Fig. 9). These deposits are interpreted to have formed in an alluvial fan system, based on the uniformly coarse conglomeratic nature of K1c, dominance of streamflow and sheetflood processes, and association with gravity-driven slide blocks and rock avalanche deposits (Blair and McPherson, 1994; Friedmann, 1997).

The basin on the northern flank of the Daqing Shan antiform contains K1a, K1b, and K1c, although the K1c unit is relatively thin. K1a and K1b are difficult to separate in this basin and are generally considered one unit that is easily distinguished from K1c, based on its greater content of red fine-grained sediment, volcaniclastic detritus, and debris flow deposits. Intense faulting in this basin inhibits measurement of a complete section (Fig. 10); a maximum of only about 200 m of continuous section can be measured without crossing significant normal faults. However, a composite section was constructed by correlating like-parts of repetitive lithostratigraphic sequences, which suggests a minimum basin thickness of nearly 400 m with at least 200 m of K1c sediment (Fig. 3). Angular unconformities are present in the basin (Fig. 11) and indicate syn-depositional rotation of Lower Cretaceous strata. Large slide blocks and rock-avalanche breccias are common within this northern basin (Fig. 7).

The basin on the southern flank of the Daqing Shan antiform also contains K1a, K1b, and K1c, with a much thicker K1c member. K1a and K1b are distinguished from

Fig. 9: Photograph of slide block within K1c. Slide block is white, Proterozoic marble encased in darker K1c conglomerate.

Fig. 10: Profile showing transect in northern basin with stratigraphic columns, paleocurrent data, and clast compositions.

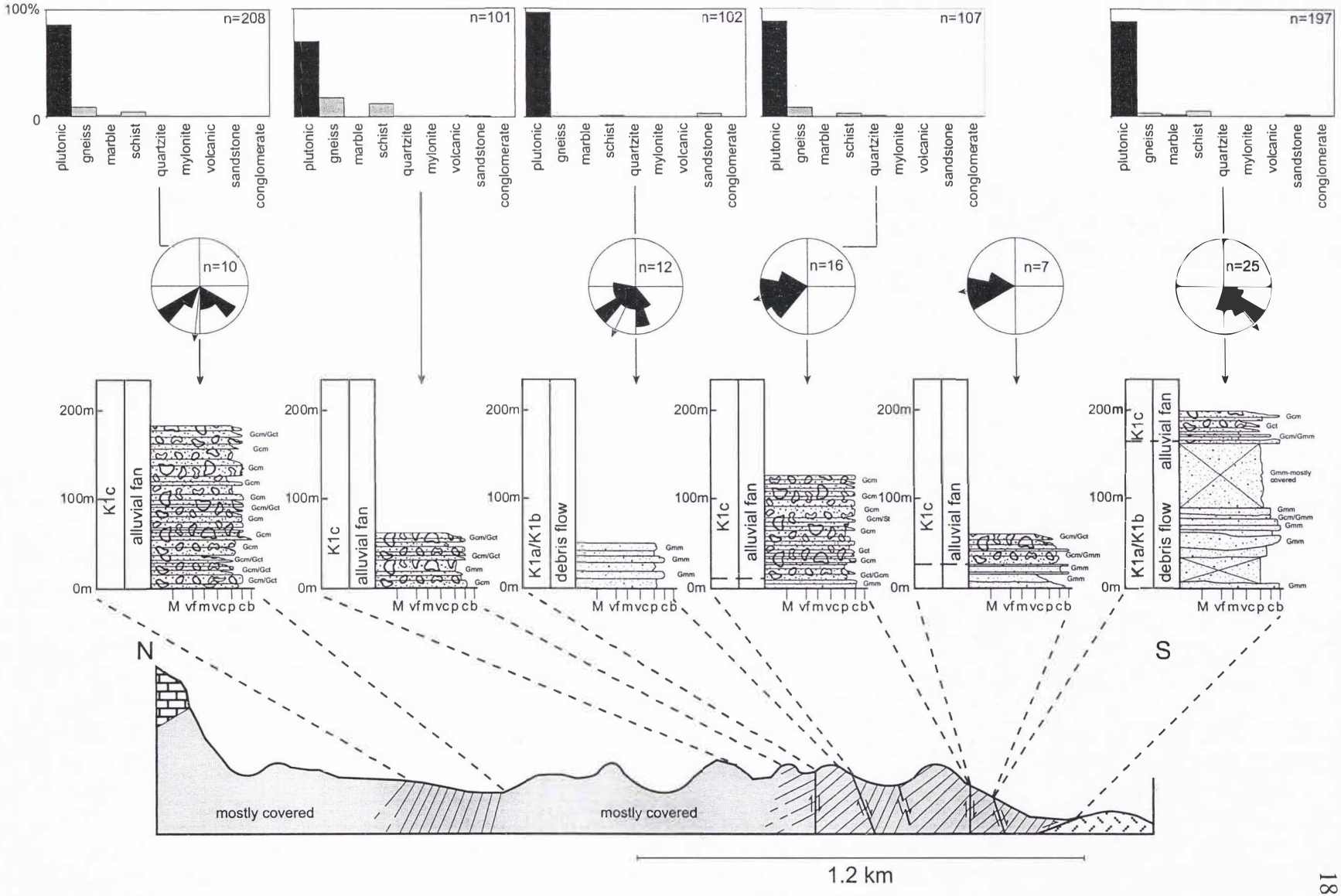
100%
0
n=208
n=101
n=102
n=107
n=197
plutonic
gneiss
marble
schist
quartzite
mylonite
volcanic
sandstone
conglomerate
n=10
n=12
n=16
n=7
n=25
200m
100m
0m
K1c
alluvial fan
K1a/K1b
debris flow
M vf m vc p cb
Gcm/Gct
Gcm
Gmm
Gct
Gcm/Gmm
Gmm-mostly covered
Gcm/St
Gct/Gcm
N
S
mostly covered
mostly covered
1.2 km

Fig. 11: Photograph of angular unconformity in Lower Cretaceous strata. Red line marks change from upper gently dipping beds to lower more steeply dipping beds.

each other in this basin based on the presence of volcanic flows. K1a and K1b are clearly distinguished from K1c based on their greater content of red fine-grained sediment, volcanic detritus, and debris flow deposits. The measured thickness of the southern basin is a minimum of 1120 m, including 900 m of K1c strata (Fig. 3). Pebble-to-cobble conglomerate is dominant in the section, but sandstone content increases upsection (Fig. 3). The sand-rich upper portion of the section still contains interbedded conglomerate beds and areally, coarse conglomerate is present at every location in this basin.

Packages of beds are generally continuous and can often be traced laterally around the southern basin (Fig. 12). Large, easily defined normal faults commonly cut the strata, but do not inhibit section measurement. The K1a and K1b part of the section in the southern basin is more pervasively faulted than the K1c section. Offset on these normal faults range from cm-scale to several meters and dips span from horizontal to moderately dipping (Fig. 13). The slip direction determined from fault planes is consistent with south-southeast extension.

Paleocurrent and Provenance Data

Paleocurrent data were collected about both basins (Fig. 14). The average paleocurrent directions for combined K1a and K1b are 155° in the northern basin and 214° in the southern basin. The paucity of imbricated clasts within K1a and K1b makes paleocurrent measurement within these units difficult. Well-imbricated conglomerate is abundant in K1c in both basins, and yields south-directed paleocurrent directions averaging 187°. K1c paleocurrents show little variability, except in the upper 200 m of

Fig. 12: Photograph showing laterally continuous strata. K1c conglomerate beds can be traced laterally around the basin.

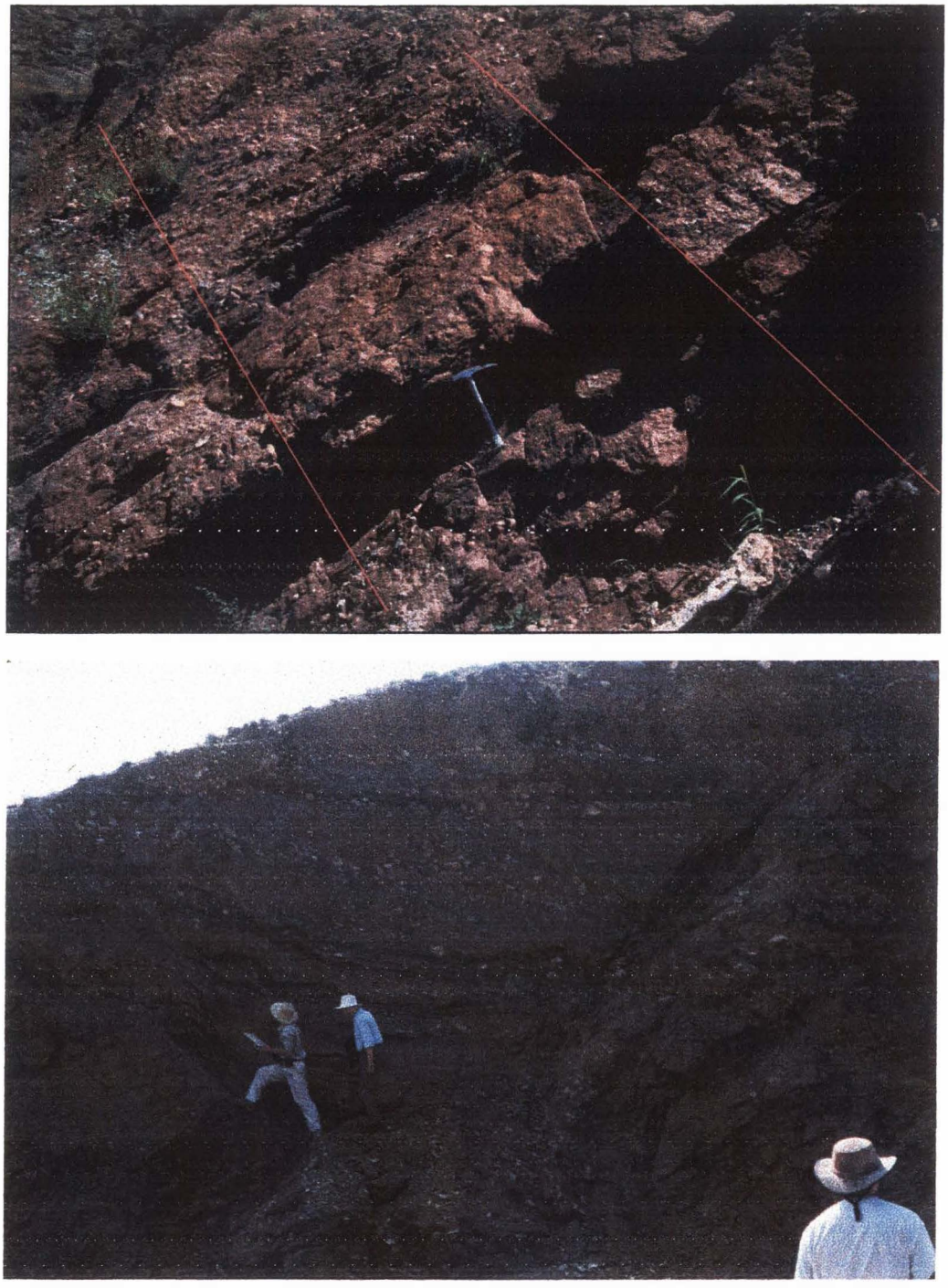

Fig. 13: Photographs of intra-K1b normal faults. Red lines on top photo mark fault planes. Lower photo shows intra-member half-graben.

Fig. 14: Aerial distribution of paleocurrent data.

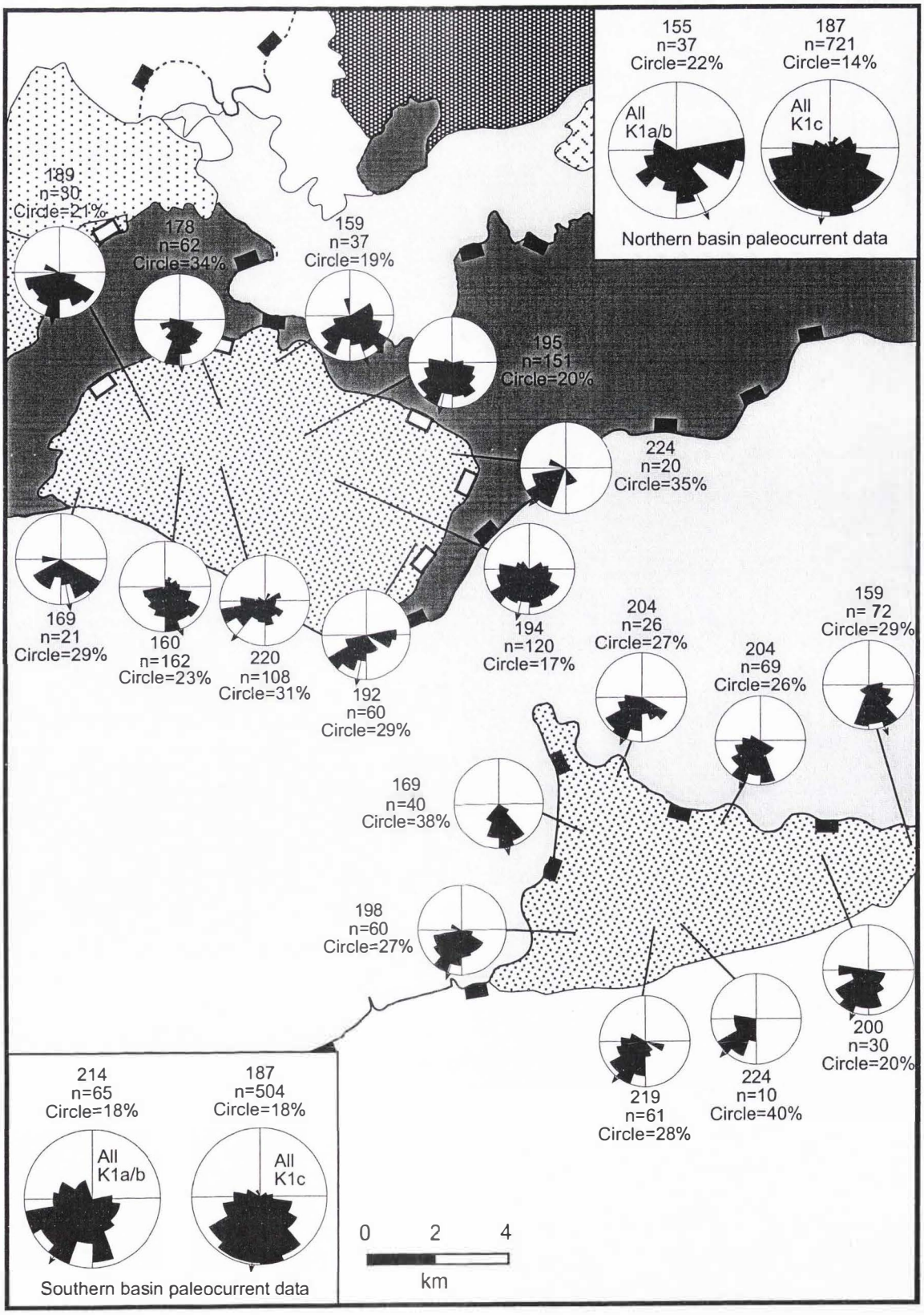
155
n=37
Circle=22%
187
n=721
Circle=14%
All
K1a/b
All
K1c
Northern basin paleocurrent data
189
n=30
Circle=21%
178
n=62
Circle=34%
159
n=37
Circle=19%
195
n=151
Circle=20%
224
n=20
Circle=35%
169
n=21
Circle=29%
160
n=162
Circle=23%
220
n=108
Circle=31%
192
n=60
Circle=29%
194
n=120
Circle=17%
204
n=26
Circle=27%
204
n=69
Circle=26%
159
n= 72
Circle=29%
169
n=40
Circle=38%
198
n=60
Circle=27%
219
n=61
Circle=28%
224
n=10
Circle=40%
200
n=30
Circle=20%
214
n=65
Circle=18%
187
n=504
Circle=18%
All
K1a/b
All
K1c
Southern basin paleocurrent data
0
2
4
km

the section in the southern basin, coincident with the increase in sandstone:conglomerate ratio (Fig. 3).

Areally distributed clast-count data clearly demonstrate the dominance of clasts derived from the footwall of the detachment throughout both basins (Fig. 15). Granitoid plutonic clasts are dominant, with foliated plutonic, conglomerate, and sandstone clasts spatially distributed fairly uniformly. Marble and volcanic clasts are locally important in parts of each basin, with volcanic clasts concentrated along the western margin of each basin (where volcanic rocks of K1a or older are still preserved).

There is little vertical stratigraphic variability in clast composition, with plutonic clasts dominating throughout the section. However, minor clast types show some important vertical trends (Fig. 3). Gneiss clasts are common in K1c, but are not present in K1a or K1b (Fig. 3, 10, and 15); similarly, mylonitic clasts are not observed in K1a or K1b and are not commonly seen in the lower part of K1c. These mylonitic clasts appear in the upper 200 m of the section in the southern basin, but are not found in the northern basin (Fig. 3 and 15). Sandstone clasts, some of which may be recycled Lower Cretaceous clasts, decrease in abundance up section (Fig. 3).

Discussion

Geologic Evolution of the Hohhot Basins

The evolution of the basins can be broadly subdivided into two phases, based on the contrasting depositional and deformational styles in K1a-K1b and K1c (Fig. 16). The

Fig. 15: Areal distribution of clast composition data.

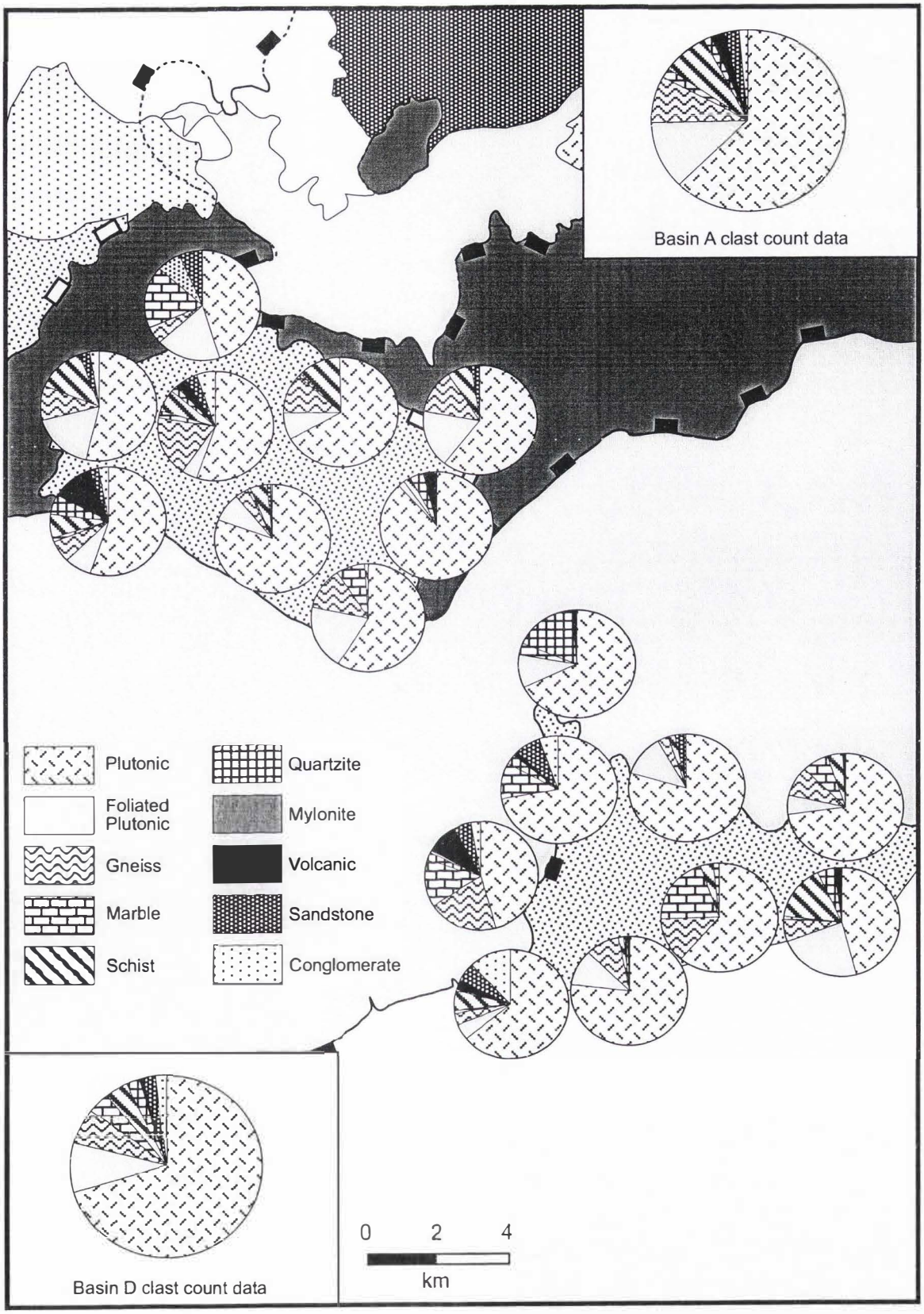
Basin A clast count data
Plutonic
Foliated Plutonic
Gneiss
Marble
Schist
Quartzite
Mylonite
Volcanic
Sandstone
Conglomerate
Basin D clast count data
0
2
4
km

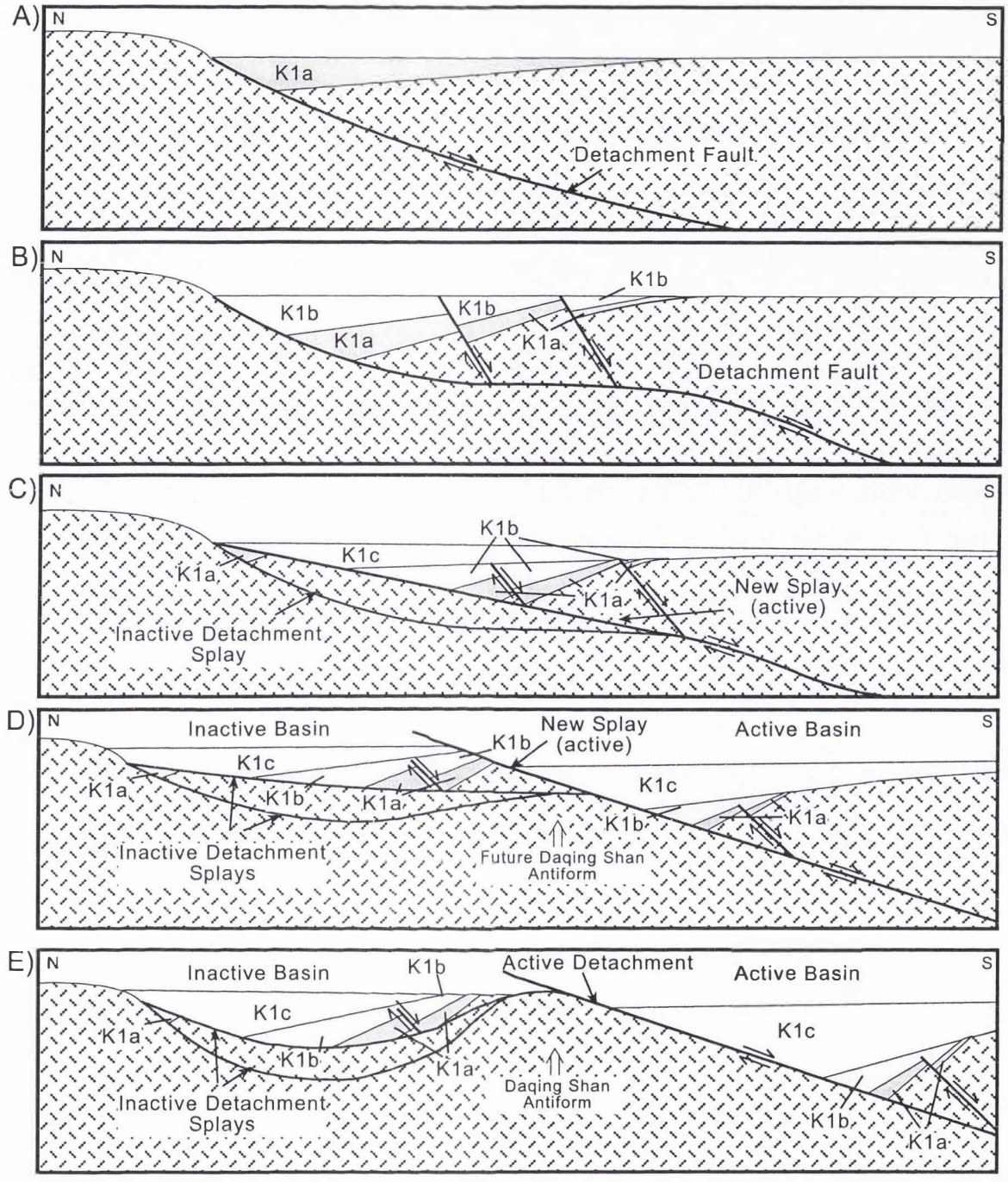

Fig. 16: Model for tectonic evolution of northern and southern basins. A) Initial faulting and syn-extensional basin filling. B) Continued extension and beginning of upperplate break-up with deposition in isolated half-graben. C) Continued extension and deposition with uplift of the upper plate causing folding and propagation of new detachment splay. D) Continued extension and deposition with uplift causing folding and propagation of a third detachment splay. E) Exhumation of Daqing Shan antiform. Northern basin is inactive with continued extension and deposition of Lower Cretaceous sediment on the southern flank of the Daqing Shan antiform.

bulk of the basin fill consists of K1c, suggesting longer-lived basins later in the evolution of the system.

K1a and K1b are dominated by proximal alluvial fan facies and include abundant debris flow, rock avalanche, and slide block deposits. These units were deposited with the onset of extension and the concomitant creation of topographic relief and isolated basins. Early stage sedimentation was concurrent with volcanism, which ceased by the K1a-K1b boundary.

The Hohhot basins were deformed and dissected by normal faults synchronous with deposition of K1a-K1b, as evidenced by the much greater density and multiple generations of normal faults in K1a and K1b versus K1c. Further evidence for dissection are angular unconformities between volcanic rocks and Lower Cretaceous strata in the northern basin (Fig. 11), and the abundance of reworked volcaniclastic detritus in sandstone and conglomerate of K1b (Fig. 17). Intrabasinal breakup of the Hohhot basins during K1a and K1b sedimentation, as well as the creation of intrabasinal graben (Fig. 13) resulted in variable paleocurrent directions and local changes in clast sources (Fig. 14 and 15).

K1c is a much more consistent unit laterally and stratigraphically, dominated by sheetflood and streamflow processes in an alluvial fan setting with additional deposition by rock-avalanche and large gravity-driven slide blocks. Paleocurrent indicators are uniformly south-directed in both basins, and demonstrate a well-developed transverse paleodrainage system flowing away from the detachment fault in the direction of extension. However, local variation in clast composition (but not depositional style or

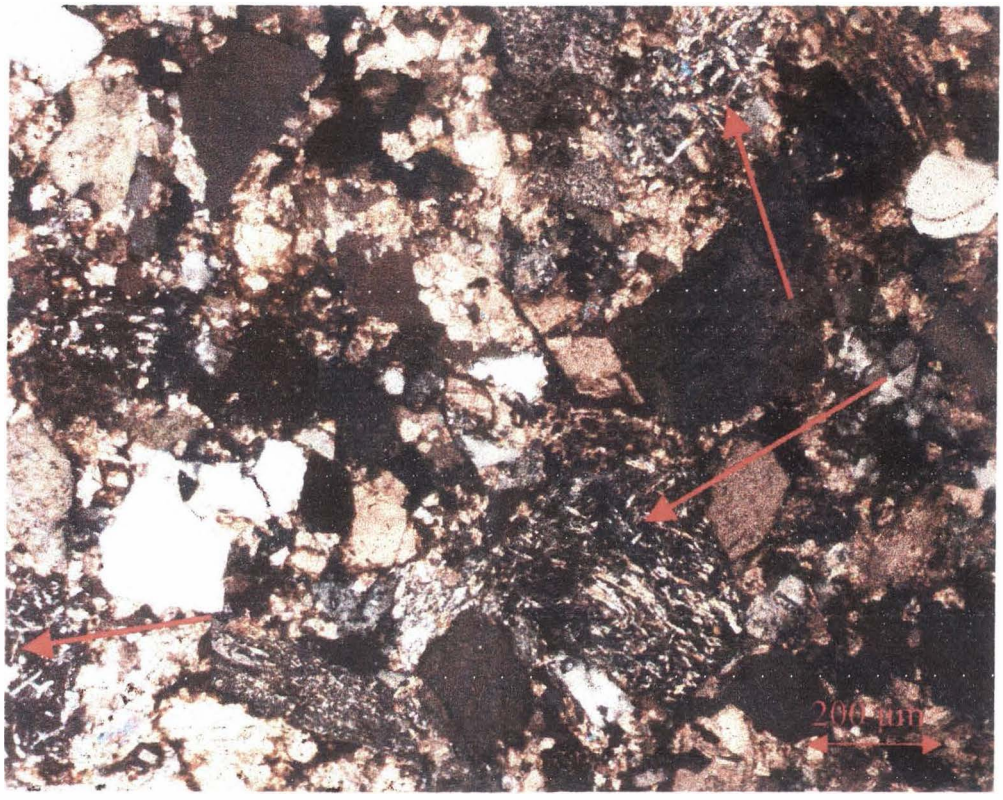

Fig. 17: Photomicrograph of K1b. Arrows mark volcanic lithic grains with plagioclase laths.

paleocurrent) suggest that these fans were not being deposited in a homogenized drainage basin, but rather were deriving sediment from small catchments or source regions of spatially variable rock types (Ingersoll, 1990). Paleocurrent trends around the basins do not reflect primary corrugation of the detachment fault. This observation does not address the presence or absence of the corrugations as primary features, given that energetic depositional systems flowing down the axis of the corrugation are expected to obscure any more minor flow components off the sides of the corrugations.

These data suggest that the basins on both flanks of the Daqing Shan antiform were originally contiguous during deposition of K1a, K1b and the lower portion of K1c (Fig. 16). Both basins exhibit K1a-K1b strata of similar thickness that were deposited by debris flow and rock-avalanche processes. Units K1a and K1b are overlain by K1c sediment that was deposited by similar processes in both basins. Transport direction for K1c in the northern basin is 187°, suggesting that the exhumed lower plate, currently a topographic high, was not exposed and bisecting the basins during deposition of the lower portion of the section. Clast types in K1a, K1b, and the lower part of K1c are also similar. Granitoid plutonic clasts dominate and clasts of reworked Lower Cretaceous conglomerate and sandstone clasts are present. Also, gneiss clasts do not appear in either basin until K1c is deposited. Age relationships from intrabasinal volcanic rocks and footwall cooling ages suggest concurrent sedimentation was occurring in both basins.

The appearance of higher metamorphic grade, including mylonitic, clasts high in the section in the southern basin suggests progressive unroofing of deeper crustal material as extension and uplift of the lower plate continued. Likewise, the absence of such clasts

in the northern basin suggests that the northern basin had stopped receiving sediment by the time those clast types were exposed in the source terrane. This apparent shorter-lived deposition on the northern flank of the core complex, also supported by the much thinner K1c section, is interpreted to record the uplift of the Daqing Shan antiformal dome during unroofing of the metamorphic core complex. Specifically, midway through deposition of K1c in the southern basin, exhumation of the lower plate and uplift of a mid-crustal dome separated the previously contiguous northern and southern basins (Fig. 16). Much as uplift of the metamorphic core complex resulted in deactivation of the folded northern splays of the Hohhot detachment (Davis et al., 2002), uplift of the core complex resulted in deactivation of the northern basin. Following uplift of the core of the metamorphic core complex, continued extension on the southern splay of the Hohhot detachment (Davis et al., 2002) continued to create accommodation space in the southern basin, where K1c continued to accumulate (Fig. 16).

Supradetachment Basin Evolution and Style

Previous work concerning supradetachment basins has presented conceptual models suggesting that supradetachment basins exhibit predictable characteristics that are a result of the structural controls exerted by the unique setting in which they form (Fillmore et al., 1994; Friedmann and Burbank, 1995). The general applicability of these models has been disputed, largely due to the variability of sedimentary styles in documented supradetachment basins, as well as the imprecision with which supradetachment basin nomenclature is applied (e.g. Janecke et al., 1999).

The most widely cited and applied model for sedimentation is supradetachment basins is that of Friedmann and Burbank (1995), who classify supradetachment basins as an end-member basin style in extensional continental settings opposite the better-known half-graben rift basin of Leeder and Gawthorpe (1987) (Table 1). Friedmann and Burbank (1995) describe supradetachment basins as those that form "above a low-angle normal fault system." More specifically, "the term also represents the end-member model presented [in Friedmann and Burbank, 1995]." These basins are thin, short-lived and are dominated by coarse, predominantly footwall-derived sediments delivered to the basin by transverse drainages and often deposited by mass-wasting processes (Table 1). Supradetachment basins generally are expected to lack either significant fine-grained, lacustrine deposits or axial drainage systems, which are commonly found in half-graben (Leeder and Gawthorpe, 1987). This type of extensional basin tends to occur in back-arc regions where the crust has recently experienced dramatic thickening, and rock may be warmer due to magmatism and high radiogenic heat flow (Friedmann and Burbank, 1995). In contrast, most rifts occur in areas with cold normal crust lacking recent contractile tectonism (Friedmann and Burbank, 1995).

The geological characteristics documented for both our northern and southern study basins, conform well to the Friedmann and Burbank (1995) end-member supradetachment basin model. The Hohhot basins are thin (<1200 m), contain angular unconformities, and are dominated by coarse conglomerate derived from the footwall of the detachment fault and transported to the basin in transverse drainage systems with paleocurrents parallel to the extension direction. Rapid rates of footwall uplift relative to

Table 1: CHARACTERISTICS OF EXTENSIONAL BASINS. (Modified from Friedmann and Burbank, 1995. Additional data sourced from: a) Davis et al., 2002 b) Stewart and Diamond, 1990; Diamond and Ingersoll, 2002)

Basin / Characteristics	Lake Baikal	Mid-continent Rift	Shadow Valley	Chemehuevi	Hohhot[a]	Esmarelda[b]
Bounding fault geometry	Steep (50-70°), listric, planar	Steep (60-65°), multiple planar	~31°, curviplanar, corrugated	12-26°, curviplanar, corrugated	15-30°, curviplanar, corrugated	25-30°, corrugated, curviplanar
Total Extension (km)	10-25	??	11-26	40-75	>40	~11
Extension rate (km/Myr)	0.3-0.84	??	12-1	10.1-4.5	??	1.2-1.8?
Duration of sedimentary record (Myr)	35-30, in progress	15-30	<7	7-9	3-7	6-9
Fill thickness (km)	4-6	3.3-7.3	3	2-3	0.3-1	4.4-5.4
Dominant provenance	Hanging wall	??	Footwall	Hanging wall and footwall	Footwall	Hanging wall and footwall
Dominant transport pathways	Hanging wall	??	Transverse, ext. parallel	Transverse, ext. parallel	Transverse, ext. parallel	Transverse, ext. parallel
Sedimentary style	Fluvial (meandering), delta Deep lake (muds, turbiditic)	Fans, fluvial (braided, meandering) Shallow lake, mudflat	Mass wasting, fans Major lake (playa, perennial)	Mass wasting, fans Major lake (playa, perennial)	Mass wasting, fans Fluvial (?) sandstone	Mass wasting, fans, braided fluvial, major lake (playa, perennial)
Associated magmatism	Alkalic, tholeitic	Alkalic, tholeitic	Calc-alkaline	Calc-alkaline	Rhyolitic, minor basalt	Calc-alkaline

basin subsidence minimized proximal accommodation space and prevented proximal trapping of sediment adjacent to the fault (as occurs in half-graben), thus promoting distal deposition of coarse material derived from the lower plate. The Hohhot basins show no evidence of axial drainage and do not contain fine-grained lacustrine intervals as with Friedmann and Burbank (1995) type supradetachment basins. Instead, coarse conglomerate is present from the detachment fault to the most distal strata exposed. Finer grained rocks may exist further into the basin, as is preserved in some supradetachment basins (Diamond and Ingersoll, 2002; Stewart and Diamond, 1990), but Neogene cover prevents observation beyond the mountain front and coarse sediment is present everywhere we see Lower Cretaceous strata. The only prominent distinction between the two Hohhot supradetachment basins described in this study is that the northern basin is thinner and has experienced more deformation as a result of the uplift of the metamorphic core of the Hohhot core complex.

In contrast to these characteristics, other workers have documented syn-extensional basins that form above detachment faults but do not conform to the Friedmann and Burbank (1995) end-member. For example, Fedo and Miller (1992) studied the Crestview Wash basin, located above the Sacramento Mountain detachment fault in the Colorado River extensional corridor, wherein they describe a basin that resembled a half-graben above a low-angle normal fault. The Crestview Wash basin has three facies associations indicating (1) small, high-gradient, mass movement dominated alluvial fans; (2) lake and lake margin; and (3) large, low-gradient, streamflow dominated alluvial fans (Fedo and Miller, 1992). This basin is dissected by a series of normal faults

that are consistent with detachment movement, but no angular unconformities or growth strata were observed. Structural reconstruction accomplished with the aid of younger sedimentary deposits and dated volcanic rocks, and the lack of growth strata lead Fedo and Miller (1992) to interpret the Crestview Wash basin fill as deposited during a period of tectonic quiescence after an initial extensional event.

Although the basin is located above a regional detachment, is thin, and contains coarse sediment from mass-wasting and alluvial fan processes. It has relatively little distally located, coarse sediment, contains a significant lacustrine component, and is lacking in angular unconformities. The structural setting, with respect to the domed lower plate, of the Crestview Wash basin is similar to the northern basin in the Daqing Shan, but these basins clearly do not share similar tectonic histories. The Crestview Wash basin may have formed with the onset of extension at the detachment breakaway, but was not involved in the uplift and exhumation of the Chemehuevi-southern Sacramento metamorphic core complex. The basin was also not continuous with the basins that formed on the eastern flank of the Chemehuevi-Sacramento ranges.

The Chemehuevi-Sacramento detachment basin was cited by Miller and John (1999) as a good example of a Friedmann and Burbank-style supradetachment basins. The Chemehuevi-Sacramento detachment basin is dominated by coarse deposits formed by sediment-gravity and streamflow processes on alluvial fans, with minor fine-grained playa and shallow-lake deposits (Miller and John, 1999). The basin is also thin (2-3 km), located above a gently dipping normal fault, and has had a tectonic history similar to the Hohhot basins. These basins thus fit the Friedmann and Burbank model well.

Janecke et al. (1999) describe the Muddy Creek basin of south-west Montana as a basin formed above a low-angle normal fault that contrasts with the end-member supradetachment basin model. This basin is bounded by three *en echelon*, left-stepping normal faults with dips ranging from 8°-60° that flatten at depth. The basin contains centrally deposited lacustrine shale, mudstone, and sandstone and is bordered by a fringe (<1.5 km) of coarse alluvial fan and fan delta conglomerate and sandstone, proximal to the basin bounding faults (Janecke et al., 1999). Angular unconformities are only observed in the syn-tectonic fill and rock-avalanche material is present but rare. Extension magnitude is low (1.8-2.9 km) as is rate of extension (0.2-0.35 km Myr^{-1}) (Janecke et al., 1999).

The Muddy Creek basin does not conform to the end-member supradetachment basin for several reasons. The basin formed above a series of normal faults that have inconsistent dips ranging from 8°-60° and are not corrugated on the scale of other detachment faults. Also, extension rate and magnitude on these faults is extremely low in comparison to other regions where supradetachment basins form. Basin sediments include a significant fine-grained interval and lack significant amounts of distally deposited coarse conglomerate, rock-avalanche deposits, or angular unconformities. Sediment accumulation was relatively long-lived (47.1 to < 35 Ma) in comparison to other supradetachment basins. Collectively, the data indicate that the Muddy Creek basin is not a supradetachment basin (as described by Friedmann and Burbank, 1995), but more closely resembles a typical half graben that, in places, is bounded by low-angle normal faults.

An earlier model for supradetachment basin sedimentation based on the Pickhandle basin of the western United States (Fillmore et al., 1994) contrasts with the more Friedmann and Burbank-like model K1c interval of the Hohhot basins. Fillmore et al. (1994) described the Pickhandle basin as forming early in the evolution of a regional detachment, prior to uplift of the central Mojave metamorphic core complex. The Pickhandle basin is characterized by deposition of epiclastic volcanic rocks, pyroclastic rocks, and coarse sediment by alluvial fan and rock-avalanche processes. Paleocurrent indicators in the Pickhandle imply a complex drainage pattern providing evidence for transverse sediment transport, a hanging wall-derived sediment source, and an axial drainage system. Comparison with the Hohhot basins reveals that the Pickhandle basin shares characteristics with the K1a and K1b units in the lower part of the section. Both basins are dominated by coarse clastic sediments that were deposited with variable drainage patterns by alluvial fan and rock-avalanche processes into asymmetrical half-graben. These similarities follow from the structural setting shared by the K1a, K1b, and Pickhandle basins, all of which formed early in movement of the detachment and record local break-up of the upper plate. Thus the Fillmore et al. (1994) supradetachment basins and the Friedmann and Burbank (1995) supradetachment basins may be more appropriately considered evolutionary steps in the same model. Specifically, Fillmore et al. (1994) style basins may form with early extension on a detachment, as is observed with K1a and K1b strata in the Hohhot basins. However, with the large-magnitude extension (generally expected on detachment faults), supradetachment basins evolve

quickly into larger Friedmann and Burbank (1995) style basins, as is observed in K1c strata of the Hohhot basins.

The Hohhot basins as well as many basins in the western United States all display Friedmann and Burbank (1995) supradetachment basin type characteristics (Diamond and Ingersoll, 2002; Miller and John, 1999), further justifying the applicability of such an end-member model to continental extensional basin study. Other examples of basins that do not seem to work with the established model can be explained by structural variability that contributes to lower rates of extension and higher angle fault geometry. Assignment of strict models for basins associated with detachment faulting is difficult due to structural variation in different settings, yet a type basin model is useful as a guide. Further examination of these types of basins in different settings will help understanding of specific controls on supradetachment basin geometry, and the probable range of variation in sedimentary style that accompanies structural variability.

Conclusions

- The supradetachment basins near Hohhot are thin basins formed above multiple splays of the low-angle Hohhot detachment fault. Sedimentation in these basins was dominated by mass-movement and alluvial fan processes that transported coarse, predominantly footwall-derived conglomerate transversely away from the detachment. No fine-grained lacustrine sediments are preserved in these basins.

- The basin on the northern flank of the Daqing Shan antiform is thinner, was shorter-lived, and is more highly faulted than the basin on the southern flank of the Hohhot metamorphic core complex.
- These basins are syn-extensional sedimentary deposits associated with the formation of the Hohhot metamorphic core complex. The northern and southern basins were originally contiguous with the onset of extension, but were bisected as extension unroofed the lower plate and triggered isostatic uplift and exhumation of the metamorphic core of the core complex. Folding of the Hohhot detachment fault caused the Daqing Shan antiform and resulted in propagation of new detachment splays on the southern flank of the metamorphic core complex that allowed further extension and created accommodation space for Lower Cretaceous basins there.
- The basins associated with the Hohhot metamorphic core complex strongly reflect the supradetachment basin model presented by Friedmann and Burbank (1995) in the K1c interval, which is the bulk of the basin volumetrically. However, the earlier basin history, recorded by K1a and K1b is similar to the early-breakup supradetachment basin model proposed by Fillmore et al. (1994). These results suggest that the Friedmann and Burbank (1995) model is applicable for systems, or for stages during the evolution of a system, where low-angle normal faults rapidly accommodate large amounts of extension.

CHAPTER III

LATERAL VARIATION IN SUPRADETACHMENT BASIN STYLE, DAQING SHAN, INNER MONGOLIA, CHINA

Introduction

Supradetachment basins have been the focus of many recent studies concerning continental extensional basins (Beratan, 1991; Beratan and Nielson, 1996; Dickinson, 1991; Dorsey and Becker, 1995; Dorsey and Roberts, 1996; Fedo and Miller, 1992; Fillmore and Walker, 1996; Fillmore et al., 1994; Forshee and Yin, 1995; Friedmann and Burbank, 1995; Friedmann et al., 1996; Janecke et al., 1999, in press; Miller and John, 1988, 1999; Nielson and Beratan, 1995; Yarnold, 1994). The goals of these studies have been many, including constraining timing relationships between basins and basin-bounding structures, determining the structural setting from characteristics of basin sediments, and simply establishing a definition for a supradetachment basin. Though examples of supradetachment basins have been described an inadequate understanding of specific controls on basin geometry remains (Janecke et al., 1999).

A series of newly documented Lower Cretaceous extensional basins associated with the Early Cretaceous Hohhot detachment and its splays in the Daqing Shan of Inner Mongolia, China, presents an opportunity to identify geometric differences of sedimentary basins located in variable positions within detachment settings. The well-documented structural geology and evolution of the Hohhot detachment and Hohhot metamorphic core complex (Davis et al., 2002), as well as preservation of well-exposed

basins in several distinct structural settings for more than 120 km along strike, and on both flanks of the metamorphic core complex make the Hohhot extensional system an excellent natural laboratory for studying the sedimentary geology of such systems. Comparing and contrasting the depositional facies, detrital provenance and paleodrainage patterns in these basins will help to gain a greater understanding of specific controls on basin formation associated with detachment-style faulting.

Previous research concerning supradetachment basins provides conceptual models for supradetachment basins (Fillmore and Walker, 1994; Friedmann and Burbank, 1995). However, the general applicability of these models has been disputed (Janecke et al, 1999), largely due to variability of sedimentary styles in various structural settings. This research was undertaken to document a newly discovered series of basins above low-angle normal faults, as well as to provide a case study for comparison with previously studied supradetachment basins and related conceptual models. The preservation of the Daqing Shan basins in a variety of structural settings allow us to examine changes in basin geometry in response to variability of the controlling structures.

Geologic Setting

Daqing Shan Geologic History

The geology of the Daqing Shan has recently been the subject of extensive study (Darby et al., 2001; Ritts et al., 2001; Davis et al., 2002). The Daqing Shan, which borders the northern edge of the Ordos basin, compose a segment of the east-west trending Yinshan belt, an intracontinental mountain belt that spans from northeast of

Paleozoic as a result of the complex amalgamation of northern China. The current understanding of the history of the Daqing Shan is divided into 6 stages (Darby et al., 2001; Ritts et al., 2001): 1) A poorly understood period of broad-wavelength folding in the Middle Paleozoic; 2) Post-Permian through pre-Early Jurassic contractile deformation characterized by north-vergent basement-involved thrusts; 3) Early Jurassic extensional normal faulting and half-graben basin development; 4) Late Jurassic contractile faulting with north-vergent basement involved thrusts, folding, and inversion of Lower Jurassic half-graben; 5) Early Cretaceous detachment faulting and metamorphic core complex formation; 6) Neogene normal faulting. The high strain extension following Late Jurassic contraction is seen throughout northern China and Mongolia (Davis et al., 2001; Webb et al., 1999), and is responsible for the detachment faulting and the formation of the metamorphic core complex and associated supradetachment basins of interest to this study.

The Hohhot Detachment and Hohhot Metamorphic Core Complex

The Hohhot detachment fault is a south-dipping, low-angle (15-30°) normal fault that is exposed along strike for > 120 km (Fig. 1 and 18). A minimum of 40 km of extension occurred along the Hohhot detachment, accommodating rapid crustal extension that followed Late Jurassic through Earliest Cretaceous contraction (Davis et al., 2002). Siliceous volcanic rocks exposed to the west-northwest of Hohhot, located in the upper

Fig. 18: Photographs of Hohhot detachment fault.

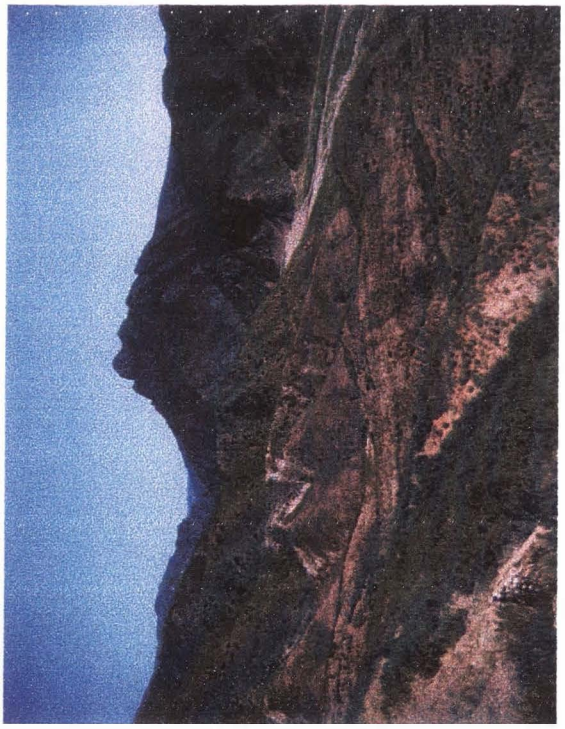

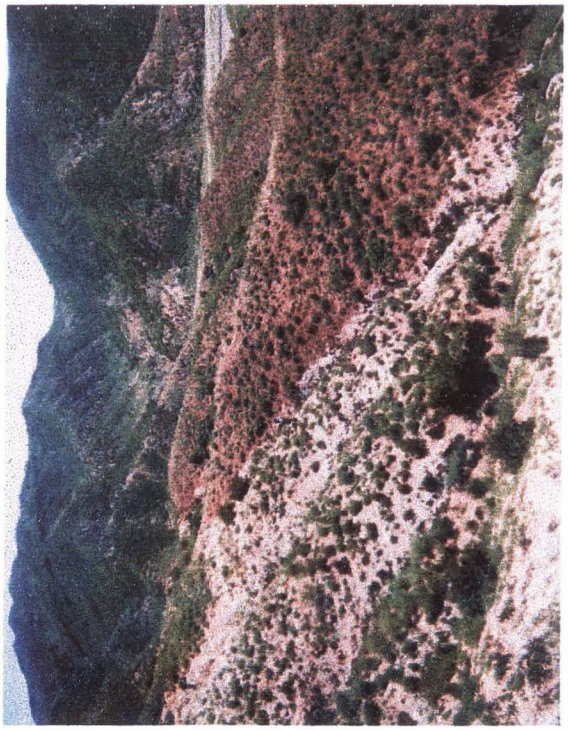

plate have yielded Early Cretaceous $^{40}Ar/^{39}Ar$ ages (127.2 ± 1.0 Ma, whole rock isochron; 125.5 ± 0.7 Ma, single-crystal sanidine weighted mean) (Davis et al., 2002). Also, syn-sedimentary volcanic rocks above the Hohhot master detachment fault yield Early Cretaceous $^{40}Ar/^{39}Ar$ ages (125.2 ± 0.7 Ma, 125.7 ± 0.6 Ma, and 125.8 ± 0.6 Ma (sanidine single-crystal weighted means) (Davis et al., 2002). Footwall biotite and hornblende cooling ages determined using $^{40}Ar/^{39}Ar$ methods show coincident Early Cretaceous ages (121.4 ± 0.9 Ma and 121.5 ± 1.3 Ma, respectively) (Davis et al., 2002). The age relationships reported here show that deposition of Lower Cretaceous syn-extensional strata began ca. 125 Ma and that extension on the Hohhot detachment fault began prior to rapid cooling of the footwall at ca. 121 Ma (Davis et al., 2002).

Large magnitude extension on the Hohhot detachment fault most likely occurred due to gravitational collapse of over-thickened crust (Darby et al., 2001; Davis et al., 1998, 2001, 2002). Dramatic extension resulted in an isostatic response in the footwall of the detachment that exhumed the Daqing Shan antiform, an east-west trending culmination of metamorphic and other crystalline rocks (Fig. 1 and 2). The master Hohhot detachment fault is located on the southern flank of this antiform. Along this flank, the detachment is corrugated with synforms that preserve numerous syn-extensional non-marine clastic basins. North of the antiform, two detachment faults are stacked and synformally folded, with top-to-the-south slip on both fault splays (Fig. 1 and 2). These faults were active early in the evolution of the detachment. The lower detachment separates mylonitic rocks from non-mylonitic, primarily Proterozoic crystalline rocks and Permian granitic gneisses (Davis et al., 2002). The upper

detachment carries a highly deformed succession of Cretaceous volcanic and sedimentary rocks. The lower, oldest detachment was the original detachment, but with extension, the footwall was progressively unloaded triggering an isostatic up-warp in the lower plate. The resultant antiformally folded detachment was deactivated and a new detachment splay propagated to the surface to accommodate further extension. The new splay, in turn, was also antiformally folded due to continued uplift with further unloading. The Hohhot detachment, on the southern flank of the Daqing Shan antiform, is the youngest fault splay and accommodated the remaining extension (Davis et al., 2002).

These processes of extensional exhumation resulted in the formation of the Hohhot metamorphic core complex, one of the most important structural features of the eastern Daqing Shan (Davis et al., 2002). The Hohhot metamorphic core complex is located north and northeast of Hohhot and consists of the Daqing Shan antiform, the Hohhot detachment, and an upper plate of pre-Cretaceous crystalline and sedimentary rocks and Lower Cretaceous syn-extensional strata (Fig. 1 and 2). The footwall of the detachment contains a mylonitic fabric within the limits of the metamorphic core complex. The mylonitic front exposed in the Daqing Shan (Fig. 1) represents a thermally controlled strain boundary below which quartz has undergone penetrative crystal-plastic deformation (Davis and Lister, 1988; Davis et al., 2002).

The Hohhot detachment extends to the east and west of the Hohhot metamorphic core complex, where the magnitude of extension is lower. East of the Hohhot metamorphic core complex, the detachment separates Lower Cretaceous clastic sedimentary rocks and upper plate crystalline rocks from non-mylonitic footwall rocks.

West of the Hohhot metamorphic core complex, the crystalline hanging wall is preserved, though it is cut by several normal faults responsible for doming of the detachment fault to a lesser degree than what is documented within the metamorphic core complex.

Hohhot Supradetachment Basins

Lower Cretaceous sedimentary basins are found discontinuously along the length of the Hohhot detachment for its 120 km length along strike. These basins occur on both the southern and northern sides of the Daqing Shan, and in the central part of the detachment, north of Hohhot (Fig. 1). This study describes all of the Lower Cretaceous basins of the Daqing Shan for the purpose of comparison in order to establish how basin geometry is affected by variability in the controlling structures.

Lower Cretaceous sedimentary basins above the detachment are interpreted to be syn-extensional for several reasons. First, Lower Cretaceous rocks are separated from older rocks by the Hohhot detachment or related normal faults, and occur only in the upper plate. Second, these rocks are cut by low and high angle normal faults as a result of southeast-directed extension, consistent with movement on the detachment. Third, volcanic rocks in the base of the Lower Cretaceous section have been dated at 125.2 ± 0.7 Ma, 125.7 ± 0.6 Ma, and 125.8 ± 0.6 Ma (sanidine single-crystal weighted mean $^{40}Ar/^{39}Ar$ age), coincident with the age of faulting determined by cooling ages and cross-cutting relationships in the footwall of the detachment (Davis et al., 2002). Fourth, these rocks consist predominantly of coarse conglomerate derived from sources that include footwall mylonite and other metamorphic rocks common in the lower plate of the

detachment. Fifth, intraformational unconformities are present indicating rotation of strata due to continued upper-plate faulting after deposition.

Basins are located in several structurally distinct settings in the Daqing Shan, and now occur as unconnected basins. The basins are labeled N1, N2, S1, S2, S3, and S4 in this paper simply to facilitate discussion (Fig. 19). Basins N1 and N2 are located on the northern flank of the Daqing Shan, whereas basins S1, S2, S3, and S4 are located along the southern range front. Basins N2, S2, and S3 are located within the central part of the detachment system and adjacent to the Hohhot metamorphic core complex. Basins S2 and S3 are located in corrugations of the master Hohhot detachment and Basin N2 is located in the synformal keel, above the stacked and synformally folded detachment splays. Basin S4 is preserved in a corrugation of the master Hohhot detachment east of Basin S3 and outside the boundary of the Hohhot metamorphic core complex. The mylonitic front is mapped northwest of this basin where extension magnitude is greater within the bounds of the metamorphic core complex. Basin N1 is also located above the master Hohhot detachment, west of basin S2. The detachment fault sweeps to the northwest beyond basin S2 and the magnitude of extension is again less than that of the metamorphic core complex. Finally, basin S1 is located within the hanging wall of the master Hohhot detachment. This intra-hanging wall basin is bounded by a less extensive, low angle normal fault, which soles into the master detachment at depth.

The Hohhot basins comprise a dominantly clastic sedimentary section that is more than 1200 m thick (Fig. 3). We informally divide the basins into three lithostratigraphic members, K1a, K1b, and K1c from bottom to top. These units are recognized in most of

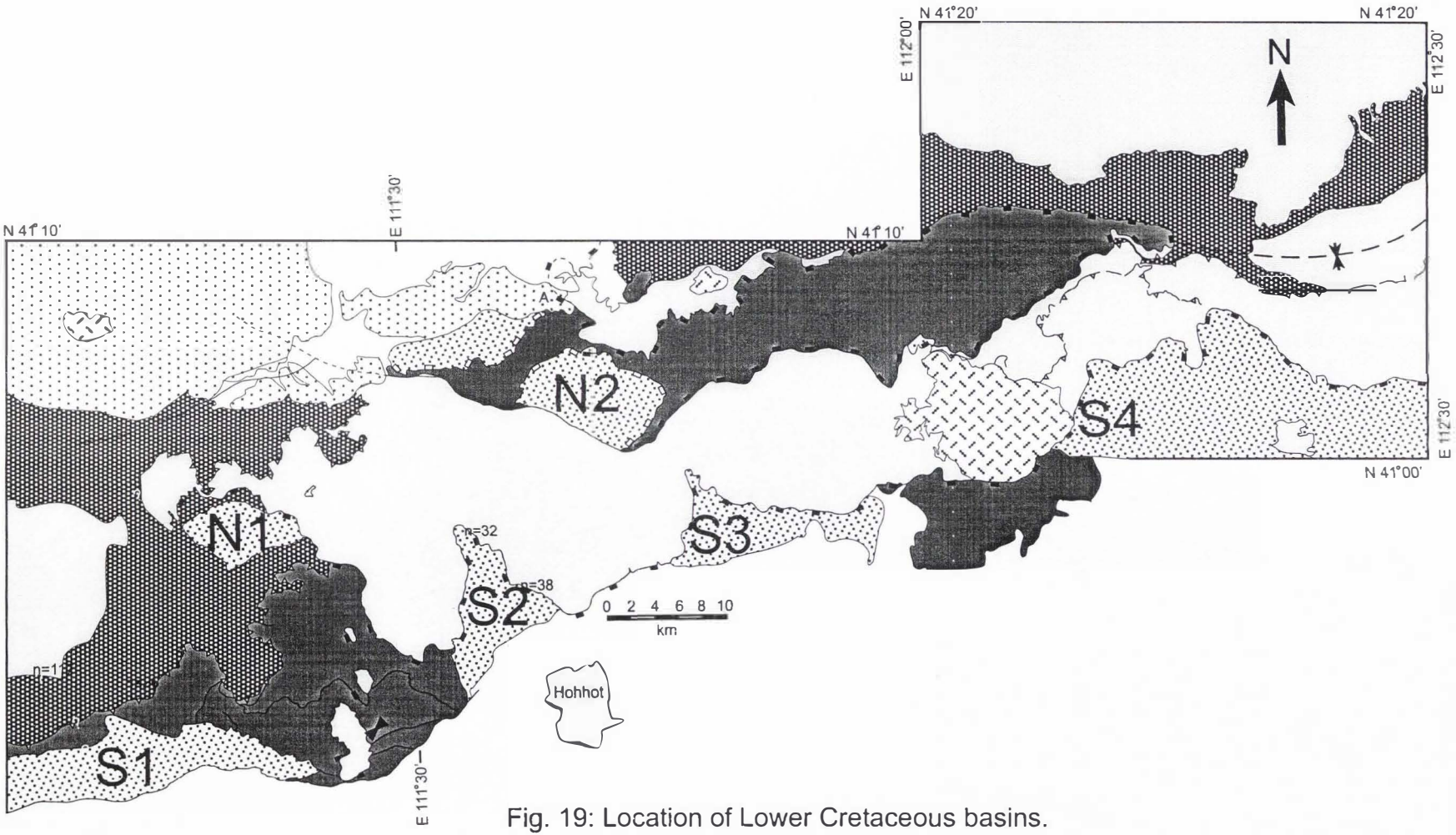

Fig. 19: Location of Lower Cretaceous basins.

Table 2: DISTRIBUTION OF SEDIMENTARY MEMBERS IN LOWER CRETACEOUS BASINS

Member	Thickness	Lithofacies	Sedimentologic Interpretation
K1a	75 m	• Red, unorganized, matrix-supported conglomerate • Interbedded bimodal volcanic rocks	• Debris flow deposits and volcanic flows in an alluvial fan setting
K1b	125 m	• Red, unorganized, matrix-supported conglomerate • Contains lesser well-organized, clast supported conglomerate • Volcaniclastic detritus • Contains monolithologic blocks and breccias	• Dominantly debris flow deposits in an alluvial fan setting • Lesser subaqueous streamflow and sheetflood deposits • Gravity-driven slide blocks
K1c	200-400 m	• Well-organized, clast-supported conglomerate • Contains monolithologic blocks and breccias	• Subaqueous streamflow and sheetflood deposits in an alluvial fan setting • Gravity-driven slide blocks

the Lower Cretaceous basins, although thickness and internal stratigraphy varies considerably throughout the study area (Table 2). K1a and K1b are composed dominantly of unorganized, red, matrix-supported conglomerate. K1a is distinguished by the presence of interbedded bimodal volcanic rocks, while K1b contains minor clast-supported lenticular conglomerate, lacks volcanic flows, and contains monolithologic blocks and megabreccia units (Fig. 7), and are most commonly composed of Proterozoic marble. K1c consists of well-organized, clast-supported conglomerate, and displays tabular to lenticular beds that can be traced laterally in the basin.

Basin N2

Basin N2 is located on the northern flank of the Daqing Shan antiform, east and slightly south of Wuchuan city (Fig. 19). Structurally, it occupies the synformal keel of the Hohhot metamorphic core complex, and lies above the second detachment splay and below the third detachment splay (Fig. 1 and 2) (Davis et al., 2002).

Sedimentology and Stratigraphy. Sedimentary strata are Early Cretaceous in age, defined by $^{40}Ar/^{39}Ar$ ages on interbedded rhyolite flows (Davis et al., 2002). The sediments rest directly on the upper detachment splay, and this relationship can be seen in numerous locations around the basin. Pervasive normal faulting in this basin inhibits measurement of a complete section (Fig. 10); a maximum of only about 200 m of continuous section can be measured without crossing significant normal faults. However, a composite section has been constructed by correlating like-parts of repetitive lithostratigraphic sequences, and suggests a minimum basin thickness of 400 m (Fig. 20). Basin N2 contains three informally divided lithostratigraphic members, K1a, K1b, and K1c from bottom to top. The lowest two units, K1a and K1b, are difficult to separate in this basin and are generally considered one unit that is easily distinguished from the overlying unit, K1c.

K1a-b is composed dominantly of unorganized, red, matrix-supported conglomerate that has a minimum thickness of 175 m (Fig. 4, 6, and 20). Beds are 1 m to 2 m thick and have erosive bases particularly in the less common, more clast-supported portions of the sequence. Maximum clast size increases upwards within beds. Large monolithologic blocks and megabreccia units, most commonly composed of Proterozoic

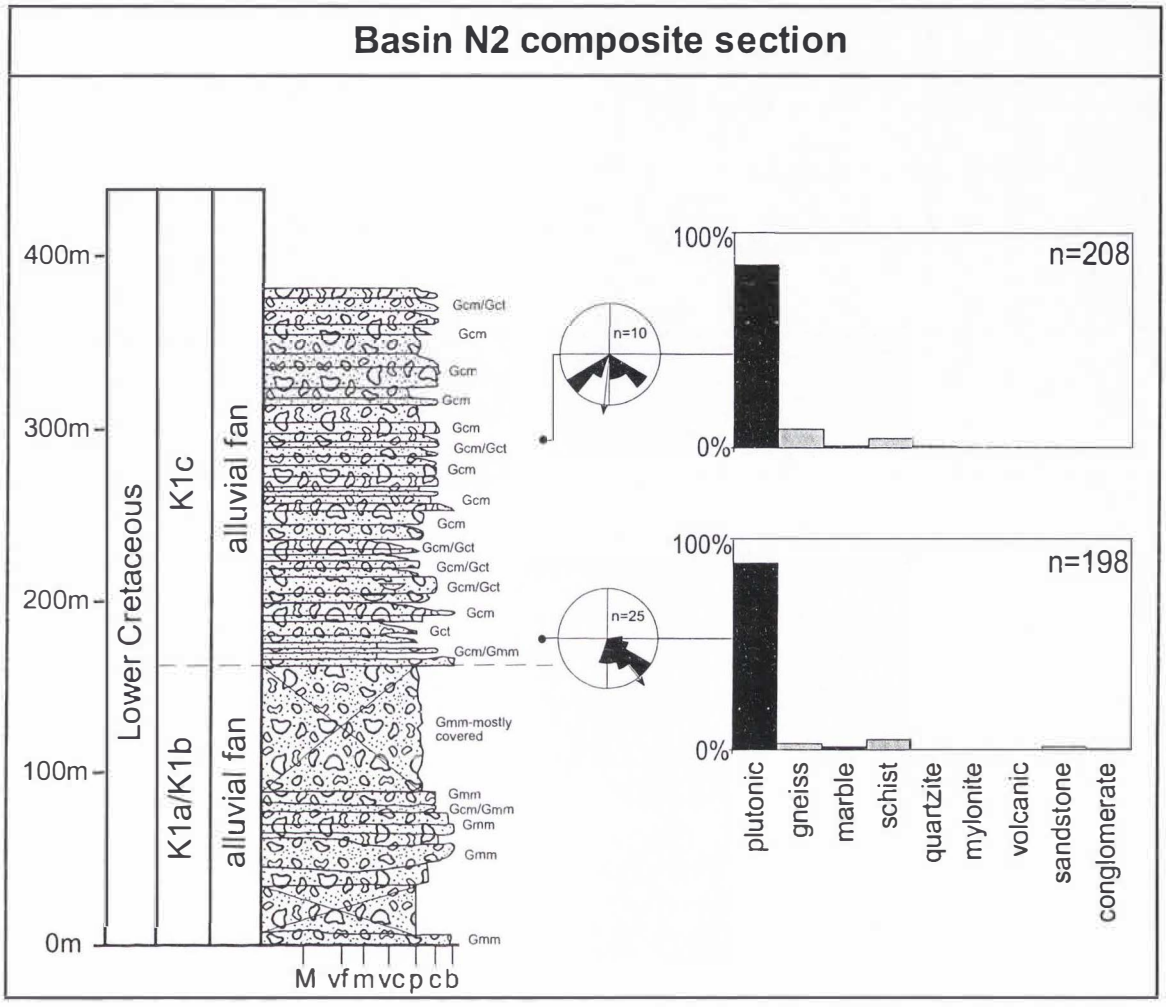

Fig. 20: Basin N2 composite section.

marble, are contained in K1b. The marble can be fairly intact, but is usually intensely fractured and brecciated and may be injected with the silty, red matrix common in K1b (Fig. 6).

K1a-b is interpreted as dominantly debris flow deposits based on the matrix-supported, disorganized nature of the conglomerate beds, with lesser streamflow and sheetflood deposits marked by the well-organized, clast-supported, lenticular to tabular, and better organized conglomerates. The combination of minor waterlain deposits and debris flow deposits is interpreted to represent a proximal alluvial fan environment (Blair and McPherson, 1994). The monolithic blocks and megabreccia units are interpreted as gravity-driven slide blocks and rock-avalanche deposits because they are completely encased in Lower Cretaceous strata and exhibit characteristics of being emplaced as coherent to semi-coherent units (Friedmann, 1997). The contact with the overlying unit, K1c, is generally gradational and appears as an increasing amount of clast-support and sand content that replaces the fine, red matrix seen in K1a/b.

K1c is the uppermost unit dominantly consisting of well-organized, clast-supported conglomerate (Fig. 8). Beds are tabular to lenticular with erosive bases, 1 m to 2 m thick, and interbedded with coarse sandstone and rare mudstone ranging in thickness from 10 cm to 80 cm. Individual beds are organized into relatively tabular units on the order of a few meters to 10 m thick and that extend for at least hundreds of meters laterally. Packages of trough cross-stratified conglomerate fining upward to medium trough cross-stratified sandstone are preserved at the 20 cm to 80 cm scale, but are not as common as the dominant imbricated conglomerate and conglomerate displaying low-

angle cross-stratification. Imbrication is abundant, as is trough cross-stratification and planar lamination in the sandstone. Large monolithologic, brecciated, gravity-driven slide blocks are common in K1c, and reach >2 km (long axis) in size, and are typically composed of Proterozoic marble (Fig. 9). The minimum thickness of this unit is ~200 m, determined by the largest length of continuous section in this transect (Fig. 3 and 20).

These conglomerates are interpreted as subaqueous channelized and sheetflood deposits based on their clast-supported, well-organized character. These deposits are interpreted to have formed in an alluvial fan system, based on the uniformly coarse conglomeratic nature of K1c, dominance of streamflow and sheetflood processes, and association with gravity-driven slide blocks and rock-avalanche deposits (Blair and McPherson, 1994; Friedmann, 1997).

Normal faults that cut the strata are roughly east-west striking consistent with extensional slip on the detachment splays. Angular unconformities in this basin indicate syn-depositional rotation of Lower Cretaceous strata (Fig. 11).

Paleocurrent and Provenance Data. Paleocurrent data were collected around the basin (Fig. 14, 21). The average paleocurrent direction for K1a-b is 155°. The paucity of imbricated clasts within K1a-b makes paleocurrent measurement within theses units difficult. Well-imbricated conglomerate is abundant in K1c, and yields south-directed paleocurrents that average 187°. K1c paleocurrents show little variability in this basin. Stratigraphically, some variation in paleocurrent direction is seen, but paleocurrents are always confined to southern hemisphere (Fig. 20).

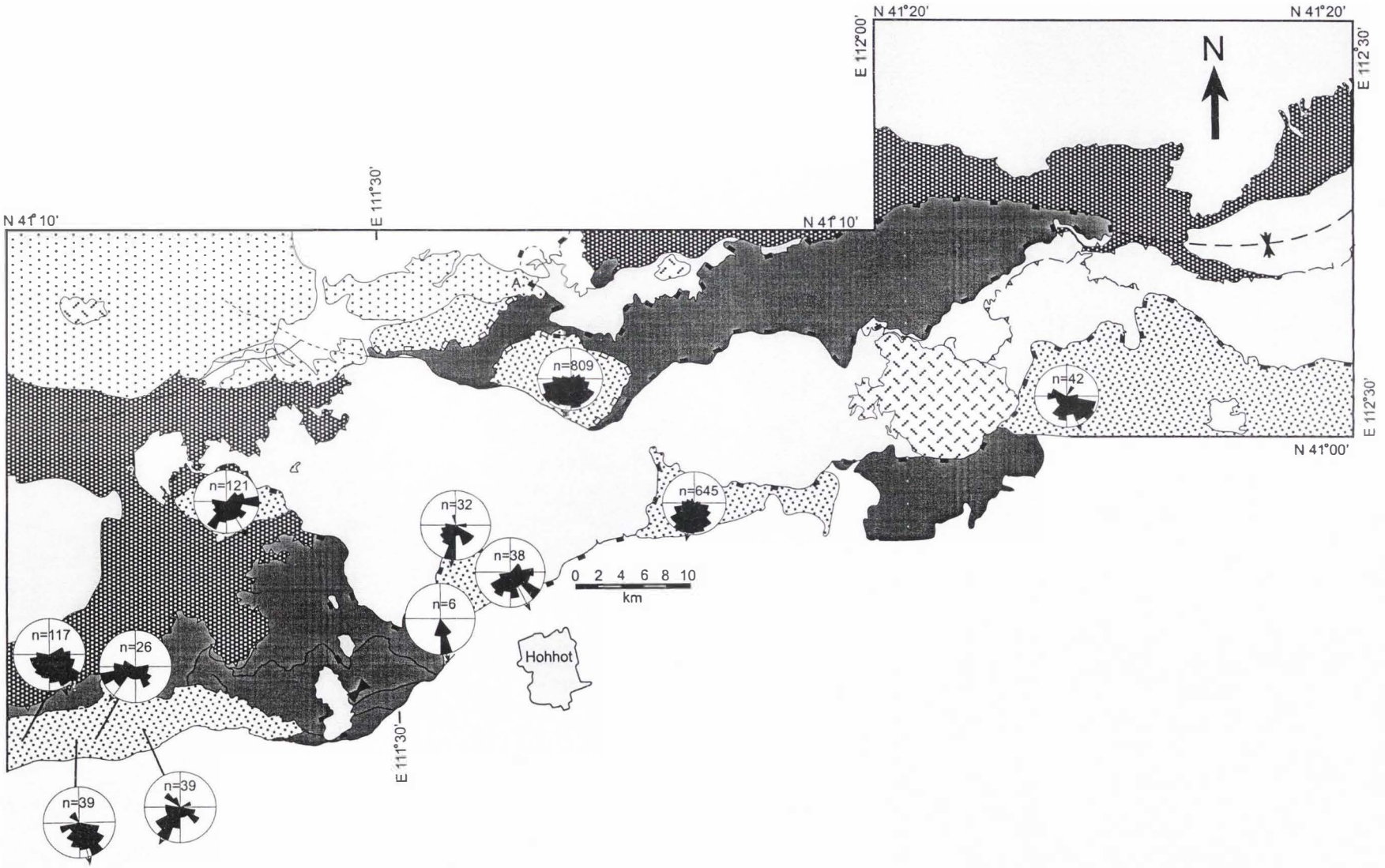

Fig. 21: Aerial distribution of paleocurrent data.

Areally distributed clast count data demonstrate the dominance of clast derived from the footwall of the detachment throughout the basin (Fig. 15, 22). Granitoid plutonic clasts are dominant, with foliated plutonic, conglomerate, and sandstone clasts distributed uniformly. Marble and volcanic clasts are locally important, with volcanic clasts, usually rhyolite and rare basalt, concentrated on the western side of the basin (where volcanic rocks of K1a are still preserved).

Clast composition vertically through the section varies little, although minor components show some important trends (Fig. 20). First, gneiss clasts are common in K1c, but not present in K1a-b. Second, sandstone clasts, some of which may be recycled Lower Cretaceous clasts, decrease in abundance up section. Finally, it should be noted that mylonite clasts, which are common in many of the other Lower Cretaceous basins are not present in this basin.

Basin S3

Basin S3 is located on the southern flank of the Daqing Shan antiform, just northeast of Hohhot, Inner Mongolia (Fig. 19). Lower Cretaceous strata overlie either the Hohhot detachment fault or an unconformity above older rocks (Fig. 5). Lower Cretaceous strata in this basin are cut, tilted, and/or folded by post-depositional normal faulting, and a large Neogene normal fault limits exposure of these rocks to within the Daqing Shan range front.

Sedimentology and Stratigraphy. Basin S3 contains a three-part stratigraphy as seen in surrounding basins. K1a, the lowest unit in the Lower Cretaceous section, is composed dominantly of unorganized, red, silty, matrix-supported conglomerate with

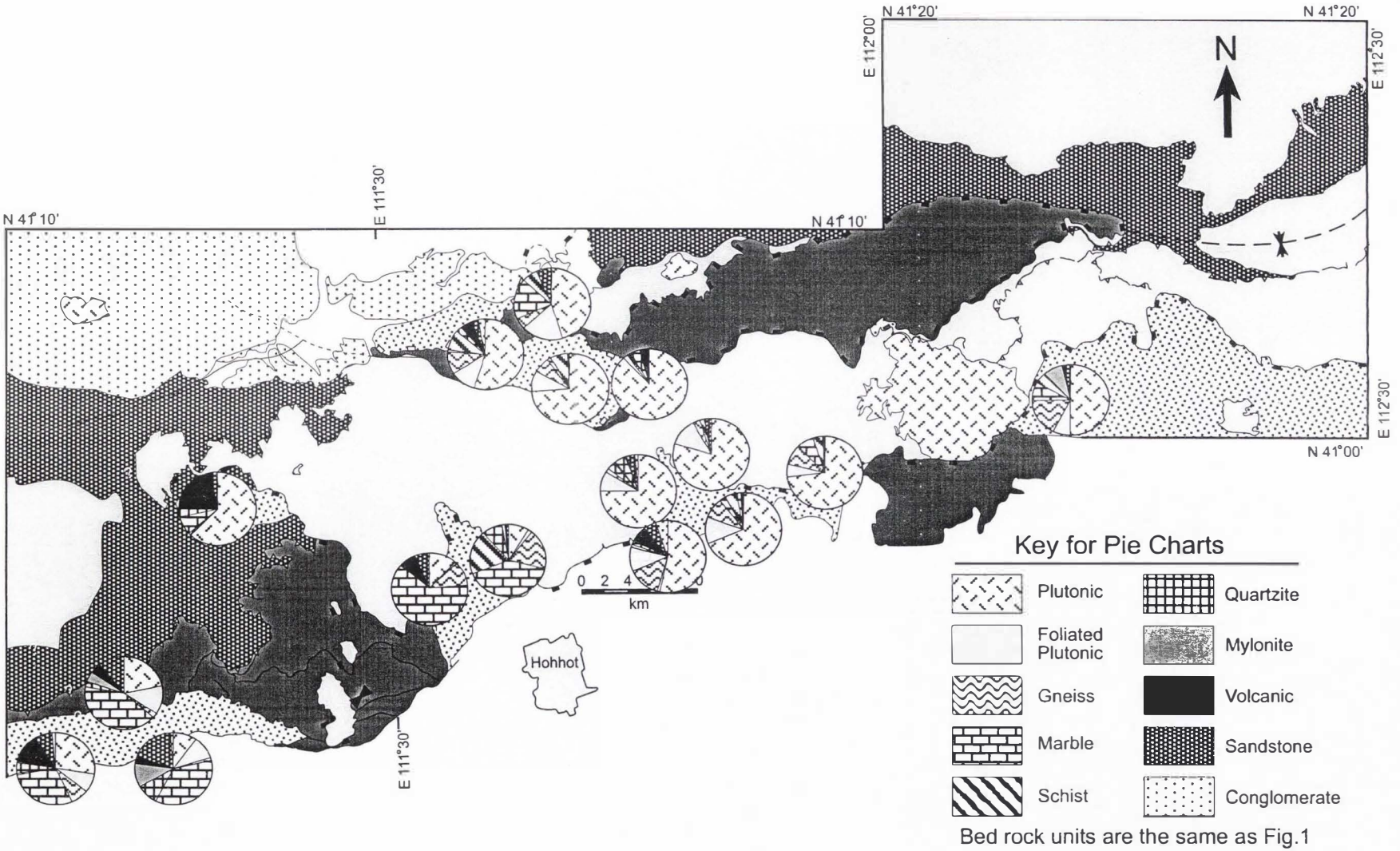

Fig. 22: Aerial distribution of clast count data.

interbedded bimodal volcanic rocks (Fig. 4). This unit is 75 m thick where the section was measured (Fig. 23). Beds are generally 1 m to several meters thick where defined.

K1a is interpreted as dominantly debris flow deposits with intermittent volcanic flows based on the matrix-supported, disorganized nature of the conglomerate beds. The dominance of debris flow deposits is interpreted to represent a proximal alluvial fan environment (Blair and McPherson, 1994).

Overlying this unit is K1b, composed dominantly of similar red, silty, matrix-supported conglomerate with beds 1 m to several meters thick (Fig. 6). This unit is distinguished from K1a by the lack of volcanic flows and the presence of minor clast-supported conglomerate, which appears as lenticular beds up to several meters thick (Fig. 6). The lenticular packages are generally not amalgamated, but are isolated within the matrix-supported conglomerate (Fig. 6). This unit also contains large (several meters to >10 m) monolithologic blocks and megabreccia units that are most commonly composed of Proterozoic marble (Fig. 7). The marble can be fairly intact, but is usually intensely fractured and brecciated and may be injected with the silty, red matrix common in K1b. K1b is ~125 m thick in this basin (Fig. 23).

K1b is interpreted as dominantly debris flow deposits based on the matrix-supported, disorganized nature of the conglomerate beds, with lesser streamflow and sheetflood deposits marked by the clast-supported lenticular to tabular, and better organized conglomerates. This combination of minor waterlain deposits and debris flow deposits is interpreted to represent a proximal alluvial fan environment (Blair and McPherson, 1994). Large blocks and megabreccia units are interpreted as slide blocks

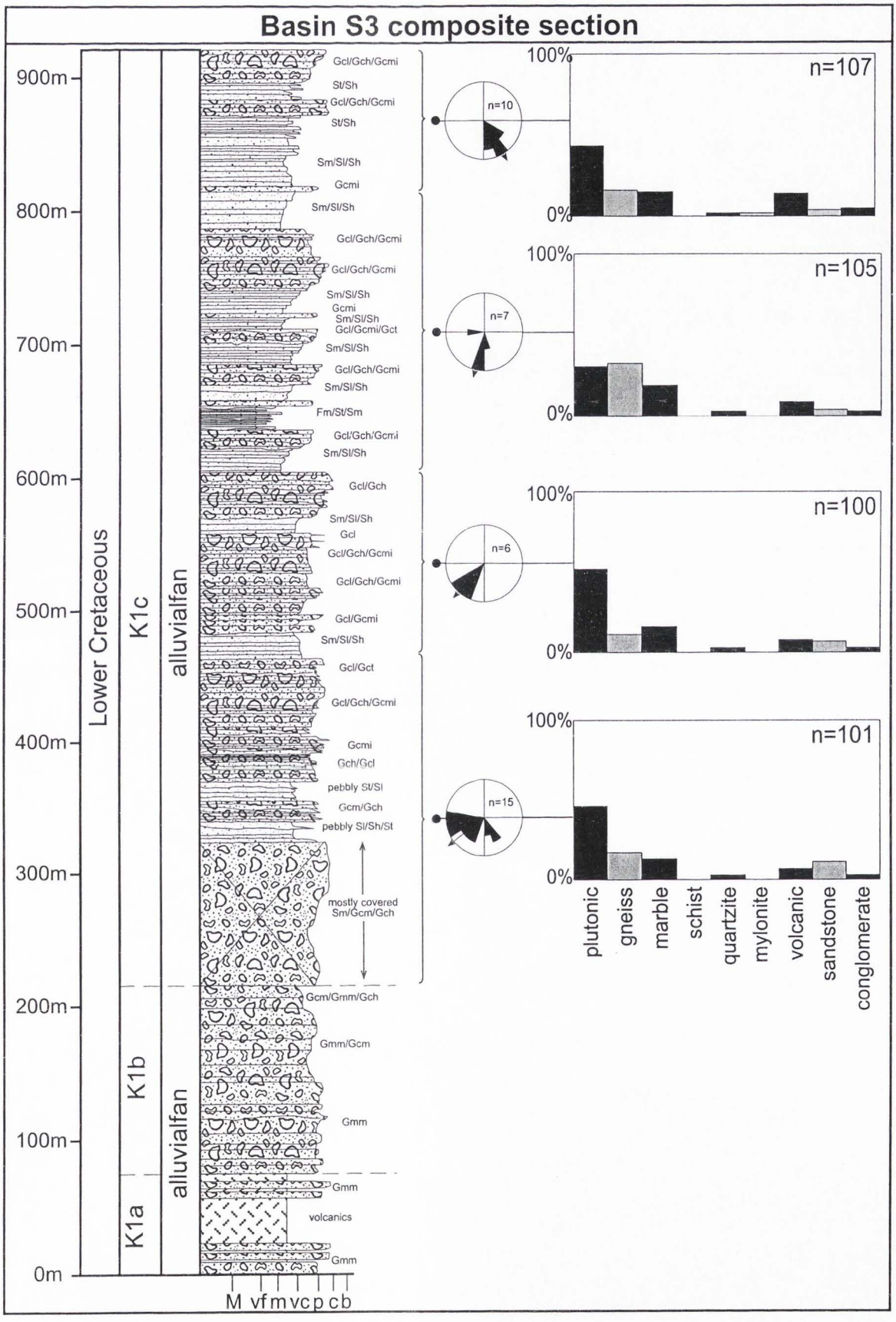
Basin S3 composite section
900m
800m
700m
600m
500m
400m
300m
200m
100m
0m
Lower Cretaceous
K1c
K1b
K1a
alluvialfan
alluvialfan
Gcl/Gch/Gcmi
St/Sh
Gcl/Gch/Gcmi
St/Sh
Sm/Sl/Sh
Gcmi
Sm/Sl/Sh
Gcl/Gch/Gcmi
Gcl/Gch/Gcmi
Sm/Sl/Sh
Gcmi
Sm/Sl/Sh
Gcl/Gcmi/Gct
Sm/Sl/Sh
Gcl/Gch/Gcmi
Sm/Sl/Sh
Fm/St/Sm
Gcl/Gch/Gcmi
Sm/Sl/Sh
Gcl/Gch
Sm/Sl/Sh
Gcl
Gcl/Gch/Gcmi
Gcl/Gch/Gcmi
Gcl/Gcmi
Sm/Sl/Sh
Gcl/Gct
Gcl/Gch/Gcmi
Gcmi
Gch/Gcl
pebbly St/Sl
Gcm/Gch
pebbly Sl/Sh/St
mostly covered
Sm/Gcm/Gch
Gcm/Gmm/Gch
Gmm/Gcm
Gmm
Gmm
volcanics
Gmm
M vf m vc p cb
n=10
n=7
n=6
n=15
100%
0%
n=107
n=105
n=100
n=101
plutonic
gneiss
marble
schist
quartzite
mylonite
volcanic
sandstone
conglomerate

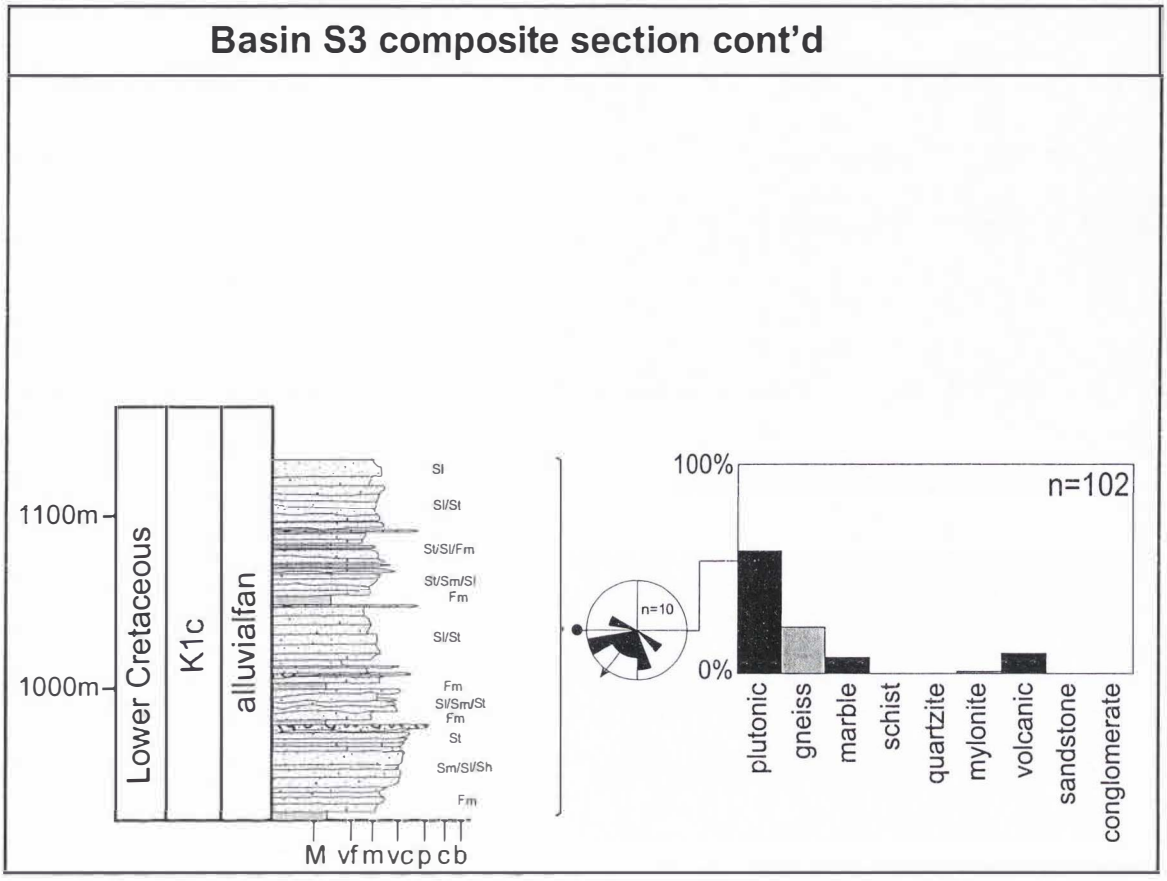

Fig. 23 cont'd: Basin S3 composite section.

and rock-avalanche deposits, because they are completely encased in the K1b strata, and exhibit characteristics of being emplaced as coherent to semi-coherent units (Friedmann, 1997).

Although normal faults cut all of the units, K1a and K1b are more pervasively faulted and contain normal faults that cut only these units, and are consistent with south-southeast extension on the master detachment (Fig. 13).

The upper unit, K1c, is a well-organized, clast-supported conglomerate (Fig. 8). The unit is 900 m thick in this basin (Fig. 23). Beds are 1 m to several meters thick and are tabular to lenticular with erosive bases. Individual beds are organized into relatively tabular units on the order of a few meters to 10 m thick and that extend for at least hundreds of meters laterally. The conglomerate is interbedded with coarse sandstone beds that are decimeter to several meters thick and rare mudstone beds several cm to decimeters thick. Imbrication is abundant, as is cross-stratification and planer lamination in the sandstone. The section fines upward overall, but coarse conglomerate is seen even in the most distally exposed parts of the basin.

This unit has been interpreted as subaqueous channelized and sheetflood deposits based on the well-organized, clast-supported character. These deposits are interpreted to have formed in an alluvial fan system, based on the uniformly coarse conglomeratic nature of K1c and dominance of streamflow and sheetflood processes (Blair and McPherson, 1994).

Paleocurrent and Provenance Data. Paleocurrent data were collected aerially about the basin (fig. 14, 21). Average paleocurrent direction for combined K1a and K1b

is 214°. The paucity of imbricated clasts within K1a and K1b makes paleocurrent measurement for these units difficult. Well-imbricated conglomerate is abundant in K1c, and yields paleocurrents that average 187°. Stratigraphically, K1c paleocurrents show little variability, except in the upper 200 m of the section where sand content increases (Fig. 23).

Areally distributed clast count data clearly demonstrate the dominance of clasts derived from the footwall of the detachment (Fig. 15, 22). Granitoid plutonic clasts dominate, and foliated plutonic, conglomerate, and sandstone clasts are distributed uniformly. Volcanic clasts, usually rhyolite and rare basalt, are more concentrated on the western side of the basin (where volcanic rocks of K1a or older are still preserved). Stratigraphically, clast composition is fairly consistent with some exceptions (Fig. 23). First, gneiss clasts are common in K1c, but are not present in K1a or K1b (Fig. 15). Similarly, mylonite clasts are not observed in K1a or K1b, and are not seen in the lower part of K1c (Fig. 23). These mylonite clasts first appear at 850 m, and persist through the remaining stratigraphy. Finally, sandstone clasts, some of which may be recycled Lower Cretaceous clasts, decrease in abundance up section.

Basin S4

Basin S4 is the most easterly exposed Lower Cretaceous basin in the Daqing Shan (Fig. 19). It is located above the master Hohhot detachment fault, still a low-angle normal fault, but not within the main Hohhot metamorphic core complex. The eastern extent of the mylonitic front mapped in the Daqing Shan is located to the northwest of this basin in the lower plate (Fig. 3). Exposure in this area is limited by cover, which

prevents measurement of a complete section in this basin. Where measured, strata are tilted with beds dipping to the north, but the basin is cut by numerous normal faults. Exposure is limited to the range front. Maximum basin thickness is estimated at 2250 m from a cross-section using sparse stratal dips. The common occurrence of normal faults in the basin suggests that the actual basin thickness is thinner, probably similar to the thickness in Basin S3 ranging from 1200 m to 1500 m in thickness.

Sedimentology and Stratigraphy. Only lithostratigraphic member K1c is observed in this basin (Fig. 24). K1c is composed dominantly of well-organized, clast-supported conglomerate with tabular to lenticular beds with erosive-based bases (Fig. 8). Bedding thickness is 1 m to several meters thick. Individual beds are organized into relatively tabular units on the order of a few meters to 10 m thick. The conglomerate is interbedded with trough cross-stratified sandstone beds ranging from decimeters to meters in thickness and mud-to-siltstone beds that are several centimeters to decimeters thick. Imbrication is abundant, as is cross-stratification and planar lamination in the sandstone.

No monolithologic, brecciated, gravity-driven slide blocks were observed in this basin, though exposure is limited and slide blocks are less common in K1c than in K1b. The limited measured section at this locality is 333 m thick (Fig. 24).

The conglomerates are interpreted as subaqueous channelized and sheetflood deposits based on their well-organized, clast-supported character. These deposits are interpreted to have formed in an alluvial fan system, based on the uniformly coarse conglomeratic nature of K1c and dominance of streamflow and sheetflood deposits (Blair and McPherson, 1994).

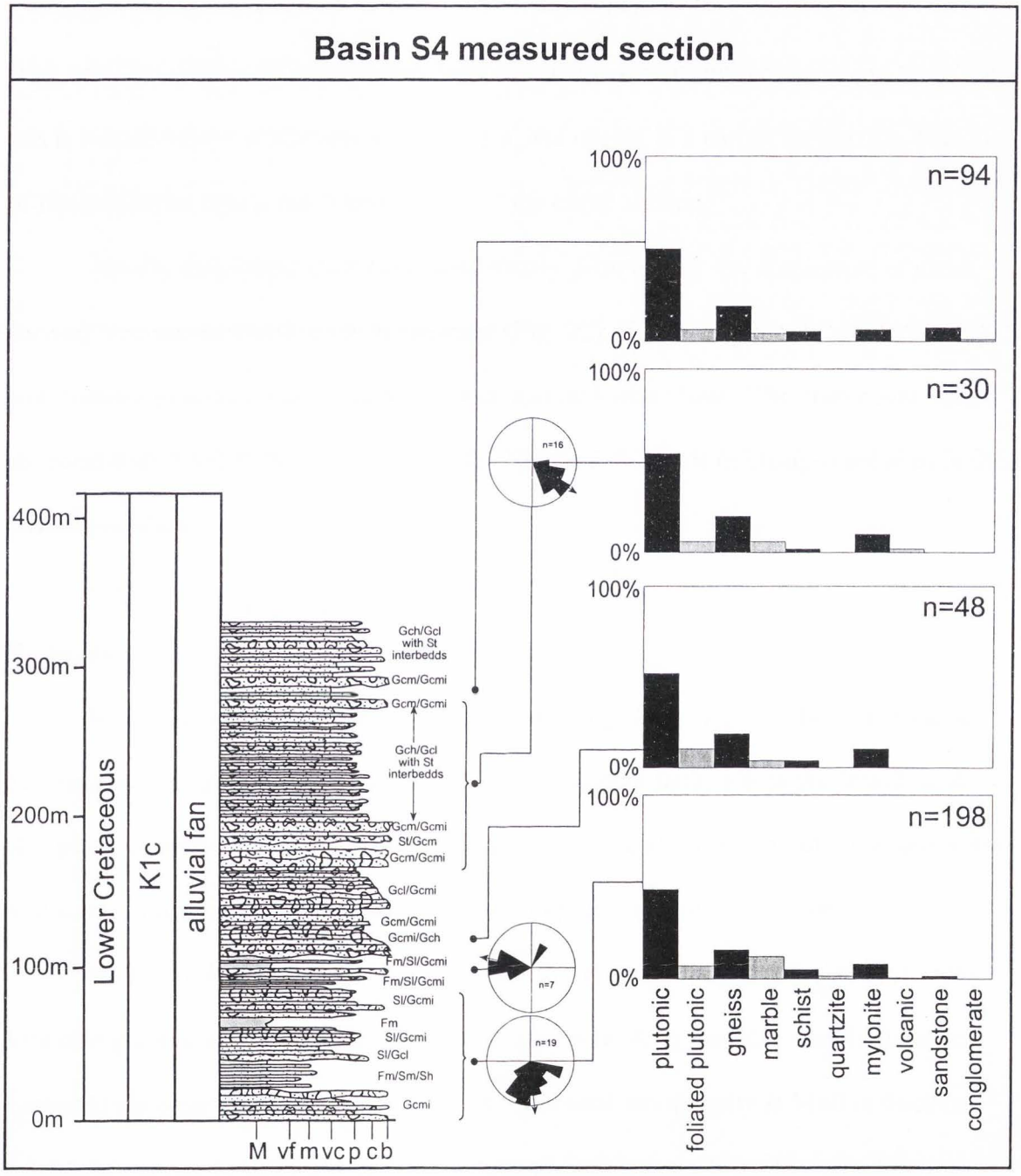

Fig. 24: Basin S4 section.

Paleocurrent and Provenance Data. Paleocurrent data were collected areally around the basin (Fig. 21). Well-imbricated clasts within K1c are abundant and yield an average paleocurrent direction of 159°. Some variability is seen vertically in the section (Fig. 24). At ~100 m into the section, west directed paleocurrent indicators are seen, but this is a small subset of the data for this basin, and occurs in a part of the section with lots of fine mudstone that is not representative of the entire section.

Areally distributed clast count data clearly demonstrate the dominance of clasts derived from the footwall of the detachment (Fig. 22). Granitoid plutonic are dominant, with foliated plutonic, gneiss, marble, schist, and mylonite clasts. The clast count data are consistent through the section (Fig. 24). No obvious trends or changes are seen in the provenance data.

Basin N1

Basin N1 is located southwest of Wuchuan city (Fig. 19). This basin is located above a folded segment of the master Hohhot detachment fault, where the detachment abruptly cuts northward into the Daqing Shan (Fig. 1). Extension magnitude at this point in the detachment is less than within the metamorphic core complex proper.

Sedimentology and Stratigraphy. Basin N1 is again divided into three informal lithostratigraphic units, but these units differ from K1a, K1b, and K1c seen in the other Lower Cretaceous basin in the Daqing Shan. The total stratigraphy is 1140 m thick in this basin and can be divided into three lithostratigraphic units (Fig. 25). The first unit is 130 m thick and rests on the detachment fault. This unit consists of clast-supported and

Fig. 25: Basin N1 stratigraphic section.

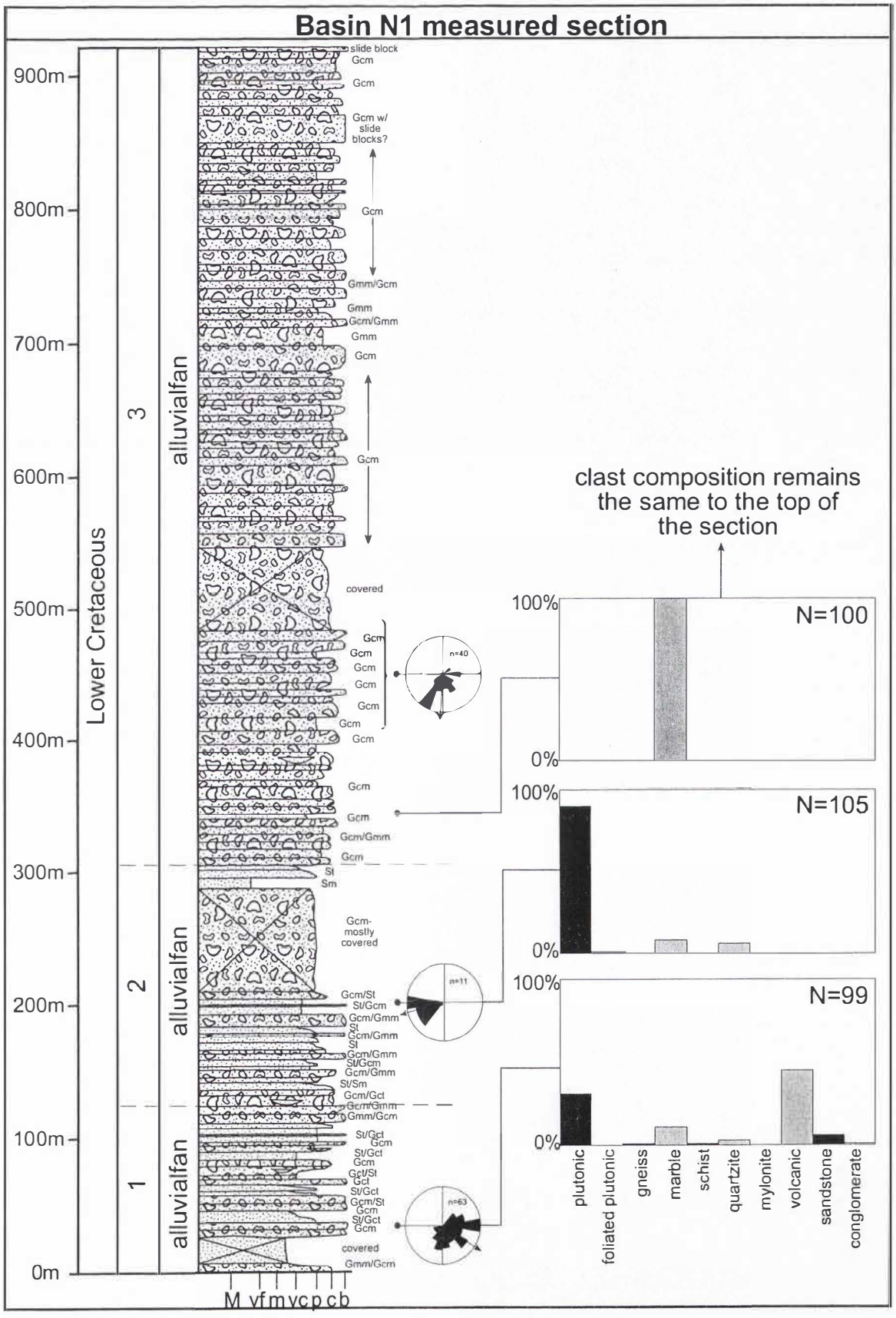
Basin N1 measured section
900m
800m
700m
600m
500m
400m
300m
200m
100m
0m
Lower Cretaceous
3
2
1
alluvialfan
alluvialfan
alluvialfan
slide block
Gcm
Gcm
Gcm w/ slide blocks?
Gcm
Gmm/Gcm
Gmm
Gcm/Gmm
Gmm
Gcm
Gcm
covered
Gcm
Gcm
Gcm
Gcm
Gcm
Gcm
Gcm
Gcm
Gcm/Gmm
Gcm
St
Sm
Gcm-mostly covered
Gcm/St
St/Gcm
Gcm/Gmm
St
Gcm/Gmm
St
Gcm/Gmm
St/Gcm
Gcm/Gmm
St/Sm
Gcm/Gct
Gcm/Gmm
Gmm/Gcm
St/Gct
Gcm
St/Gct
Gcm
Gct/St
Gct
St/Gct
Gcm/St
Gcm
St/Gct
Gcm
covered
Gmm/Gcm
M vf m vc p c b
n=40
n=11
n=63
clast composition remains the same to the top of the section
100%
0%
N=100
N=105
N=99
plutonic
foliated plutonic
gneiss
marble
schist
quartzite
mylonite
volcanic
sandstone
conglomerate

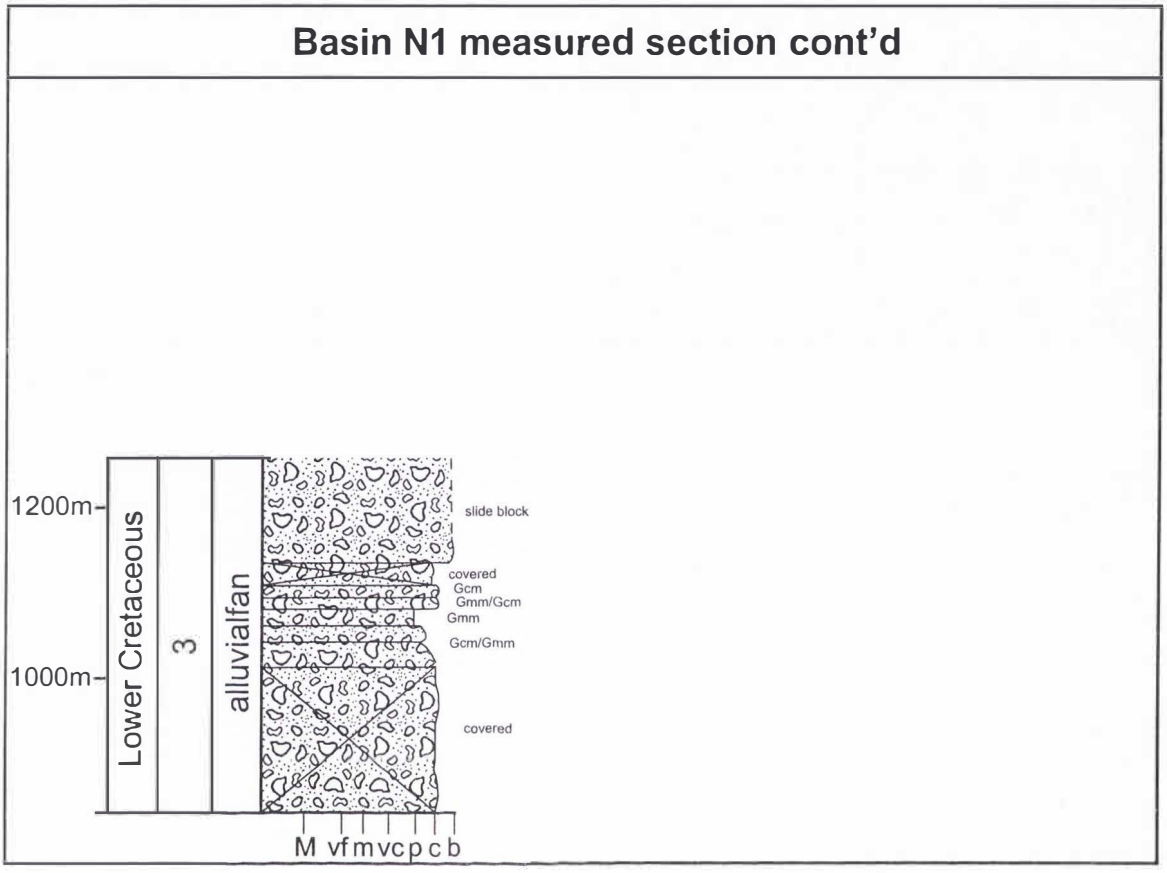

Fig. 25 cont'd: Basin N1 section.

lesser matrix-supported cobble to boulder conglomerate with boulders ranging in diameter from 86 cm to 197 cm (Fig. 26). Beds are lenticular and erosive-based, ranging from 80 cm to 2.5 m thick. The conglomerate is massive, but imbrication is common, and large-scale trough cross-stratification is seen in some of the beds. The matrix is red to maroon in color with very coarse sand and pebbles. Above the basal conglomerate, numerous broad, trough cross-stratified sandstone beds are interbedded with pebble to boulder, organized, clast-supported conglomerate. The sandstone beds display 20 cm to 30 cm upward fining packages from pebble to medium sand size. These deposits are interpreted to be subaqueous channelized and sheetflood deposits based on clast-support, lack of fine-grained material, imbrication and trough cross-stratification, and lenticular, erosive nature of the bedding. These deposits are interpreted to have formed in an alluvial fan system, based on the uniformly coarse conglomeratic nature and dominance of streamflow and sheetflood deposits (Blair and McPherson, 1994)

The second unit is 170 m thick (Fig. 25). The unit dominantly consists of well-imbricated, clast-supported cobbler to boulder conglomerate interbedded with trough-cross stratified sandstone (Fig. 27). The conglomerate beds are tabular to lenticular with erosive bases and range from 1 m to 3 m in thickness. The sandstone beds are 10 cm to 20 cm thick, fining upward packages that contain occasional cobbles and boulders. Maximum boulder diameter in this unit is 140 cm. Overall, this unit is finer than the underlying unit.

This unit is interpreted as dominantly subaqueous channelized and sheetflood deposits based on the presence of trough cross-stratified sandstone interbedded with

Fig, 26: Photographs of lowest unit in basin N1. This unit is clast-supported, pebble to boulder conglomerate. Large boulder in lower photo is basalt.

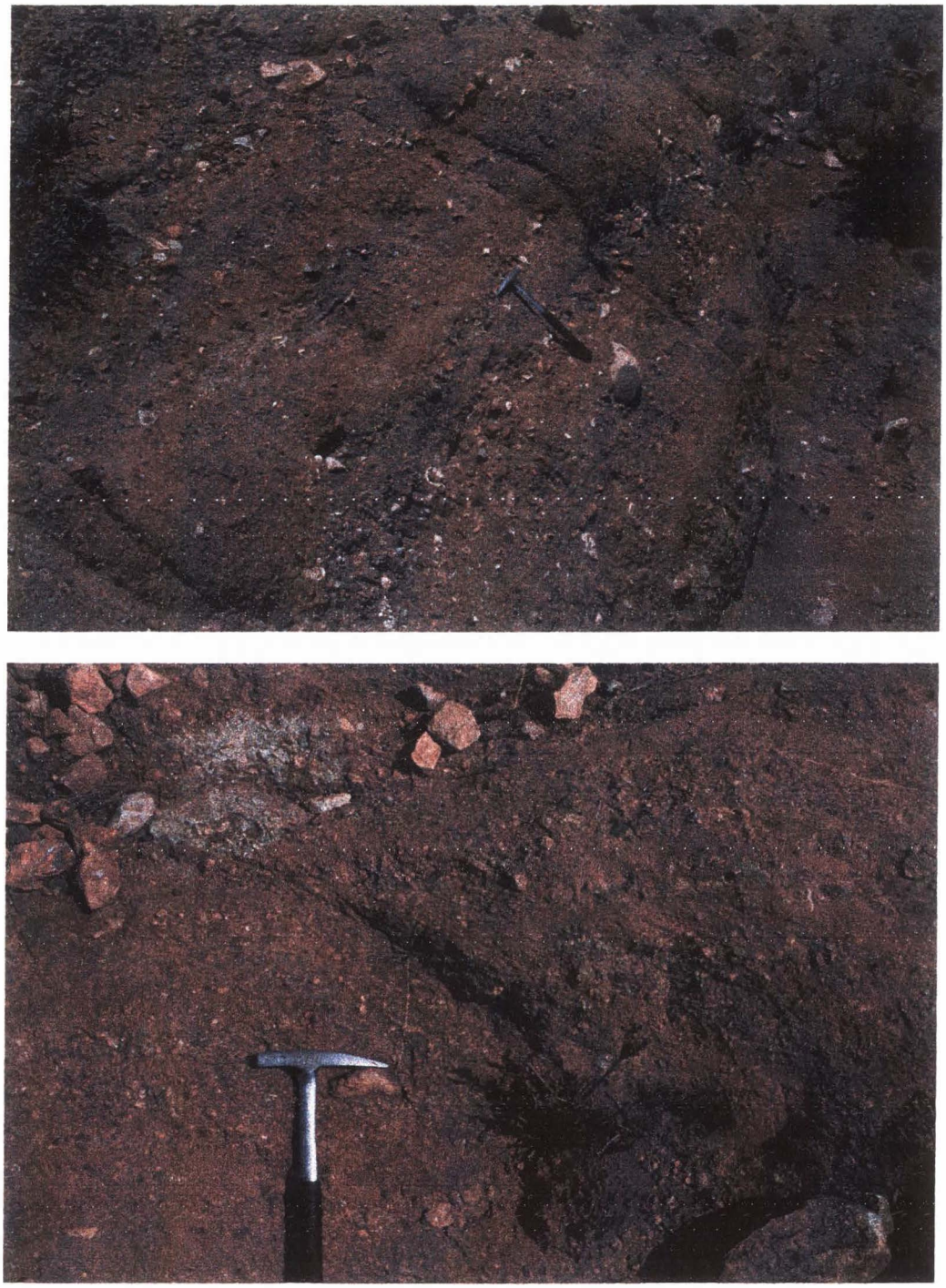

Fig. 27: Photographs of middle unit in basin N1. This unit is very coarse to pebble sand with pebble to boulder interbeds.

clast-supported conglomerate, and the lack of fine grain sediment. These deposits are interpreted to have formed in an alluvial fan system, based on the dominance of streamflow and sheetflood processes and the coarse nature of the deposits (Blair and McPherson, 1994). This unit and the lowest unit are consistent with units seen in the other Daqing Shan basins.

The third unit comprises the remaining stratigraphy in this basin (Fig. 25). The base of this unit is composed of poorly organized, yet predominantly clast-supported pebble-to-boulder conglomerate with a red, silty matrix (Fig. 28). The conglomerate, which consists of entirely of marble clasts, outcrops as 20 m to 40 m thick packages without well-defined bedding (Fig. 28). Clasts are generally angular and some of the boulders are fractured and injected with red matrix (Fig. 28). Higher in the section, the unit consists of boulder to cobble conglomerate with red, silty matrix, which remains clast-supported and poorly organized, but becomes locally well-imbricated and more organized in individual beds. Towards the top of the section, the matrix of the conglomerate was gradationally replaced with calcite-rich cement, resulting in resistant packages (Fig. 29). A high percentage of sand to pebble, marble derived clasts due to transport induced brecciation and cataclasis may contribute to the high calcite content in the matrix (Friedmann, 1997). Clast size in these conglomerate packages ranges from pebble to >2 m. Recrystalization of the matrix with calcite is common from this point upward in the stratigraphy, but red matrix is still present in the conglomerate when beds are traced laterally. Also at this point in the section, large monolithologic blocks contained in the conglomerate become common, some greater than >30 m in diameter

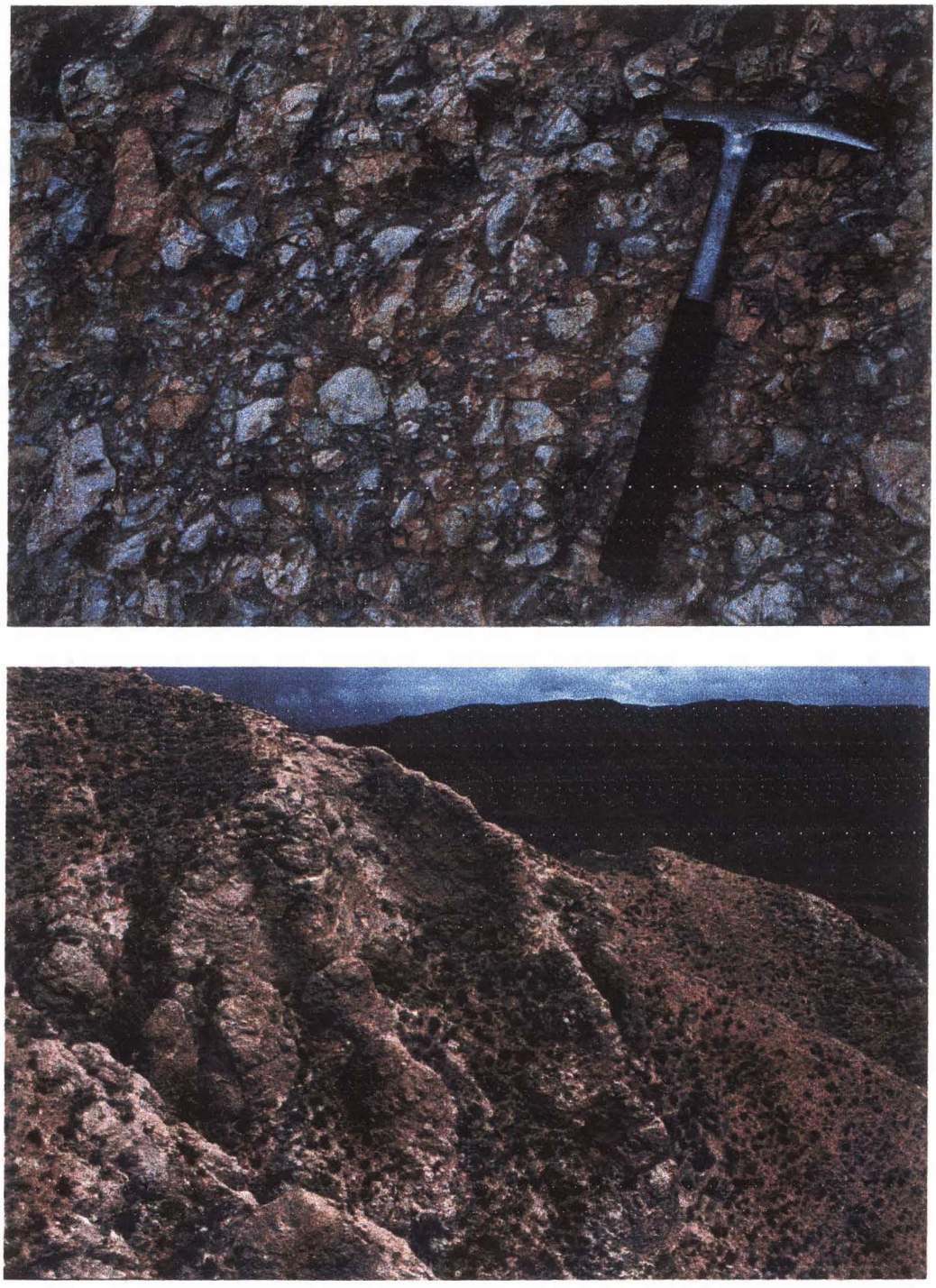

Fig. 28: Photographs of upper unit in basin N1. Top photo is clast-supported, matrix-rich, angular, pebble to cobble conglomerate. Bottom photo shows thick package of this conglomerate.

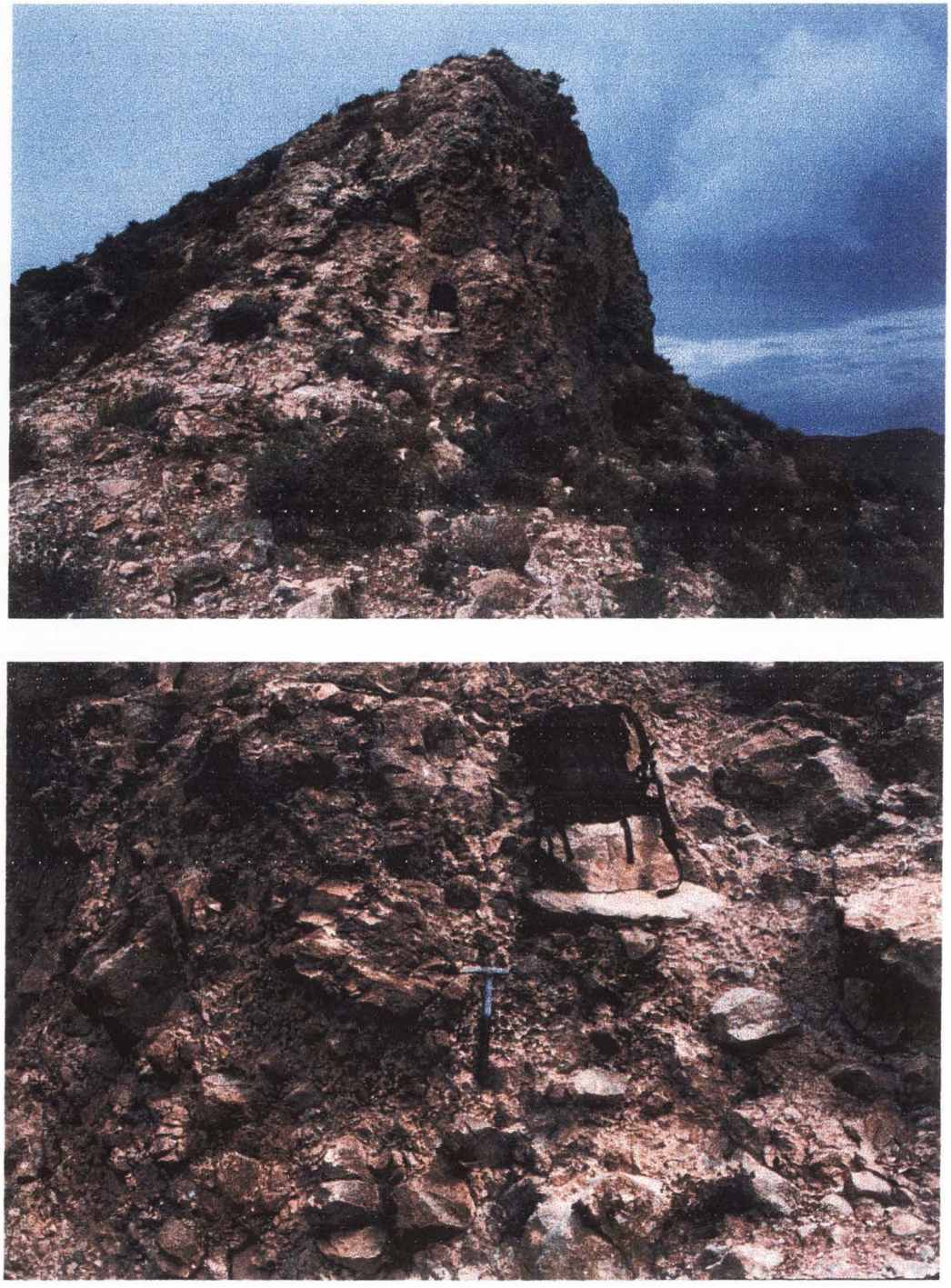

Fig. 29: Top photo shows resistant pod of upper unit in basin N1. Lower photo is a closer shot of the pod (backpack is in same location on both photographs) showing the individual clasts within the bed.

(Fig. 30). These blocks are generally fractured and intensely brecciated. A monolithic block of marble that is 100-200 m thick caps the section.

This unit is interpreted as debris flow deposits, hyperconcentrated flow deposits, and rock-avalanche deposits with interbedded gravity-driven slide blocks. The debris flow interpretation is based on the presence of unorganized, matrix-rich conglomerate, some of which is well-imbricated, yet retains a significant amount of fine-grained matrix. The megabreccia units are interpreted as rock-avalanche deposits based on the coarse, angular, monolithologic clasts that are unorganized and both clast and matrix supported (Friedmann, 1997). Bedding is often difficult to see with in each package, but packages may represent individual flows or several amalgamated rock-avalanches. Large blocks are interpreted as gravity-driven slide blocks because they are completely contained within the Lower Cretaceous conglomerate and exhibit characteristics of being emplaced as coherent to semi-coherent units (Friedmann, 1997).

Paleocurrent and Provenance Data. Paleocurrent data were collected areally in this basin (Fig. 21). Well-imbricated clasts yield an average paleocurrent direction of 154°. Stratigraphically, paleocurrent data were difficult to obtain as well-imbricated conglomerate is rare due to the dominance of debris flow deposition (Fig. 25). Near the base of the section, southeastern paleocurrents are dominant with a significant east-directed component. At around 200 m, paleocurrents make a dramatic swing, becoming west directed. Between 410 m and 475 m, average paleocurrent direction from imbricated clasts is nearly south.

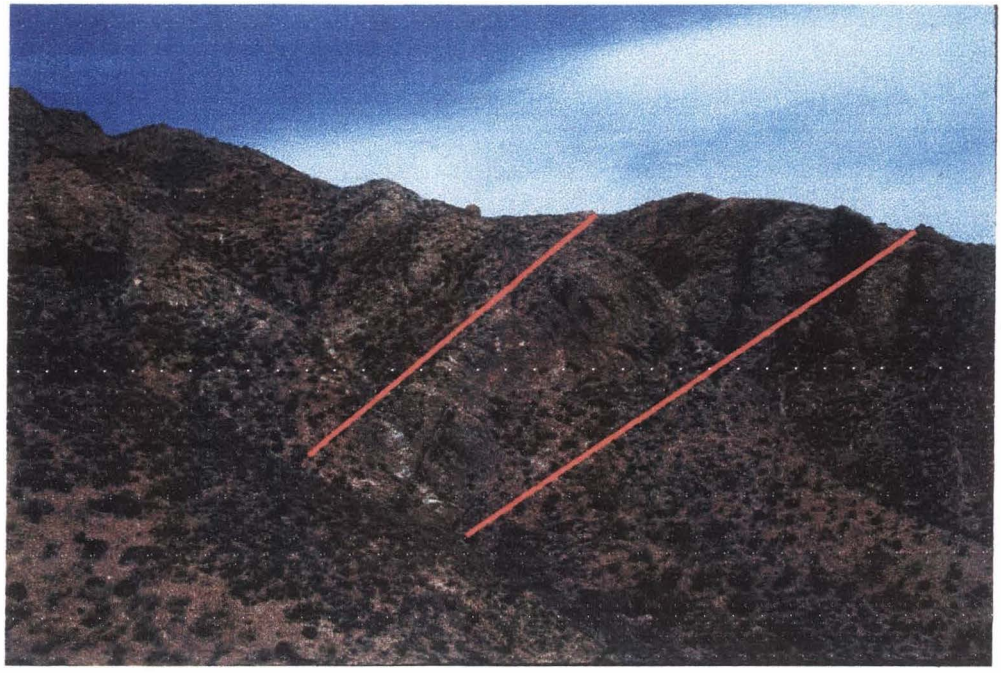

Fig. 31: Gravity-driven slide block near top of section in basin N1. Red lines mark top and bottom of block which is encased in red, Lower Cretaceous conglomerate.

Areally distributed clast-count data clearly demonstrate the dominance of clasts derived from the footwall of the detachment (Fig. 22). Granitoid plutonic clasts are dominant, with foliated plutonic, quartzite, and conglomerate representing minor percentages of the clast composition. Marble content decreases from west to east, and volcanic clasts (rhyolite and basalt ranging from pebbles to boulders) compose ~25% of the basin overall clast composition (Fig. 22). Stratigraphically, clast composition changes dramatically (Fig. 25). The base of the section contains high percentages (57%) of volcanic clasts, both rhyolite and large, well-rounded boulders (1 m to 2 m) of basalt. A large basalt flow is located near the base of the section and is the likely source of these boulders. Granitoid plutonic clasts are common and are accompanied by lesser quantities of marble, sandstone, quartzite, schist, and gneiss clasts. Up section, volcanic, gneiss, schist, and sandstone clasts are not seen, and granitoid plutonic clasts become dominant. The most dramatic change in clast composition occurs at a ~305 m where only marble, which is commonly silicified, is present within the conglomerate. Marble content remains constant through the remainder of the section.

Discussion

Tectonic Evolution of Lower Cretaceous Basins

The data from the supradetachment basins allow us to better understand the coupled structural and stratigraphic evolution of this extensional system. Comparison of controls emplaced by distinct basin settings highlights the more influential factors to supradetachment basin geometry.

The data from basin N2 and basin S3 allow us to establish a model for these basins that relates to the evolution of the Hohhot metamorphic core complex (Fig. 16). This model can be broadly subdivided into two phases, based on the contrasting depositional and deformational styles in K1a-b and K1c (Fig. 16). The bulk of the supradetachment basin fill consists of K1c, suggesting longer-lived basins later in the evolution of the system.

Units K1a and K1b were deposited by debris-flow and mass-wasting processes, with the onset of extension and concomitant creation of topographic relief and isolated basins. Volcanic flows were interbedded with these deposits as extension began, but ceased by the K1a-K1b boundary. Syn-depositional normal faulting consistent with extension direction deformed and dissected the basin. Further evidence of dissection consists of angular unconformities and abundant reworked volcaniclastic detritus in the sandstone and conglomerate (Fig. 11, 17). Intrabasinal breakup of these basins during K1a and K1b sedimentation, as well as the creation of intrabasinal graben (Fig. 13) resulted in variable paleocurrent directions, and local changes in stratigraphy and provenance (Fig. 14 and 15).

K1c is very consistent areally and stratigraphically, dominated by waterlain sheetflood and streamflow processes in an alluvial fan setting with additional rock-avalanche deposits and gravity-driven slide blocks. Paleocurrent indicators are uniformly south-directed in both basins indicating transverse transport of sediment away from the detachment breakaway. Gneiss clasts are common in K1c, but do not appear in K1a or K1b.

Data from the Lower Cretaceous sedimentary rocks suggests that the basins on both flanks of the Daqing Shan antiform were previously contiguous during deposition of K1a, K1b and the lower portion of K1c (Fig. 16). Both basins exhibit K1a-K1b strata of similar thickness that were deposited by debris flow and rock-avalanche processes. Units K1a and K1b are overlain by K1c sediment that was deposited by waterlain sheetflood and streamflow deposits in an alluvial fan setting. Mean transport direction in K1c summed for both basins is 187°, despite the presence of the current topographically-high metamorphic core complex that would have inhibited south-directed flow. Clast types in K1a, K1b, and the lower part of K1c are also similar. Granitoid plutonic clasts dominate and clasts of reworked Lower Cretaceous conglomerate and sandstone clasts are present. Also, gneiss clasts do not appear in either basin until K1c is deposited. Volcanic rocks are present along the west side of the basins and $^{40}Ar/^{39}Ar$ dates in basin N2 coincide with the age of movement on the master Hohhot detachment underlying basin S3 (Davis et al., 2002).

The appearance of higher-grade gneiss and mylonitic clasts high in the section suggests progressive unroofing of deeper crustal material as extension and uplift of the lower plate continued. The absence of such clasts in the northern basin implies that the northern basin had stopped receiving sediment by the time those clast types were exposed in the source terrane. The apparent shorter-lived deposition on the northern flank, supported by the much thinner K1c deposit in basin N2, is interpreted to record the uplift of the Daqing Shan antiform during unroofing of the metamorphic core complex. Uplift of the metamorphic core resulted in, not only deactivation of the folded northern splays

of the Hohhot detachment, but also resulted in cessation of sedimentation in basin N2. Following uplift of the Daqing Shan antiform, extension was accommodated by propagation of a new detachment splay on the southern flank of the Daqing Shan antiform (Davis et al., 2002) that, created additional accommodation space in basin S3, and resulted in the thicker K1c deposit.

Basin S2 exhibits many similarities to basin S3. The basin consists of predominantly coarse conglomerate deposited by subaqueous channelized and sheetflood deposits in an alluvial fan setting. Paleocurrents are south-directed, indicating transport of sediment transversely away from the detachment fault (Fig. 21). Clast composition in basin S2 is similar to basin S3, but marble is much more common (Fig. 22). Sediment sources elsewhere in the Daqing Shan tend to be very localized, but the numerous brecciated, slide blocks composed of Paleozoic marble present in the strata may influence high marble content in this basin. We cannot determine if basin S2 and basin S3 were connected during their evolution, but were most likely deposited in separate corrugations of the detachment fault. The basins may be connected at some distance beyond where Lower Cretaceous rocks are exposed at the surface. If more distal exposure of these basins was available, the Daqing Shan basins may be found similar to the Esmarelda basin of Nevada, where sediments above the bounding detachment fault are deposited into a very broad, shallow lake, distal from the detachment breakaway (Diamond and Ingersoll, 2002; Stewart and Diamond, 1990).

The early history of basin S4 is not discernible because the only exposed unit is K1c. This unit is identical to the K1c seen in other basins. Paleocurrent directions are

south-directed indicating transverse transport of sediment away from the detachment. Clast composition in basin S4 is similar to other Lower Cretaceous basins, but mylonite content is much higher in this basin indicating a western source terrane where the mylonitic front of the metamorphic core complex is exposed. It should be noted that sedimentary processes and provenance in this basin are very similar to that in the basins further west, though the magnitude of extension is less.

Extension at this point in the detachment was not as great as in the basins directly adjacent to the Hohhot metamorphic core complex, but the resulting basin geometry is identical to the other K1c supradetachment basins described. The basin is bounded by a low-angle, corrugated normal fault that accommodated significant, rapid extension. With this extension, the lower plate was unloaded, triggering an isostatic response in the footwall. Uplift of these rocks minimized proximal accommodation space, promoting distal deposition of coarse sediment in an alluvial fan setting.

Basin S1 formed above a major low-angle fault, but this normal fault system is within the hanging wall of the Hohhot detachment fault. Coarse conglomerate was shed into the basin by alluvial fans that prograded into a shallow lacustrine environment. Paleocurrent indicators west of the lacustrine interval show southeast-directed flow into the lake. East of the lacustrine interval, paleocurrent directions are southwest directed again suggesting progradation into the lake.

Basin N1 differs from the other Lower Cretaceous basins in the Daqing Shan. Basin N1 does not contain the same lithologic members, K1a, K1b, and K1c, described in the other basins, and sedimentation in this basin is dominated by debris flow and rock-

avalanche deposition throughout the section. The upper portion of the section contains numerous monolithologic, brecciated, gravity-driven slide blocks that are hundreds of meters in diameter. Paleocurrent directions average near south, but significant east-west flow indicators are seen low in the section. Clast composition low in the stratigraphy is similar to that in other basins in this study, though they are high in volcanic clast content. Higher, the clast composition is nearly 100% marble, which persists through the top of the section.

Although Basin N1 displays some differences in sedimentary style when compared to the other Daqing Shan basins, it probably shares a similar history. The basin is thin (<1200 m), located above a low-angle normal fault, and dominated by debris flow and rock-avalanche deposits that were transported transversely away from the detachment. From these data, we cannot infer a similar period of hanging wall break up as seen in the other supradetachment basins, but the section studied strongly resembles a supradetachment basin based on the afore mentioned sedimentary characteristics.

The large presence of rock-avalanche and megabreccia deposits in basin N1 may be due to the characteristics of the source area. Generally, rock-avalanche source regions have three main requirements: slopes in excess of 25°, vertical falls in excess of 150 m, and a highly fractured source terrane (Friedmann, 1997; Keefer, 1984). Though the basin-bounding fault is low-angle, it may have exceeded 25° during the evolution of the basin, and high topography is common in regions that have experienced isostatic uplift of the lower plate with dramatic extension. Also, detachment faults commonly have breccia layers that form due to shear stress along the fault surface during tectonic transport

(Davis and Lister, 1988; Friedmann, 1997). As the footwall was elevated and exposed to surficial processes, the brecciated layer would have provided excellent source of fractured material to the basin. Any one, or combination, of these processes may have been responsible for the intense amount of rock-avalanche and megabreccia material in this basin.

Many studies have proposed that corrugated geometry of detachment faults is primary (Davis and Lister, 1988; John, 1987; Spencer and Reynolds, 1991). The paleocurrent data from the Hohhot basins neither supports nor refutes this statement, but the isolation of these basins from other Lower Cretaceous basins in the Daqing Shan and the differences in provenance characteristics implies that corrugations are primary. These corrugations would have been a strong geomorphologic control on Cretaceous drainage patterns, and which are still the major through-going drainages present in the Daqing Shan.

Supradetachment Basin Systems

The most widely cited and applied model for sedimentation in supradetachment basins is that of Friedmann and Burbank (1995), which classify supradetachment basins as an end-member basin style in extensional continental settings opposite the better-known half-graben rift basin of Leeder and Gawthorpe (1987) (Table 1). Friedmann and Burbank (1995) describe supradetachment basins as those that form "above a low-angle normal fault system." More specifically, "the term also represents the end-member model presented [in Friedmann and Burbank, 1995]." These basins are thin, short-lived and are dominated by coarse, predominantly footwall-derived sediments delivered to the

basin by transverse drainages and often deposited by mass-wasting processes (Table 1). These basins generally are expected to lack either significant fine-grained, lacustrine deposits, or axial drainage systems, which are commonly found in half-graben basins (Leeder and Gawthorpe, 1987). Also, supradetachment basins tend to occur in back-arc regions where the crust has recently experienced dramatic thickening in rock that may be warmer and have had considerable radiogenic heat flow (Friedmann and Burbank, 1995). Most rifts occur in areas with cold normal crust lacking recent contractile tectonism (Friedmann and Burbank, 1995).

The Lower Cretaceous basins in the Daqing Shan all represent supradetachment basins though they are located in structurally distinct sub-settings. Our study basins may have formed within a variety of these settings and allow us to further understand how location within the detachment-metamorphic core complex system controls supradetachment basin geometry.

Basin S2, basin S3, and basin S4 were all formed in similar settings: they are in the upper plate of a metamorphic core complex that evolved during basin formation. The basins all display units from the Lower Cretaceous stratigraphy, best described in basin S3 (Fig. 25). Sediment in these basins was deposited directly above the Hohhot detachment, which rapidly accommodated high magnitudes of extension. The basin fill is thin and dominated by coarse conglomerate shed from the footwall by mass-wasting, sheetflood, and streamflow processes in an alluvial fan setting. Although exposure of Cretaceous rock is limited to within 5-6 km of the master detachment fault, coarse sediment is present everywhere in these basins, suggesting distal deposition of this

material. Rapid rates of footwall uplift relative to basin subsidence would exclude proximal accommodation space, promoting distal deposition of sediment. Basin S2, and basin S3 are located within the boundary of the Hohhot metamorphic core complex, an excellent indicator of the large amount of extension accommodated by the Hohhot detachment. Basin S4 is located east of the mylonitic front, which marks the edge of the metamorphic core complex. Though the amount of extension was less at this point in the detachment, the rates were probably comparable, and the detachment bounding this basin is low-angle and corrugated. These factors suggest a similar mechanism for proximal exclusion of sediment in this basin, and signify the importance of extension rate and fault geometry to supradetachment basin formation. Several studies have documented supradetachment basins of this type without the presence of an exposed mylonitic metamorphic core (Friedmann and Burbank, 1995; Diamond and Ingersoll, 2002; Miller and John, 1988, 1999; Stewart and Diamond, 1990).

Basin N2 is preserved in an interesting structural setting not generally observed in other metamorphic core complexes. Doming of the metamorphic core complex kinematically deactivated the detachment on this flank of the metamorphic core complex leading to the cessation of syn-extensional sedimentation. The geometry and depositional style of this basin clearly establish that this is a supradetachment basin, demonstrating that supradetachment basin geometry may form early during basin formation and does not require an exhumed metamorphic core complex or mid-crustal dome.

Basins located in the structural setting of basin N2 may have existed in other highly-extended regions of the world, but may not have been preserved, or are covered by

later sedimentation. In the Central Mojave metamorphic core complex, syn-extensional strata of the Pickhandle Formation are mapped overlying mylonitized footwall rocks of the metamorphic core (Fillmore et al., 1994; Fillmore and Walker, 1996). The sedimentary rocks of this formation are suggested to have formed in a basin adjacent to the detachment breakaway, but are not preserved in this adjacent locality (Fillmore et al., 1994; Fillmore and Walker, 1996). Basin N2 is provides an example of another structural setting for basin development within detachment metamorphic core complex settings that seems to be rarely preserved.

The intra-hanging wall setting of basin S1 is quite different than that of basins S2, S3, S4, which form directly above the detachment fault. However, many characteristics of a supradetachment basin are still present that clearly distinguish it from a typical rift. The basin is both bounded by a low-angle normal fault and underlain by the master Hohhot detachment. The basin is thin and dominated by coarse, footwall-derived conglomerate that was deposited dominantly by streamflow and sheetflood processes of an alluvial fan system, and displays predominantly transverse paleocurrents. The major difference this basin exhibits is the presence of a centrally located lacustrine interval. Extension magnitude in this basin may have been less and at a slower rate, which would have resulted in more basin subsidence, and made it possible for the lacustrine interval to form. This lacustrine interval is accompanied by variable paleocurrent patterns from alluvial fan progradation into the lake and possibly a minor axial component. If a large shallow lake was present south of the Daqing Shan, the lacustrine interval preserved in

basin S1 may be a factor of its southerly location, and not due to specific controls such as rate footwall uplift or rate of basin subsidence.

Basin N1 is located in similar structural setting as basin N2. Both basins are located above a synformally folded detachment fault that has experienced doming of the lower plate to the south, but the basin stratigraphy is different. The stratigraphic thickness is greater than in basin N2, and the majority of the basin fill was deposited by debris flow processes as seen in K1a and K1b, but lacking a K1c waterlain unit. Doming of the detachment occurred as the upper plate was unloaded, but the extension magnitude was not great enough to exhume deep crustal material as in the Hohhot metamorphic core complex. Therefore, we again see a basin exhibiting supradetachment basin characteristics early in the basin history.

All of the Lower Cretaceous basins described in the Daqing Shan exhibit supradetachment basin characteristics (Friedmann and Burbank, 1995), regardless of location within the detachment-metamorphic core complex setting. The basins all formed above low-angle normal faults that accommodated rapid crustal extension in a region that has a complex tectonic history, including a period of significant contraction immediately prior to extension. These characteristics provide the conditions necessary to exclude proximal accommodation space and promote distal deposition of coarse sediment.

Conclusions

- Nonmarine extensional basins associated with the Hohhot detachment in the Daqing Shan of Inner Mongolia, China, are end-member supradetachment basins

(Friedmann and Burbank, 1995 *sensu stricto*) that are characterized by a definite structural style, thin basin fill, and prominence of mass-wasting and alluvial fan deposition of footwall-derived, coarse sediment through transverse transport paths.

- Supradetachment basins that form above the lower plate metamorphic dome evolve from being integrated early in the history of the detachment to separate as metamorphic core complex is exhumed and dissects the formerly contiguous basins. Accordingly, the basins that form above the youngest detachment splay are longer-lived as accommodation space is created by continued extension. Basins preserved in the synformal keel north of the structural culmination, do not continue to receive sediment because folding results in inactivation of their kinematically-linked detachment, and thus cessation in creation of accommodation space.
- Depositional environment, depositional processes, lithology, and transport patterns in the Daqing Shan supradetachment basins have little variation, but sediment sources are local and poorly mixed.
- Supradetachment basins associated with detachment faulting in the Daqing Shan are of the style described by Friedmann and Burbank (1995) regardless of the magnitude of extension by the time of K1c deposition. Metamorphic core complex exhumation is not a necessary requirement for end-member supradetachment basin geometry.

- Intra-hanging wall basins display Friedmann and Burbank (1995) characteristics. They are controlled largely by the detachment and metamorphic core complex sediment supply, not local upper plate sources.

CHAPTER IV

CONCLUSIONS

Nonmarine extensional basins associated with the Hohhot detachment in the Daqing Shan of Inner Mongolia, China, are end-member supradetachment basins (Friedmann and Burbank, 1995 *sensu stricto*) that are characterized by a definite structural style, thin basin fill, and prominence of mass-wasting and alluvial fan deposition of footwall-derived, coarse sediment through transverse transport paths. These supradetachment basins associated with detachment faulting in the Daqing Shan are of the style described by Friedmann and Burbank (1995) regardless of the magnitude of extension by the time of K1c deposition. Metamorphic core complex exhumation is not a necessary requirement for end-member supradetachment basin geometry.

The supradetachment basins that form above the lower plate metamorphic dome evolve from being integrated early in the history of the detachment to separate as metamorphic core complex is exhumed and dissects the formerly contiguous basins. Accordingly, the basins that form above the youngest detachment splay are longer-lived as accommodation space is created by continued extension. Basins preserved in the synformal keel north of the structural culmination, do not continue to receive sediment because folding results in inactivation of their kinematically-linked detachment, and thus cessation in creation of accommodation space.

Intra-hanging wall basins also display Friedmann and Burbank (1995) characteristics. They are controlled largely by the detachment and metamorphic core complex sediment supply, not local upper plate sources.

Overall, depositional environment, depositional processes, lithology, and transport patterns in the Daqing Shan supradetachment basins have little variation, but sediment sources are local and poorly mixed.

REFERENCES

Beratan, K.K., 1991, Miocene synextension sedimentation patterns, Whipple Mountains, southeastern California: Implications for the geometry of the Whipple detachment system: Jour. Geophys. Research, v. 96, no. B7, p. 12,425-12,442.

Beratan, K.K., and Nielson, J.E., 1996, Tests of detachment fault models using Miocene syntectonic strata, Colorado River extensional corridor, southeastern California and west-central Arizona, in: Beratan, K.K., ed. Reconstructing the structural history of Basin and Range extension using sedimentology and stratigraphy: Geol. Soc. America Special Paper 303, p. 171-182.

Blair, T.C., and McPherson, J.G., 1994, Alluvial fans and their natural distinction from rivers based on morphology, hydraulic processes, sedimentary processes, and facies assemblages, Jour. Sedimentary Research, v. A64, no., p. 450-489.

Darby, B.J., Davis, G.A., and Zheng, Y., 2002, Extensional collapse of a nonconventional fold-thrust belt, Daqing Shan, Inner Mongolia, China: *Am. Geophysical Union abstracts for Fall meeting*, p. 47.

Darby, B.J., Davis, G.A., and Zheng, Y., 2001, Structural evolution of the southwestern Daqing Shan, Yinshan belt, Inner Mongolia, China, In: Hendrix, M.S. and Davis, G.A. (eds.), Paleozoic and Mesozoic tectonic evolution of central and eastern Asia -- from continental assembly to intracontinental deformation: Geol. Soc. America Memoir 194, p. 119-214.

Davis, G.A., and Lister, G.S., 1988, Detachment faulting in continental extension; perspectives from the southwestern U.S. Cordillera, in: Sydney, Burchfiel, and Suppe, eds., Processes in Continental Lithospheric Deformation, Geol. Soc. America Special Paper 218, p. 133-160.

Davis, G. A., Cong, W., Zheng, Y. D., Zhang, J. J., Zhang, C. H., and Gehrels, G. E., 1998, The enigmatic Yinshan fold-and-thrust belt of northern China: new views on its intraplate contractional styles: Geology, v. 26, no. 1, p. 43-46.

Davis, G.A., Darby, B.J., Zheng, Y.D., and Spell, T.L., 2002, Geometric and temporal evolution of an extensional detachment fault, Hohhot metamorphic core complex, Inner Mongolia, China: Geology, v. 30, no. 11, p. 1003-1006.

Davis, G.A., Zheng, Y.D., Cong, W., Darby, B.J., Zhang, C.H., and Geherls, G.E., 2001, Mesozoic tectonic evolution of the Yanshan fold and thrust belt, with emphasis on Hebei and Liaoning provinces, Northern China, in: Hendrix, M.S. and Davis, G.A. eds., Paleozoic and Mesozoic tectonic evolution of central and eastern Asia

– from continental assembly to intracontinental deformation: Geol. Soc. America Memoir 194, p. 171-197.

Diamond, D.S., and Ingersoll, R.V., 2002, Structural and sedimentologic evolution of a Miocene supradetachment basin, Silver Peak Range and adjacent areas, west-central Nevada: International Geology Review, v. 44, p. 588-623.

Dickinson, W.R., 1991, Tectonic setting of faulted Tertiary strata associated with the Catalina core complex in southern Arizona, Geol. Soc. America Special Paper 264, p. 1-106.

Dorsey, R.J., and Becker, U., 1995, Evolution of a large Miocene growth structure in the upper plate of the Whipple detachment fault, northeastern Whipple Mountains, California: Basin Research, v. 7, p. 151-163.

Dorsey, R.J., and Roberts, P., 1996, Evolution of the Miocene North Whipple basin in the Aubrey Hills, western Arizona, upper plate of the Whipple detachment fault, In: Beratan, K.K., ed., Reconstructing the structural history of Basin and Range extension using sedimentology and stratigraphy: Geol. Soc. America Special Paper 303, p. 127-146

Fedo, C.M., and Miller, J.M.G., 1992, Evolution of a Miocene half-graben basin, Colorado River extensional corridor, southeastern California: Geol. Soc. America Bulletin, v. 104, p. 481-493.

Fillmore, R.P., and Walker, J.D., 1996, Evolution of a supradetachment extensional basin: The Lower Pickhandle basin, central Mojave Desert, California: Geol. Soc. America Special Paper 303, p. 107-126.

Fillmore, R.P., Walker, J.D., Bartley, J.M., and Glazner, A.F., 1994, Development of three genetically related basins associated with detachment-style faulting: Predicted characteristics and an example from the central Mojave Desert, California: Geology, v. 22, p. 1087-1090.

Forshee, E.J., and Yin, A., 1995, Evolution of monolithological breccia deposits in supradetachment basins, Whipple Mountains, California: Basin Research, v. 7, 181-197.

Friedmann, S.J., 1997, Rock-avalanche elements of the Shadow Valley Basin, eastern Mojave Desert, California: Processes and problems: Jour. Sedimentary Research, v. 67, p. 792-804.

Friedmann, S.J., and Burbank, D.W., 1995, Rift basins and supradetachment basins: Intracontinental extensional end members: Basin Research, v. 7, p. 109-127.

Friedmann, S.J., Davis, G.A., and Fowler, T.K., 1996, Geometry, paleodrainage, and geologic rates from the Miocene Shadow Valley supradetachment basin, eastern Mojave Desert, California, in Beratan, K.K., ed., Reconstructing the structural history of Basin and Range extension using sedimentology and stratigraphy: Geol. Soc. America Special Paper 303, p. 85-105.

Ingersoll, R.V., 1990, Actualistic sandstone petrofacies: Discriminating modern and ancient source rocks: Geology, v. 18, p. 733-736.

Janecke, S., McIntosh, W., and Good, S., 1999, Testing models of rift basins: Structure and stratigraphy of an Eocene-Oligocene supradetachment basin, Muddy Creek half graben, south-west Montana: Basin Research, v. 12, p. 143-167.

Janecke, S.U., Carney, S.M., Perkins, M.E., Evans, J.C., Link, P.K., Oaks, Jr., R.Q., and Nash, B.P., in press, Late Miocene-Pliocene detachment faulting and Pliocene-recent Basin-and-Range extension inferred from dismembered rift basins of the Salt Lake Formation, southeast Idaho, in: Raynolds, R., and Flores, R., eds., Cenozoic systems of the Rocky Mountains: SEPM Special Publication.

John, B.E., 1987, Geometry and evolution of a mid-crustal extensional fault system: Chemehuevi Mountains, southeastern California, in Coward, Dewey, and Hancock, eds., Continental extensional Tectonics: Geol. Soc. London Special Publication 28, p. 313-335.

Keefer, D.K., 1984, Rock avalanches caused by earthquakes: source characteristic, Science, v. 223, p. 1288-1290.

Leeder, M.R., and Gawthorpe, R.L., 1987, Sedimentary models for extensional tilt block/half-graben basins, in Coward, Dewey, and Hancock, eds., Continental extensional Tectonics: Geol. Soc. London Special Publication 28, p. 139-152.

Lister, G.S., and Davis, G.A., 1989, The origin of metamorphic core complexes and detachment faults formed during Tertiary continental extension in the northern Colorado River region, U.S.A.: Jour. Structural Geology, v. 11, p. 65-94.

Miller, J.M.G., and John, B.E., 1988, Detached strata in a Tertiary low-angle normal fault terrane, southeastern California: A sedimentary unroofing, breaching, and continued slip: Geology, v. 16, p. 645-649.

Miller, J.M.G., and John, B.E., 1999, Sedimentation patterns support low-angle normal faulting, southeastern California and western Arizona: Geol. Soc. America Bulletin, v. 111, no. 9, p. 1350-1370.

Nielson, J.E., and Beratan, K.K., 1995, Stratigraphic and structural synthesis of a Miocene extensional terrane, southeast California and west-central Arizona: Geol. Soc. America Bulletin, v. 107, no. 2, p. 241-252.

Ritts, B.D., Darby, B.J., and Cope, T., 2001, Early Jurassic extensional deformation and Basin Formation in the Daqing Shan segment of the Yinshan belt, northern North China Block, Inner Mongolia: Tectonophysics, v. 339, no. 3-4, p. 239-258.

Spencer, J.E., and Reynolds, S.J., 1991, Tectonics of mid-Tertiary extension along a transect through west-central Arizona: Tectonics, v. 10, no. 6, p. 1204-1221.

Stewart, J.H., and Diamond, D.S., 1990, Changing patterns of extensional tectonics; overprinting of the basin of the middle and upper Miocene Esmeralda Formation in western Nevada by younger structural basins, in: Wernicke, B.P., ed., Basin and Range extensional tectonics near the latitude of Las Vegas, Nevada: Boulder, Colorado, Geol. Soc. America Memoir 176, p. 447-476.

Webb, L.E., Graham, S.A., Johnson, C.L., Badarch, G., Hendrix, M.S., 1999, Occurrence, age, and implications of the Yagan-Onch Hayrhan metamorphic core complex, southern Mongolia: Geology, v. 27, no.2, p. 143-146.

Yarnold, J.C., 1994, Tertiary sedimentary rocks associated with the Harcuvar core complex in Arizona (U.S.A.): Insights into paleogeographic evolution during displacement along a major detachment fault system: Sedimentary Geology, v. 89, p. 43-63.

APPENDIX

APPENDIX EXPLANATION

This appendix presents the field data collected in this study in table format. Station refers to the numerical representation of a geographical location where data was collected. Latitude and longitude refer to the coordinates of that station given in decimal minutes. Strike and Dip values describe the attitude of bedding at that station in degrees. Imbrication is the corrected measurement of the plane of imbrication in degrees. Paleocurrent roses presented in the thesis were created by plotting poles to these planes. Trough Axis refers to corrected trough axis in degrees, but may also represent data from imbrication that is corrected and recorded as a line instead of a plane. When used for paleocurrent roses they were plotted as lines or poles. Clast Type refers to the type of clast recorded in a clast count. Clast Count refers to the frequency of a particular clast type in a clast count. Max Clasts refers to the maximum long axes of the largest clasts found at a particular station.

In the Clast Count Data, the table is arranged by basin and shows the frequency of clast types for each station. These clast types were grouped from the raw data to present a standardized assemblage that is consistent for all of the basins. The data is provided in the raw groupings as well as by percentages for each clast count.

Station	Unit	Latitude		Longitude		Strike	Dip	Imbrication		Trough Axis		Clast Type	Clast Count	max clasts
Basin N2														
1														
2	K2	41	1.497	111	43.521									
3	K2	41	1.608	111	43.522									
4	K2	41	1.769	111	43.687									
5	K2	41	1.825	111	43.747									
6	K2?K3	41	1.982	111	43.484	22	53W	291	55N			plutonic	40	
								316	61E			gneiss	12	
								329	53E			foliated plutonic	19	
								324	48E			schist	1	
								298	27N			volcanic	2	
								301	22N			conglomerate	1	
								330	49E			weathered plutonic	15	
								313	55N			white marble	8	
								314	44N			porphyritic plutonic	1	
								312	51N			green plutonic	1	
								332	55E					
								303	40N					
								291	28N					
								328	30E					
								338	54E					
								321	50E					
								320	30E					
								318	27E					
								297	33N					
								323	42E					
								310	29N					
								332	67E					
								329.2	45.4E					
7	K3	41	2.093	111	41.584									
8	Basemen	41	1.81	111	42.059									
9	K2/K3?	41	1.953	111	42.097							plutonic	52	34
								222.2	65.1W			green plutonic	4	29

												schist	6	37
												maroon plutonic	35	34
												marble	2	49
												intermediate plutonic	2	27
												gneiss	1	36
														38
10	K2/K3?	41	1.994	111	42.082	74	53N							
11	K2/K3	41	2.013	111	42.079									
12	K3	41	2.069	111	42.064			236	47N			plutonic	53	36
								238.2	51.1N			gneiss	5	25
								263.2	34.7N			maroon plutonic	21	32
								267.1	31.1N			foliated plutonic	8	25
								235.1	15.1N			marble	1	43
								281.5	25.4N			conglomerate	1	29
								281.1	27.6N			weathered plutonic	1	
								261.1	35.4N			schist	3	
								286.1	32.6N			green ss	3	
								217.4	62.4W			green plutonic	3	
								220.7	68W			phyllite	1	
								213.3	34.4W					
								212.5	36.6W					
								241.7	61.3N					
								227.9	55.2N					
								181.5	86.9W					
								224.1	62.5W					
								225.2	74.4W					
								216.7	77.9W					
								200	65W					
								205.4	61.1W					
								210.7	70.1W					
								220.3	66W					
13	K2	41	2.086	111	42.007	69	32NV	12.4	37.1E					43
						57	40NV	356.6	38.1E					39
								345.9	49E					75

								330.3	45.2E					49
														46
14	K2/K3	41	2.114	111	42.026	63	44N	344.7	26.4E					32
								358.1	21E					29
								6.1	21.8E					39
														30
														28
														47
														52
														34
15	K2/K3	41	2.134	111	42.032									
16	K2/K3	41	2.181	111	41.982	46	36N	340.1	58.3E			plutonic	43	55
								332.4	74.6E			maroon plutonic	17	33
								341	57.6E			foliated plutonic	12	44
								345.3	65.1E			green plutonic	8	39
								329.4	49.4E			intermediate plutonic	1	33
								320.5	57.9E			schist	3	31
								315.9	43.3E			quartzite	1	27
								326.2	54.1E			gneiss	9	36
												weathered plutonic	1	45
														41
17	K3	41	2.2	111	41.985	46	65N	12.9	37.4E					
								354.9	39.2E					
								338.5	35.1E					
								354.5	32E					
								356.4	37.8E					
								1.3	36E					
								20.5	47.7E					
								4.5	38.4E					
18	K3	41	2.266	111	42.01									
19		41	2.34	111	41.993									
20		41	2.347	111	41.907									
21		41	2.374	111	41.943									
22	K2?	41	2.384	111	41.965	78	40N					plutonic	81	

												maroon plutonic	10	
												schist	1	
												weathered plutonic	4	
												ss	1	
												foliated plutonic	3	
23	K2/K3	41	2.419	111	41.977			265.1	33.8N			plutonic	43	
								295.1	45.1N			gneiss	18	
								312	43.4N			maroon plutonic	16	
								323.2	36.7E			foliated plutonic	9	
								319.7	40.5E			schist	12	
												weathered plutonic	2	
												red ss	1	
24	K3	41	2.477	111	41.981	30	28N	262	34.2N					48
								270.5	32.7N					36
								261.2	28.1N					31
								238.1	40.8N					
								331.2	27.2N					
								317.5	42.7N					
								350.9	32E					
25	K3	41	2.512	111	41.984	73	58S	274.4	55.7N					33
								290.1	61.3N					44
								291.5	60.5N					29
								292.5	64.3N					32
														27
26		41	2.546	111	41.977									
27	K3?	41	2.579	111	42.022							plutonic	50	
												weathered green schi	16	
												weathered plutonic	8	
												maroon plutonic	20	
												gneiss	3	
												foliated plutonic	4	
												schist	2	
28		41	2.608	111	42.016									

29	K3	41	2.753	111	42.049							plutonic	42	28
												foliated plutonic	12	26
												gneiss	15	29
												maroon plutonic	19	27
												intermediate plutonic	6	
												green plutonic	1	
												schist	6	
												phyllite	1	
												quartzite	1	
												marble	2	
30	K3	41	2.764	111	42.019				77.8W					
								219.9	61.2W					
								214.9	65.1W					
31	K3	41	2.778	111	42			235	89.2N					22
								267.8	88.3N					27
								323.7	89.6E					24
								328.2	87.2E					25
								308.3	77.9N					29
								310.5	84.9N					
								315.2	80.9E					
32	K3	41	2.792	111	41.968	36	80N							
33	detach	41	2.361	111	36.225									
34	K1/K2	41	2.613	111	36.351	34	28S	258	81N			plutonic	37	
								243	63N			rhyolite	16	
								251	80N			schist	3	
								223	71W			red ss	5	
												foliated plutonic	17	
												phyllite	9	
												quartzite	7	
												basalt	3	
												conglomerate	1	
												white marble	2	
35	K1/K2	41	3.267	111	38.09									
36	K3	41	3.381	111	38.028	165	17W	329	72E			volcanic	28	84

								336	65E			gneiss	11	68
								320	63E			plutonic	31	29
								345	71E			quartzite	12	34
								325	72E			marble	3	35
								271.5	15.6N			intermediate plutonic	1	
								286.4	33N			foliated plutonic	5	
								293.1	52.5N			weathered plutonic	2	
								298.7	41.1N			green plutonic	4	
								286.5	19.8N			schist	2	
								284.4	25.8N			maroon plutonic	1	
								255	76.4N					
37	K3	41	3.496	111	37.977	80	32N	339	47E					41
								320	50E					88
								11	22E					
								306	7N					
								345	17E					
								228	6N					
								342	19E					
								275.9	23.9N					
								289	62.8N					
								305.6	49.4N					
								273.8	75.6N					
								294.8	66.3N					
								227.1	21.7N					
								251	25.3N					
38	K3	41	4.01	111	37.701	44	48NW	250.3	23.9N			gneiss	14	33
								236.3	34.6N			plutonic	46	29
								227.4	36N			red ss	1	39
								219	37.1W			dark ss	1	34
								211.2	44.7W			quartzite	1	27
								197.2	58W			weathered plutonic	5	
												maroon plutonic	7	
												intermediate plutonic	3	
												green plutonic	4	

											foliated plutonic	4	
											green ss	2	
											schist	3	
											volcanic	9	
39	K2	41	2.695	111	44.244	194	78NW	173.3	72.4W		plutonic	35	
								172.5	68W		foliated plutonic	11	
								192.6	40W		gneiss	19	
								195.5	37W		maroon plutonic	15	
								178.5	53.1W		weathered plutonic	14	
								196.5	43W		schist	2	
								187.1	56.5W		intermediate plutonic	3	
								188.5	59.3W		phyllite	1	
								172.1	56.5W				
								204.1	28.4W				
								169.8	31.7W				
								247.4	68.9N				
40	K2	41	2.69	111	44.22	198	5NE	313.8	31.9N				
41	K2	41	2.71	111	44.17	22	44N	303.9	46.1N				
								283.4	53.7N				
								298.7	47.6N				
								289.3	39.1N				
								319.6	45.9E				
								316.2	45.5E				
								311.4	43.2N				
42	K2	41	2.711	111	44.126	42	48N						
43	K3	41	2.732	111	44.047	111	41W	291.6	80N				42
								274.3	76.4N				77
								290.2	62N				44
								303.6	71.3N				49
								292.4	67N				83
								283.8	76.5N				43
								275.8	67.4N				88
								287.9	64.9N				98
													59

														48
44		41	2.72	111	43.982							plutonic	71	
												mylonite	1	
												weathered plutonic	10	
												foliated plutonic	2	
												granodiorite	9	
												volcanic	4	
												quartzite	4	
												schist	2	
45	K2	41	2.738	111	33.977									
46	K2	41	2.718	111	43.949	94	26N	244.7	67.7N					32
								258.2	66.7N					38
								257.8	68.6N					31
								246.6	69.3N					25
								252.8	73.8N					29
														58
														57
														62
47a	K2	41	2.72	111	43.925	352	50N	199.1	76.5W					240
								195.6	67.7W					84
								185.8	77.5W					85
														205
														225
47b		41	2.655	111	43.844									
48	K2	41	2.691	111	44	171	61W							
49	K2	41	2.682	111	43.804									
50	K2	41	2.664	111	43.759									
51	K2	41	2.656	111	43.709									
52	K2	41	2.652	111	43.68									
53	K3	41	3.397	111	39.511	36	54N	248	41N			plutonic	47	
								276	22N			maroon plutonic	16	
								328	13E			foliated plutonic	8	
								267	68N			phyllite	12	
								252	24N			gneiss	4	

								240.2	21.5N	weathered plutonic	5	
								219.7	33.1W	schist	5	
								233.9	38.4N	black igneous	1	
								266.8	71N	conglomerate	1	
								285.9	80.2N	red ss	1	
								284.6	78.7N			
								262.8	68N			
								281.9	77.1N			
54	K3	41	3.31	111	39.533	84	55N	230	49N			
								258	17N			
								153	31W			
								299	28N			
								124	19S			
								284	20N			
								264	51N			
								226	59N			
								261	58N			
								238.4	38.8N			
								224.2	68.5W			
								220.5	68.5W			
								220.2	71.2W			
								229.1	47.3N			
								256.9	53.3N			
								345.8	27.6E			
								318.8	23.1E			
								301.5	20.6N			
								264	33N			
								310.3	30.4N			
55	K3	41	3.423	111	39.411	62	64N	329	21E			
								287	14N			
								359	34E			
								343	20E			
								340	24E			
								324	32E			

325	27E
342	64E
331	65E
357	25E
308	13N
342	39E
292	18N
346	20E
343	36E
339	39E
349.8	32.2E
344.9	67.1E
344	43.2E
359.8	63.4E
12.8	39.7E
329.8	63.3E
350.8	58.1E
321.1	48.4E
324.4	67.2E
345.5	44.9E
318.8	40.7E
337.1	36.4E
355.9	41.9E
347.1	38.1E
352.4	35.9E
344	43.2E
329.5	48.5E
335.9	46.5E
344	43.2E
346	82.9E
2.4	70.6E
342.5	66.7E
349.8	59E
339.4	59.9E

								338.5	45.3E					
								336.4	41.9E					
								341.5	46.9E					
								334.6	60.1E					
								332.6	53.7E					
56	K3	41	3.528	111	39.422	62	79N	319	30E					
								287	40N					
								309	32N					
								352	52E					
								339	43E					
								273	39N					
								324	38E					
								342.1	41.3E					
								341.7	37.8E					
								340.1	45.6E					
								329.3	17.1E					
								311.4	13.7N					
								301.2	12.1N					
								294.7	29.7N					
								260.6	22.8N					
								329.1	65.4E					
								317.8	39.7E					
								329	61.8E					
								325.2	65.6E					
								326	34.4E					
								339.2	36.6E					
								329.6	42.4E					
57	K3	41	3.379	111	39.123	65	57N	212	66W					
								202	42W					
								240	38N					
								201	56W					
								201	37W					
								180	37W					
								213	52W					

								218.2	38.5W				
								211.1	37.8W				
								212.8	40.6W				
								333.9	43.6E				
								322.8	45.6E				
								203.8	54.6W				
								208.2	48.4W				
								203.2	53.7W				
								205.2	48.3W				
								331.2	66.6E				
								335.5	67.8E				
								334.5	70.4E				
								331	57.2E				
								336.9	50.3E				
								336.1	64.4E				
								343.3	56E				
58	K3	41	3.455	111	38.773	72	48N	185	29W		plutonic	57	
								171	8W		gneiss	6	
								161	32W		foliated plutonic	3	
								210	74W		maroon plutonic	5	
								214	67W		schist	8	
								205	65W		phyllite	13	
								277	23N		green conglomerate	10	
								227	12N		weathered conglome	1	
								278	6N		green plutonic	1	
								165	17W		weathered plutonic	1	
59	K3	41	3.357	111	38.774	168	45NE	298	41N				
								244	46N				
								253	51N				
								238	58N				
								249	27N				
								226	47N				
								226	45N				
								257	28N				

								227	43N				
								254	33N				
								243	32N				
								209	51W				
								262.3	51N				
								263.7	46N				
								271.7	47.4N				
								255.4	43.1N				
								258.6	57N				
								254.3	47.2N				
								242.6	28.2N				
								225	34N				
								228.2	53.3N				
								225.9	47.8N				
								252.7	40.3N				
								258.1	38.2N				
								229.7	49N				
								225.9	56.9N				
60	K3	41	3.195	111	38.423	12	49SE	258	38N				
								257	37N				
								250	31N				
								237	64N				
								252	66N				
								251	62N				
								232	70N				
								234	82N				
								226	76N				
								226	76N				
								222	73W				
								246.7	57.6N				
								259.7	60.4N				
								250.7	81.5N				
								214.2	88.2W				
								233.4	63.6N				

								245.4	82.6N				
								251.7	86.2N				
								248.3	75N				
								252.4	64.9N				
								262.5	83.4N				
								242.7	81.1N				
								258.6	63.7N				
								239.9	75.3N				
								245.2	89.8N				
61	K2?	41	3.113	111	38.616								
62	K2?	41	2.982	111	38.773								
63	K2	41	2.947	111	38.768								
64	K1/K2	41	2.976	111	38.992								
65	K2	41	3.012	111	39.062						plutonic	59	
											phyllite	8	
											schist	2	
											volcanic	1	
											foliated plutonic	3	
											weathered plutonic	4	
											conglomerate	10	
											maroon plutonic	10	
											quartzite	3	
66	K3	41	3.139	111	39.068								
67	K3	41	3.138	111	39.411	57	60N	164	35W				
								160	35W				
								171	30W				
								223	39W				
								166	18W				
								198	19W				
								188	28W				
								204	71W				
68	K3	41	2.955	111	39.761								
69	K3	41	2.963	111	39.824	132	60N						
70	K3?	41	3.279	111	39.928								

71	K3	41	3.572	111	41.129	171	61E	270	52N			plutonic	45
								223	40W			conglomerate	8
								234	58N			intermediate plutonic	5
								218	56W			green ss	1
								199	51W			gneiss	8
								231	80N			maroon plutonic	5
								242	32N			quartzite	4
								232	59W			volcanic	6
								9	65E			phyllite	2
								253	42N			foliated plutonic	1
								247	48N			schists	5
								247.6	56.1N			red ss	3
								240.5	33.4N			marble	5
								234.4	58.2N			green plutonic	2
								252.5	53.7N			tan ss	1
								241.2	68.4N				
								240.4	50.9N				
								251.4	46.7N				
								235.8	53.5N				
								246.3	49.3N				
								243.3	38.5N				
								253.6	57N				
								250	42.8N				
								240.3	55.2N				
72	K3	41	3.826	111	41.086	84	54N						
73	K3	41	3.865	111	41.099	69	45N	185	48W				
								206	40W				
								194	48W				
								199	51W				
								191	50W				
								354.3	63.4E				
								0.6	60.7E				
								355.8	64.8E				
								358	58.8E				

								351.8	50.5E				
								4	59.6E				
								347.6	48.3E				
								12.1	54E				
74	K3	41	3.926	111	41.104	59	69N	342.2	50.1E				
								298.2	57.6N				
								323.4	59.7E				
								317.8	42.3E				
								309.9	9.8N				
								322.1	33.5E				
								302	22.6N				
								312.6	24.4N				
								315.2	32.3E				
								307.9	29.2N				
75	K3	41	3.976	111	41.106	52	51N	332	44E				
								316	31E				
								208	11W				
								217	10W				
								184	32W				
								218	26W				
								208	30W				
								212	26W				
								327	19E				
76	K3	41	4.012	111	41.114								
77		41	4.1	111	40.958								
78	K3	41	3.952	111	40.855								
79	K3	41	4.014	111	40.827	27	68N	301	45N			plutonic	52
								302	49N			gneiss	29
								296	48N			maroon plutonic	5
								319	57E			phyllite	3
								307	57N			conglomerate	3
								304	68N			foliated plutonic	8
								228	70N			red ss	1
								226	41N			schist	3

								257	45N		green plutonic	1	
								293	34N		volcanic	1	
								299.2	23.3N				
								321	49.5E				
								281.7	31.6N				
								316.1	26E				
								303.3	56.4N				
								299.9	37.5N				
								330.4	47.2E				
								316.4	36.6E				
								318.4	34E				
								315.8	49.8E				
								317.8	54.9E				
								325	46.1E				
								338.2	44.3E				
								308	37.7N				
								309.7	36.7N				
								314.8	34.8N				
								321.3	37.6E				
								313.6	43.7N				
								303.4	43.8N				
80	K3	41	4.062	111	40.798	54	51N	276	18N				
								277	29N				
								343	59E				
								286	67N				
								384	38N				
								292	21N				
								316	29E				
								287	25N				
								281	28N				
								291	18N				
								348.5	37.9E				
								357.1	49.4E				
								327.7	35E				

								323.2	20E				
								304.5	30.9N				
								336.9	25.3E				
								295	23.9N				
								358.7	20.1E				
								343.9	25.8E				
								329.5	31.9E				
								324.5	25E				
								272.6	15.9N				
								311.6	20.7N				
								290.8	19.2N				
								330	47.5E				
								339	58.5E				
								334.3	42.3E				
81	K3	41	4.135	111	40.84	53	46N	247	75N				
								260	71N				
								266	66N				
								306	34N				
								266	60N				
								261	47N				
								249	34N				
								222	39W				
								258	47N				
								230	66N				
								229	74N				
								236	53N				
								229	74N				
								238	39N				
								296.8	27.5N				
								309	26.4N				
								292.4	29.6N				
								294	51.7N				
								289.6	57.8N				
								209.3	29.8N				

								268.9	30.1N				
								251.5	28.1N				
								267.5	38.6N				
								252.4	34.3N				
								284.9	25.3N				
								305.5	53.3N				
								280.5	49.1N				
								295.5	56.5N				
								290.4	52N				
82	K3	41	4.327	111	40.804	45	55N	270	33N				
								280	38N				
								308	33N				
								246	46N				
								257	29N				
								283	29N				
								268	34N				
								285	33N				
								271	24N				
								303	43N				
								217	30W				
500	K3?	41	1.824	111	41.948								
501	K3?	41	1.876	111	42	63	48N	335	22E				
								206	64W				
502	K3	41	2	111	41.996	95	42N	356	32E		plutonic	43	86
								261	24N		schist	8	38
								37	31E		foliated plutonic	16	71
								4	30E		gneiss	2	40
								346	26E		green plutonic	5	
								321	13E		marble	2	
						36	87N	201	29W		phyllite	2	
								261	47N		vein quartz	1	
								242	34N				
503	K3	41	1.962	111	41.97	35	50N	271	43N				29
								255	41N				25

								281	34N				30
								310	38N				
								336	55E				
								328	53E				
								300	37N				
504	K3	41	1.994	111	41.946	60	48N	151	48W				36
								204	35W				59
								238	34N				38
													27
													44
													66
													44
													42
505	K1/K2?	41	2.037	111	41.927								
	FAULT												
506	K2/K3	41	2.025	111	41.829	45	54N	335	45E				
								139	21W				
507	K3	41	2.017	111	41.742	56	43N	326	47E				
								307	18N				
								317	39E				
								161	49W				
								170	29W				
								270	25N				
508	K3	41	2.028	111	41.721	50	56N	170	27W				38
								288	71N				30
								262	31N				28
								251	62N				30
								311	27N				
509	K3	41	2.053	111	41.715	41	44N	236	37N				39
								328	47E				42
								322	39E				36
								293	30N				29
								264	19N				37
						60	50N	314	20N				36

								355	30E					45
								335	24E					
								310	22N					
								328	14E					
510	K3	41	2.064	111	41.696	45	37N	330	28E					
								301	31N					
								310	38N					
								308	21N					
								316	58E					
								320	55E					
								337	28E					
								302	55N					
								308	39N					
								324	33E					
								304	43N					
511	K3	41	2.23	111	41.771	65	67N	272	27N					41
								245	5N					28
								228	14N					27
								195	26W					
								308	16N					
								318	36E					
512	K3	41	2.211	111	41.709	51	42N	342	71E					
								322	57E					
								353	49E					
								303	41N					
								333	31E					
								271	31N					
								239	5N					
								345	59E					
513	K2/K3?	41	2.278	111	41.796									
514	K3?	41	2.359	111	41.756	52	37N	269	41N					
								230	26N					
515	K3?	41	2.373	111	41.768	79	80N							
516		41	2.405	111	41.732									

517	K1/K2	41	2.399	111	41.79									
518	K1/K2	41	2.461	111	41.881									
519	K1/K2	41	2.542	111	41.821									
520	K3?	41	2.853	111	41.819	62	46SE							
521	K3?	41	2.867	111	41.811	101	35N	265	36N					37
								257	20N					25
								259	29N					38
								341	27E					29
								281	24N					32
								178	34W					30
522	Ksb?	41	3.232	111	41.796									
523	Ksb	41	3.357	111	41.789									
524		41	3.476	111	41.864									
525		41	3.256	111	41.811									
526		41	2.696	111	36.29	95	44N	318	43E					
						103	34N	217	22W					
								232	22N					
								224	24W					
								297	27N					
								234	29N					
								241	14N					
527	K3	41	2.984	111	36.474	74	8N	354	63E					
								322	30E					
								216	50W					
								287	27N					
								214	20W					
								323	42E					
								225	31W					
								230	46N					
								292	25N					
								297	44N					
528		41	3.724	111	37.259									
529		41	3.998	111	37.326									
530		41	3.819	111	37.784									

531		41	3.643	111	38.044									
532		41	3.262	111	38.106									
533	K2	41	2.844	111	44.481	202	77W							
534	K1/K2	41	3.093	111	44.511									
535	K3	41	3.192	111	44.512	140	82W	315	58E			plutonic	45	28
								317	71E			foliated plutonic	22	39
												gneiss	13	29
												schist	4	40
												gabbro	4	65
												red ss	3	35
												phyllite	3	32
												red mudstone	1	49
														42
														43
														45
														59
														41
536	K3	41	3.242	111	44.123									
	FAULT													
537	K3?	41	3.507	111	44.187									
538	K3?	41	3.625	111	44.274									
539	K3	41	3.638	111	43.853	50	48W	298	40N			gneiss	3	
								320	28E			plutonic	50	
								315	32N			foliated plutonic	14	
								291	32N			phyllite	4	
								300	28N			schist	5	
								246	17N			red ss	2	
								268	26N			vein quartz	1	
								346	50E					
								14	57E					
								344	42E					
								341	37E					
								320	31E					
								323	24E					

								299	23N					
								305	19N					
								319	30E					
								335	41E					
								297	39N					
540	K3	41	3.531	111	38.817	61	45N	282	29N					
								224	19W					
								212	20W					
								283	45N					
								235	17N					
								257	25N					
								261	28N					
								235	29N					
								264	37N					
								275	29N					
								232	32N					
								254	38N					
								260	38N					
								276	40N					
								285	53N					
						94	42N	224	74W					
								216	55W					
								229	44N					
								214	32W					
								204	12W					
						102	54N	124	43S					
								147	35W					
								114	35S					
								152	60W					
						53	42N	200	45W					
								267	19N					
								185	18W					
								204	33W					
								192	35W					

								315	57N
								244	24N
								247	29N
								251	43N
								210	40W
								268	32N
								255	36N
								257	29N
								222	47W
								250	47N
								256	31N
								221	47W
								97	84S
								245	27N
								217	19W
541	K3	41	3.781	111	38.537				
542	K3	41	3.729	111	38.666	70	30N	249	40N
								237	41N
								242	35N
								219	37W
								236	50N
543	K2?	41	3.71	111	38.717	47	54N	279	47N
544	K3	41	3.606	111	39.151	55	51N	272	40N
								305	59N
								296	47N
								319	50E
								306	53N
								335	70E
								270	52N
								317	57E
						62	41N	272	43N
								258	45N
								262	44N
								292	49N

								251	64N				
								272	37N				
								291	39N				
								320	69E				
								308	48N				
								311	71N				
								271	53N				
								304	53N				
								303	49N				
								288	58N				
								287	47N				
								300	53N				
								305	55N				
								325	62E				
								321	54E				
								297	43N				
								237	47N				
								287	53N				
								265	45N				
								283	54N				
								256	41N				
								241	43N				
545	K2	41	3.879	111	39.049								
546	K3	41	3.939	111	39.542	64	41N	310	41N			gneiss	20
								259	32N			plutonic	42
								276	36N			foliated plutonic	29
								282	39N			phyllite	1
								275	28N			red ss	9
								254	43N			marble	1
								287	57N			gabbro	1
								283	44N				
								270	47N				
								286	50N				
								280	50N				

								298	46N					
								299	58N					
								225	38W					
								309	55N					
								284	56N					
								279	49N					
								253	43N					
								256	27N					
								285	37N					
								237	34N					
								217	32W					
								295	44N					
								256	41N					
								282	45N					
								253	44N					
								300	63N					
								274	45N					
								266	46N					
547	K3	41	4.028	111	39.598	30	35W	245	56N					
								266	59N					
								270	65N					
								258	59N					
								261	55N					
								223	52N					
								239	57N					
								264	63N					
								270	57N					
								234	57N					
								273	57N					
								270	43N					
548	K3	41	4.066	111	39.801	69	62N	357	31E					
								246	38N					
								196	30W					
								249	28N					

								218	30W					
								222	42W					
								210	22W					
								270	32N					
								280	26N					
								243	37N					
								231	44N					
549	K3	41	4.107	111	39.994	79	80N	191	37W			plutonic	49	70
								348	56E			gneiss	6	49
								346	32E			foliated plutonic	30	48
								342	20E			phyllite	2	
								334	33E			schist	2	
								221	38W			red ss/maroon quartzi	14	
								310	35N					
								282	33N					
								284	26N					
								251	44N					
550	K3	41	4.524	111	40.371	46	80N	294	27N					
								246	12N					
								167	32W					
								240	19N					
								215	22W					
								273	32N					
								303	19N					
								167	41W					
551	K3	41	4.751	111	40.433	60	68N	183	22W			plutonic	45	
								207	17W			white marble	19	
								214	23W			gneiss	5	
								226	17N			foliated plutonic	19	
								247	17N			phyllite	6	
								312	66N			vein quartz	1	
								295	53N			red ss	7	
								296	50N			green plutonic	2	
								313	47N			schist	1	

								309	46N				
								288	50N				
552	K3	41	5.126	111	40.322	50	38N	190	50W			plutonic	40
								75	11S			foliated plutonic	29
								221	15W			phyllite	9
								259	17N			gneiss	13
								241	25N			red ss	1
								324	39E			schist	8
								251	22N			green plutonic	1
								330	15E			white quartzite	2
								309	15N			volcanic	1
								223	32W			vein quartz	1
								267	22N				
553	K3	41	5.151	111	40.273	61	36N	177	41W				
								193	36W				
								249	28N				
								226	39N				
								254	31N				
								211	45W				
								195	61W				
554	K3	41	5.02	111	40.109	84	23N	317	41E			plutonic	48
												foliated plutonic	17
												schist	12
												gneiss	6
												phyllite	9
												red ss	3
												green plutonic	1

Basin S3													
Station N	Unit	Latitude		Longitude		Strike	Dip	Imbrication		Trough Axis		Clast Type	Clast Count
1	K3	40	57.38	111	53.36	129	6S	285	68N			plutonic	53
								286	62N			foliated plutonic	7
								288	36N			green ss	1
								271	51N			white marble	10
												green phyllite	3
												green plutonic	20
												coarse schist	5
2	K2	40	57.8	111	53.244								
3	K3	40	57.37	111	53.671								
4	K3	40	57.32	111	53.344								
5	K3	40	56.23	111	49.167	101	30N	295	39N				
								283	32N				
								218	41W				
								195	59W				
								202	53W				
								203	46W				
								209	46W				
								236	62N				
								279	27N				
								244	13N				
								256	19N				
								199	34N				
								286	7N				
								339	2E				
								330	18E				
								325	18E				
								269	9N				
								206	21W				
								213	22W				
								324	21E				
								245	15N				

								220	21W					
								329	32E					
								317	26E					
								236	32N					
								253	30N					
						110	28N	220	42W					
								217	41W					
								231	33N					
								232	28N					
								220	53W					
								269	29N					
								254	38N					
								244	42N					
								302	44N					
								293	48N					
								319	33E					
								278	22N					
						103	34N	269	33N					
								302	27N					
								296	28N					
								254	33N					
								245	24N					
								230	28N					
								216	27W					
								253	34N					
								260	38N					
								260	46N					
								260	53N					
								264	50N					
								224	36W					
								273	24N					
								319	35E					
								322	23E					

								329	32E						
								258	27N						
								262	27N						
								297	32N						
								262	43N						
								243	30N						
								249	31N						
								262	5N	9	116				
								357	18E						
								63	54S						
								332	34E						
								329	44E						
								302	17N						
								248	21N						
								318	19E						
								200	55W						
								256	28N						
								262	32N						
								183	46W						
								225	21W						
								294	36N						
								269	37N						
								209	49W						
								194	29W						
								237	49N						
						96	27N	254	28N						
								242	52N						
								256	39N						
								226	45N						
								239	38N						
								241	46N						
								246	56N						
								265	43N						

								266	23N				
								217	56W				
								225	51W				
								270	21N				
								243	34N				
								224	57W				
								235	48N				
								204	39W				
								237	42N				
								239	58N				
								276	18N				
								249	40N				
						74	32N	334	23E				
								219	20W				
								279	38N				
								333	36W				
								322	36E				
6	Car	40	57.66	111	48.409								
7	K2	40	58.19	111	48.285								
8	K3	40	58.21	111	48.105	111	38S	343	59E				
								20	37E				
								354	57E				
								321	16E				
								350	18E				
								313	69N				
								307	54N				
								313	89N				
9	K3	40	58.16	111	48.1	96	53S	275	63N				
								309	53N				
								291	70N				
								315	57N				
								294	57N				
								300	52N				

								317	48E					
								332	43E					
								326	40E					
								302	38N					
								288	57N					
								308	77N					
								317	79E					
10	K3	40	58.09	111	48.101	112	42S	292	57N					
								309	45N					
								287	56N					
								295	64N					
								285	40N					
								274	49N					
								339	57E					
								309	55N					
								314	72N					
								333	69E					
								310	83N					
								335	46E					
								357	44E					
11	K3	40	57.84	111	48.413	60	32S	298	35N	60	246			
								273	72N					
12	K3	40	58.19	111	48.291	280	40S	250	69N	6.1	186			
								269	76N	12.3	184			
								265	82N					
								264.1	82N					
								280.6	55N					
								267.7	55N					
								266	84N					
								273	77N					
13	K3	40	58.14	111	48.291	286	40S	341	49E					
								235	46N					
								228	52N					
								212	32W					

								267	46N				
								268.3	78.8N				
								261.1	87.4N				
								264.1	69.4N				
								262.8	86.8N				
	14	K3	40	58.11	111	48.3	100	42S				plutonic	49
												foliated plutonic	20
												green plutonic	15
												schist	3
												green ss	5
												gneiss	6
												intermediate plutonic	2
												weathered plutonic	1
	15	K3	40	58.1	111	48.309	282	45S	232	14N			24
									252	53N			27
									326	40E			21
									302	48N			25
									299	37N			28
									289.5	72.2N			
									287.6	74.6N			
									293.2	78.5N			
									295.8	77.7N			
	16	K3	40	58.06	111	48.29	272	42S	302	47N			
									256	76N			
									263	83N			
									268	66N			
									288	58N			
									268	73N			
									273	49N			
	17	K3	40	57.94	111	48.282	80	45S					
	18	K2	40	55.95	111	46.315	84	26N					
18b		K2	40	57.84	111	48.413	121	22S	27	42E			
									40	30E			
									54	44S			

								11	39E					
								333	37E					
								307	74N					
								337	54E					
								331	54E					
								325	55E					
								341	55E					
								324	33E					
19	K2?	40	55.98	111	46.248	354	71E							
20	K2?	40	56.03	111	46.111									
21	K2?	40	56.04	111	46.143	244	45N							
22	K2?	40	56.03	111	46.163									
23	K2?	40	56.13	111	46.518									
24	K1?	40	56.42	111	46.404	126	21N							
25	K2?	40	56.46	111	46.382									
26	K3	40	56.35	111	46.615							plutonic	45	59
												conglomerate	18	58
												foliated plutonic	6	45
												gneiss	4	49
												green volcanic	3	46
												green plutonic	8	59
												white marble	2	39
												rhyolite	2	
												green ss	5	
												schist	3	
												quartzite	5	
												res ss	1	
27	K3	40	56.42	111	46.751	3	33E							
28	K3	40	56.39	111	47.012	64	41SE							
29	K3	40	56.38	111	46.991									
30	K3	40	56.34	111	46.981	46	32SE							
31	K3	40	56.29	111	46.974	58	60SE							
32	K3	40	56.25	111	46.941	24	38SE							
33	K3	40	56.23	111	46.914	34	25SE							

34	K3	40	56.17	111	46.88									
35	K3	40	56.04	111	46.866	72	27SE			25	140			
										20	122			
										18	113			
36	K2?	40	58.72	111	46.424									
37	K2?	40	58.86	111	46.535									
38	K1?	40	58.99	111	46.744									
39	K1	40	58.76	111	47.456									
40	K2	40	58.73	111	47.478									
41	K2	40	58.58	111	47.62	13	27NW							
42	K2	40	58.57	111	47.641	84	50S							
43	K2	40	58.55	111	47.666	78	10S							
44	K3	40	58.48	111	47.71	101	38S							
45	K3	40	58.42	111	47.696	80	45S							
46	K3	40	58.41	111	47.696	106	46	329	61E					
								349	41E					
								286	6N					
								275.8	89.8N					
								279.3	87N					
47	K3	40	58.38	111	47.688	85	43S	3	26E			plutonic	83	
								324	9E			foliated plutonic	5	
								338	40E			green plutonic	2	
								329	45E			weathered plutonic	6	
								308	43N			ss	3	
								301	42N			schist	1	
								294	33N					
								292.1	22.2N					
								245.5	24.8N					
								259.6	28.3N					
								271.6	22.3N					
48	K3	40	58.32	111	47.715	85	57S	295	53N					
								229	65N					
								217	72W					
								225	67N					

								290.1	23.1N				
								302.9	16.2N				
								246.4	66.7N				
49													
50	K1/K2	40	59.2	111	46.378	101	40S	35	40E			plutonic	55
								57	29S			foliated plutonic	8
								167	56W			quartzite	14
								265	24N			volcanic	1
												white marble	3
						120	20N	275	44N				
								279	28N				
								12	34E				
								342	43E				
								249	14N				
51	K2?	40	59.15	111	46.79								
52	K1/K2	40	59.02	111	47.068								
53	K2	40	58.85	111	47.055								
54	K3	40	58.16	111	47.564	60	45E	316	59E				
								327	44E				
								312	49N				
55	K3	40	55.71	111	46.671	131	27E	276	29N				
								277	44N				
								309	57N				
								243	19N				
								20	33E				
								333.7	36.3E				
								318.8	34.2E				
								338.2	32.8E				
56	K3	40	55.73	111	46.71	92	25N	221	42W	7	201	plutonic	65
								221	25W	15	208	green conglomerate	5
								237	34N			phyllite	7
								226	49N			green ss	2
								305	58N			tan ss	3
								291	45N			weathered plutonic	4

								268	39N	schist	1	
								256	58N	green plutonic	1	
								334	42E	gneiss	3	
								293	60N	quartzite	1	
								290	54N			
								326	53E			
								336	33E			
								214	46W			
								201	62W			
								253	41N			
								212	33W			
								248	52N			
								289	53N			
								280	23N			
								272	55N			
								237	34N			
								296	36N			
								275	29N			
								282	27N			
57	K3	40	55.94	111	46.733	80	25S					
58	K3	40	55.96	111	46.736	80	20S					
59	K2/K3	40	56.15	111	46.704	96	59N					
						51	44S					
60								288	45.9N			
								216.7	46.4W			
								296.4	45.3N			
								224.6	44W			
								293.2	55.1N			
								232.6	53N			
								279.4	48.7N			
61								302.9	40.1N			
								298.3	45.2N			
								276.5	34.6N			
								290	39.6N			

								296.8	50.3N				
								286.5	54.1N				
								298.4	56.6N				
								314	42.4N				
								289.3	46.2N				
								194.8	64W				
								209.5	73.5W				
								213.1	58.7W				
								197	71W				
								317.3	82E				
								325.9	77.4E				
								323.7	87.2E				
								323.1	82.9E				
62								287.3	47.6N				
								282.2	53.6N				
								295.8	74.4N				
								305.5	76N				
								234.8	44N				
								246.7	41.9N				
								261.2	44.9N				
								251.9	50.2N				
								332.6	73.4E				
								328.6	74.6E				
								329.9	65.6E				
								331.7	73.2E				
								308	56.9N				
								292.6	71.4N				
								314.8	50.3N				
								287.8	58.4N				
								305.3	61.4N				
								314.8	52.4N				
								279.6	49.7N				
								324.5	54E				
								277.2	67N				

								328.9	51.9E					
								303	52.2N					
								315.9	59.1E					
								316.4	63.4E					
63								304	81N					
								305	89N					
								342.9	78.4E					
								334.7	68.7E					
								338.8	59.3E					
								328.6	74.6E					
								342.7	69.2E					
								338.4	72.5E					
64	K3	40	56.26	111	47.05	58	42S	311	87N					
								305	77N					
								312	77N					
65	K3	40	56.13	111	43.132							plutonic	74	
												foliated plutonic	13	
												gneiss	5	
												phyllite	2	
												schist	2	
												green ss	1	
												tan ss	1	
												quartzite	1	
												weathered plutonic	2	
66	K3	40	56.04	111	47.213	36	42S	254	34N					
67	K3	40	55.91	111	41.236	55	22N	237	55N					
								259	54N					
								272	38N					
68	K3	40	55.82	111	47.236	169	20NE							
69	K2	40	57.05	111	49.878	45	63N			1	350			
										1	331			
										7	32			
										2	154			
										12	155			

69B		40	56.98	111	50.481	88	48S	279.5	50.3N					
								294.1	61.4N					
								292	66.3N					
								287	63.6N					
								278.6	53.7N					
								284.3	55.8N					
								288.7	55.8N					
								280.7	54.7N					
								275.3	53.7N					
								284	54.4N					
70	K2	40	57.13	111	50.048									
71	K2													
72	K2	40	57.04	111	50.515	36	9E	287	59N					
								281	48N					
								299	54N					
								302	54N					
								290	47N					
								275	64N					
								305	60N					
								309	41N					
								273	42N					
								253	45N					
								260	38N					
								254	39N					
								246	56N					
								254	51N					
								265	38N					
								294	39N					
								270	45N					
								253	44N					
								263	42N					
								253	48N					
								347	58E					
								307	61N					

								292	34N				
								267	51N				
								294	41N				
								229	48N				
								230	30N				
								220	30W				
								234	48N				
								186	55W				
								258	16N				
								203	45W				
								206	41W				
								1	39E				
								346	26E				
								347	67E				
								344	67E				
								354	50E				
								9	32E				
								24	62E				
73	Pt	40	57.2	111	51								
300	K3	40	57.53	111	46.7	16	65S	280	67N				
								246	56N				
								277	37N				
								246	49N				
								261	69N				
								269	81N				
								289	49N				
								248.3	40.8N				
								242.8	63.9N				
								247.6	24.1N				
								233.8	26.1N				
301	K3	40	57.49	111	46.819	10	54S	252	66N			plutonic	60
								252	82N			quartzite	7
								230	67N			black quartzite	3
								252	26N			tan ss	6

								234	33N		weathered plutonic	3	
								237	42N		green plutonic	5	
								281	17N		marble	10	
								261	27N		conglomerate	5	
								259	36N		K2 clast	1	
								270	37N		green volcanic	1	
								272	31N		chert	1	
								296.6	28.5N				
								245.5	42.3N				
								301.2	37.1N				
								270.8	37.7N				
								266.1	43.7N				
								257.3	69.2N				
								263.8	70.8N				
								250.4	59.6N				
302	K3?	40	56.99	111	47.36								
303	K3	40	56.81	111	47.243	161	8SW						
304	K3	40	55.74	111	47.733	35	50S	14	78E				
								6	77E				
								9	85E				
								317	37E				
								271	43N				
								284	46N				
305	K3	40	55.76	111	47.775	45	25S	326	40E				
								195	67W				
								322	53E				
								321	49E				
								342	50E				
								320	38E				
								321	48E				
								209	78W				
								304	34N				
								303	51N				
								325	53E				

								324	53E				
306	K3	40	55.87	111	47.803	50	45S	291	33N			plutonic	80
								283	49N			foliated plutonic	15
								266	69N			gneiss	9
								333	47E			green plutonic	2
								314	34N				
								310	38N				
								280	61N				
								248	19N				
								297	16N				
								257	71N				
								299	42N				
307a	K3	40	56	111	47.874	49	15S	356	21E				
								318	34E				
								281	46N				
								281	43N				
								8	19E				
								22	34E				
307b	K3	40	56.05	111	47.733	60	17N	301	53N			gneiss	15
								307	47N			plutonic	77
								293	44N			green plutonic	7
								300	55N			quartzite	2
								285	53N			foliated plutonic	6
								278	52N			schist?	1
								298	60N				
								291	61N				
308a	K3	40	56.07	111	47.864	75	17N						
308b	K3	40	56.27	111	47.868	97	29N						
309	K3	40	56.33	111	47.875	200	32SE	303	46N			plutonic	34
								307	50N			marble	12
								323	54E			green plutonic	2
								304	45N			gneiss	8
								197	57W			schist	2

								278	34N			quartzite	1
								298	43N				
								296	39N				
								288	49N				
								294	45N				
310	K3	40	56.45	111	47.829	36	45SE						
311	K3	40	56.52	111	47.781	61	42SE	360	33E				
								314	30N				
								347	48E				
								341	51E				
								337	67E				
								346	36E				
								328	49E				
								349	37E				
312	K3	40	56.55	111	47.766	73	90						
313	K3?	40	56.81	111	47.679								
314	K3	40	56.64	111	48.061	21	32SE						
315	K3	40	56.5	111	48.183	75	54S	328	27E				
								317	54E				
								275	50N				
								294	37N				
								296	42N				
								312	58N				
								324	53N				
								335	39E				
								303	49N				
								351	35E				
316	K3?	40	56.44	111	48.217	86	54S						
317	K3?	40	56.42	111	48.22	101	33N						
318	K3	40	56.37	111	48.299	102	28N						
319	K3	40	56.3	111	48.402	146	44E						
320	K3	40	56.27	111	48.441	141	45E						
321	K3	40	56.2	111	48.447	125	36N						
322	K3	40	56.08	111	48.382	63	14SE						

323	K3	40	55.91	111	48.304	57	35SE		
324	K3	40	55.83	111	48.175	59	37SE		
325	K2	40	56.87	111	47.124				
	K2	40	56.9	111	47.089				
326	K3	40	57.02	111	47.021	10	54SE	254	49N
								261	43N
								261	36N
								253	34N
								249	37N
								273	68N
								236	22N
								276	24N
								292	24N
								215	38N
327	K1/K2	40	57.44	111	49.563				
327B	K3					35	28N	332.7	39.6E
								310.8	28.5N
								302.3	49.3N
								330.1	53.8E
								326.1	31.9E
								328.4	38.2E
								323.5	54.9E
								350.2	63.3E
								312.3	46N
								302.7	51.9N
								335.4	42.8E
								318.4	30E
								330.9	54.3E
								326.2	60.1E
328	K2	40	57.56	111	49.378				
329	K3	40	56.99	111	49.254	35	28N	282	24N
								285	35N
								313	53N
								298	57N

								289	31N					
								318	20E					
								314	38N					
								323	40E					
330	K3	40	57.34	111	53.521	56	26N							
331	K3	40	57.35	111	53.82	20	13N	299	56N			plutonic	81	
								188	49W			marble	3	
								269	62N			gneiss	14	
								270	76N			foliated plutonic	6	
								277	55N			schist	4	
								244	66N			green plutonic	4	
								263	76N			dark volcanic	1	
								252	66N			quartzite	1	
								245	63N					
								229	72N					
332	K3	40	57.41	111	53.904	52	24N	251	44N					
								251	31N					
								238	33N					
								226	31N					
								242	21N					
								261	23N					
								230	18N					
								197	4W					
								194	25W					
								218	16W					
333	K3	40	57.49	111	53.861	117	16N							
334	K3	40	57.54	111	53.881	117	27N	229	41N					
								235	54N					
								236	48N					
								253	44N					
								239	25N					
								243	36N					
								232	21N					
								228	48N					

								258	48N				
								244	37N				
335	K3	40	57.58	111	53.792	182	25E						
336	K3	40	57.54	111	53.747	190	20E						
337	K3	40	57.52	111	53.728	103	10N						
338	K2/K3	40	57.74	111	53.23	70	24S						
339	K3	40	57.63	111	53.053	114	40N	260	34N			plutonic	62
								325	18E			foliated plutonic	5
								252	52N			green plutonic	5
								235	38N			gneiss	14
								206	59W			marble	10
								220	35W			schist	1
								236	48N			weathered plutonic	3
								201	35W				
								239	23N				
								234	49N				
								234	30N				
340	K3	40	57.37	111	52.766	144	27SW	187	34W				
								283	54N				
								250	77N				
								282	63N				
								215	61N				
								201	31W				
								285	50N				
								248	50N				
								216	41W				
								233	43N				
341	K3	40	57.3	111	52.826	170	30W	280	54N				
								269	55N				
								273	34N				
								259	42N				
								257	40N				
								275	37N				
								277	61N				

								256	46N					
								239	49N					
								237	45N					
								284	57N					
								287	35N					
								258	47N					
								278	64N					
								244	34N					
								280	51N					
								284	59N					
342	K3	40	57.21	111	52.897	170	30W							
500	K3	40	56.04	111	46.927	65	31S	308	47N	24	153			
										15	161			
501	K3	40	55.94	111	46.987	44	18S	295	47N					
								291	71N					
								306	57N					
								305	70N					
								301	63N					
								310	75N					
								266	74N					
								294	65N					
								277	71N					
								318	52E					
								330	61E					
								330	39E					
								334	43E					
								321	52E					
								308	55N					
								311	51N					
								271	37N					
								264	46N					
								307	56N					

								321	47E
502	K3	40	55.84	111	46.828	31	20E	248	58N
503	K3	40	53.57	111	50.628	135	31N	256	41N
								262	22N
								286	54N
								276	20N
								247	25N
								257	40N
								244	31N
								269	53N
								221	5W
								303	38N
								283	27N
								277	33N
								319	21E
								249	32N
								314	84N
								301	35N
								312	43N
								243	49N
								233	45N
								248	35N
								244	31N
504	K3	40	56.62	111	50.615	87	28N	235	37N
								267	47N
								252	44N
								286	52N
								275	31N
								8	52E
								258	27N
								206	23W
505	K3	40	56.74	111	50.611	100	37N	352	60E
								359	57E
								321	49E

								334	30E					
								266	46N					
506	K3	40	56.76	111	50.626	94	43N	297	38N			gneiss	7	
								296	36N			plutonic	48	
								249	24N			foliated plutonic	25	
								295	26N			schist	4	
								220	26W			phyllite	14	
								311	46N			white marble	1	
								299	39N			vein quartz	1	
								278	25N			green plutonic	1	
								298	35N			quartzite	5	
								292	37N			basalt	2	
								314	33N					
								283	39N					
								295	39N					
								317	38E					
								318	29E					
								284	22N					
								260	33N					
507	K2/K3	40	56.79	111	50.645									
Brad big section										270	0	plutonic	79	
										249	0	gneiss	30	
										261	0	marble	9	
										240	0	sandstone	2	
										228	0	volcanic	5	
										263	0		125	
										236	0			
										235	0			
										198	0			
										193	0			
										259	0			
										230	0			
Tape 1														
Tape 2										215	0	Plutonic	46	

										216	0	Gneiss	18	
										220	0	Marble	13	
												Schist	0	
Tape 3												Quartzite	3	
												Mylonite	0	
Tape 4										157	0	Volcanic	7	
												Sandstone	11	
Tape 5										252	0	Conglomerate	3	
													101	
Tape 6														
Tape 7										266	0			
										256	0			
										268	0			
Tape 8										241	0			
										264	0			
										253	0			
Tape 9										231	0			
Tape 10										163	0			
										278	0			
										149	0			
Tape 11										228	0			
										214	0			
										211	0			
Tape 12										230	0			
										214	0			
Tape 13														
Tape 14												Plutonic	52	
												Gneiss	11	
Tape 15										234	0	Marble	16	
												Schist	0	
Tape 16												Quartzite	3	
												Mylonite	0	
Tape 17										181	0	Volcanic	8	
										189	0	Sandstone	7	

										190	0	Conglomerate	3	
										192	0		100	
										261	0			
Tape 18														
Tape 19										181	0			
										177	0			
Tape 20												Plutonic	32	
Tape 21												Gneiss	34	
Tape 22												Marble	20	
Tape 23												Schist	0	
Tape 24												Quartzite	3	
Tape 25										120	0	Mylonite	0	
Tape 26												Volcanic	9	
Tape 27												Sandstone	4	
Tape 28										137	0	Conglomerate	3	
										163	0		105	
										165	0			
										161	0	Plutonic	46	
										157	0	Gneiss	17	
										151	0	Marble	16	
										144	0	Schist	0	
										148	0	Quartzite	2	
										146	0	Mylonite	2	
Tape 29												Volcanic	15	
Tape 30										216	0	Sandstone	4	
										197	0	Conglomerate	5	
										162	0		107	
										134	0			
Tape 31														
Tape 32										243	0			
										239	0			
Tape 33										258	0			
Tape 34										281	0			
Tape 35										253	0	Plutonic	60	

Tape 36												Gneiss	23	
												Marble	8	
												Schist	0	
												Quartzite	0	
												Mylonite	1	
												Volcanic	10	
												Sandstone	0	
												Conglomerate	0	
													102	
Basin S4														
Station N	**Unit**	**Latitude**		**Longitude**		**Strike**	**Dip**	**Imbrication**		**Trough Axis**		**Clast Type**	**Clast Count**	
#######														
Station1		41	2.816	112	11.345			281	35N					
								206	25W					
								293	25N					
								286	28N					
								255	33N					
Tape 1								307.1	38.5N			Gneiss	15	
								297.1	41.6N			plutonic	43	
								283.8	46N			quartzite	1	
								280	31N			red ss	1	
								257.1	21.8N			white marble	9	
								313.2	63.9N			mylonite	9	
								295.8	31.7N			schist	3	
								225.5	23N			foliated plutonic	5	
								282.4	29.1N			ss	1	
								248.3	32N			brecciated marble	1	
Tape 2								249.9	19.7N					
								270.6	59.9N					

								272.3	38.9N				
								205	17W				
								309.2	57.3N				
Tape 4								239.2	26.8N		mylonite	7	
								207.7	30W		foliated plutonic	7	
								256.4	25.8N		schist	7	
								202.1	32W		plutonic	53	
											GNEISS	16	
											white marble	12	
											red ss	2	
											brecciated marble	2	
											foliated plutonic	2	
											quartzite	2	
											volcanic	1	
Tape 5								125.3	40.2S				
								356.1	67.2E				
								5.7	77.2E				
								344	36.8E				
								358.2	29.4E				
								16.8	27.7E				
								18	37E				
Tape 6											schist	2	
											gneiss	9	
											mylonite	5	
											plutonic	25	
											foliated plutonic	5	
											marble	2	
Tape 9								196.6	22.6W				
								231.1	22.3N				
TAPE 10		41	3.098	112	10.727			209.6	26.2W		plutonic	27	
								214.9	27.2W		foliated plutonic	3	
								196.1	36.1W		gneiss	10	
											marble	3	
											mylonite	5	

												volcanic	1
												brecciated marble	3
												phyllite	1
Tape 11													
TAPE 12								209.4	46.6W				
								245.1	51.1N				
								230.1	27.3N				
								211.4	29.3W				
								213	41.6W				
TAPE 13								202.1	47.7W				
								216	50.4W				
								219.2	37.1W				
								214.1	68.6W				
								188.8	78.0W				
								230.4	11.1N				
Tape 14												plutonic	47
												gneiss	18
												ss	7
												marble	4
												mylonite	6
												phyllited	3
												schist	2
												brecciated marble	1
												cgl	1
												foliated plutonic	6
Tape 15													
Tape 16		41	3.214	112	10.645								

Basin N1														
Station N	Unit	Latitude		Longitude		Strike	Dip	Imbrication		Trough Axis		Clast Type	Clast Count	Max Clasts
500		40	56.46	111	20.118									
501		40	56.51	111	20.061									
502		40	56.84	111	19.923									
503		40	57.01	111	19.927									
504		40	57.08	111	19.904									
505		40	57.13	111	22.743									
506		40	56.9	111	19.944									
507		40	57.74	111	19.572									
508		40	57.84	111	19.479									
509		40	57.29	111	19.604									
1		40	56.18	111	20.514									
2		40	56.2	111	20.495									
3		40	56.23	111	20.469									
4		40	56.28	111	20.432									
5		40	56.35	111	20.363									
6		40	56.38	111	20.341									
7														
8		40	56.43	111	20.254									
9		40	56.44	111	20.224									
10		40	56.46	111	20.115	45	32N	151	32W			Basalt	27	
								170	45W			Plutonic	30	
								169	56W			Marble	11	
								171	23W			Quartzite	3	
								179	31W			Weatherd Igneous	1	
								199	32W			Chert	1	
								186	51W			Rhyolite	18	
												Schist	1	
												Tan ss	6	
												Conglomerate	1	
												Gneiss	1	
11		40	56.47	111	20.11			275.7	56.3N					
								271.3	54.7N					

								295	57.1N				
								263.9	63N				
								245.4	51.5N				
								221.5	31W				
								244.9	48.4N				
								234.3	37.3N				
								226.4	45N				
								265.9	44.4N				
								252.9	31.1N				
								211.6	39.6W				
								211.3	31.5W				
								209.9	38.7W				
12		40	56.48	111	20.116			180.8	24.8W				
								210.1	28.6W				
								184.6	31.8W				
								220	28W				
								167.7	44.1W				
								161.4	35.8W				
								169.5	40.8W				
								140.5	32.3W				
								182.2	84.3W				
								140.7	28.5W				
								191	32.5W				
								202	35.7W				
								224	33W				
								217.7	39.1W				
								262	21.4N				
								206.7	39.1W				
								253.5	24.2N				
								240.5	22.7N				
								185.9	27W				
								186	21.4W				
								286.8	38.5N				
								165	47.9W				

								191.8	38.8W				
								170.4	41.6W				
								176.1	40.4W				
								148.9	32W				
								183.5	43.4W				
								179.1	43.8@				
								184.6	31.8W				
								164.9	43W				
								180.8	39.8W				
								202.3	32.5W				
								160.9	42.6W				
								181.2	36.3W				
								176.7	31.9W				
								154.8	40.8W				
								182	37.1W				
								177.9	72.9W				
								172.7	32.1W				
								175.1	81.5W				
								211.2	20.4W				
13		40	56.5	111	20.122								
14		40	56.52	111	20.057			276	39.7N				
								283.6	45.4N				
								263.6	45.5N				
								301	33.8N				
								331.3	20.5E				
								313.5	49.5N				
								270	31.8N				
								280.2	39.1N				
								293.5	31N				
15		40	56.51	111	20.007								
16		40	56.81	111	19.976								
17		40	56.83	111	19.942	64	65N	328	35E		Plutonic	90	110
								326	29E		Marble	8	80
								347	58E		Foliated plutonic	1	70

								328	54E			Quartzite	6	130
								349	62E					90
								355	42E					70
								356	40E					140
								354	42E					110
								356	40E					130
								353	22E					70
								333	50E					
18		40	56.85	111	19.931									
19		40	56.88	111	19.895									
20		40	56.96	111	19.949	35	70N							
21														
22		40	56.97	111	19.94									
23		40	57.01	111	19.939	25	51N	241	27N					
								244	35N					
								258	27N					
								299	40N					
								319	65E					
								240	23N					
								234	30N					
								221	31W					
								232	37N					
								255	26N					
24		40	57.03	111	19.912									
25														
26		40	57.06	111	19.903	61	47N	185	41W					
								269	33N					
								178	90W					
								212	15W					
27		40	57.07	111	19.903									
28		40	57.1	111	19.766									
29														
30		40	57.13	111	19.746									70
														85

														190
														85
														75
														45
														135
														80
														130
														120
31		40	57.15	111	19.732	42	56N							
32		40	57.17	111	19.716	25	61N							
33		40	57.18	111	19.705									
34		40	57.22	111	19.705									
35		40	57.27	111	19.672									
36		40	57.31	111	19.637									
37		40	57.32	111	19.626									
38		40	57.4	111	19.62									
39		40	57.48	111	19.577									
40														
41														
42		40	57.05	111	19.471									
43		40	56.14	111	20.382									
44		40	57.02	111	22.843	59	62NW	147.8	43.7W					
								180.9	33.5W					
								182.9	19.9W					
45		40	57.05	111	22.811									
46		40	57.08	111	22.808									
47		40	57.13	111	22.775	25	52N	304	62N			Plutonic	57	
								277	40N			Volcanic	21	
								294	53.2N			Green Plutonic	15	
								293.2	59.3N			Marble	3	
								292.6	35.1N			Foliated Plutonic	2	
								282.5	49N			quartzite	1	
								296.6	46.7N			gneiss	1	
								284.1	40.1N					

								290.9	58.3N					
								294.9	56.1N					
								300.8	46.1N					
								296.7	42.6N					
								289.5	38N					
								304.8	72.9N					
								284.9	33.3N					
								304.2	75.6N					
								296.9	55N					
								294.4	72.9N					
								319.2	64.2E					
								304.8	69.4N					
								308	56.9N					
								303.2	63.6N					
48								302.6	81.1N					
49		40	57.25	111	22.784									
50		40	57.28	111	22.762									95
														63
														65
														53
														100
														90
														64
														210

Clast Count Data													
Basin N2	A6	A9	A12	A16	A22	A23	A27	A29	A34	A36	A38	A39	A44
Plutonic	57	93	78	70	95	61	78	68	37	39	65	68	90
Foliated Plutonic	19	0	8	12	3	9	4	12	17	5	4	11	2
Gneiss	12	1	5	9	0	18	3	15	0	11	14	19	0
Marble	8	2	1	0	0	0	0	2	2	3	0	0	0
Schist	1	6	4	3	1	12	18	7	12	2	3	3	2
Quartzite	0	0	0	1	0	0	0	1	7	12	1	0	4
Mylonite	0	0	0	0	0	0	0	0	0	0	0	0	0
Volcanic	0	0	0	0	0	0	0	0	8	28	9	0	4
Sandstone	0	0	3	0	1	1	0	0	5	0	4	0	0
Conglomerate	0	0	1	0	0	0	0	0	1	0	0	0	0
Clast Totals	97	102	100	95	100	101	103	105	89	100	100	101	102
Percentages													
Plutonic	58.8	91.2	78.0	73.7	95.0	60.4	75.7	64.8	41.6	39.0	65.0	67.3	88.2
Foliated Plutonic	19.6	0.0	8.0	12.6	3.0	8.9	3.9	11.4	19.1	5.0	4.0	10.9	2.0
Gneiss	12.4	1.0	5.0	9.5	0.0	17.8	2.9	14.3	0.0	11.0	14.0	18.8	0.0
Marble	8.2	2.0	1.0	0.0	0.0	0.0	0.0	1.9	2.2	3.0	0.0	0.0	0.0
Schist	1.0	5.9	4.0	3.2	1.0	11.9	17.5	6.7	13.5	2.0	3.0	3.0	2.0
Quartzite	0.0	0.0	0.0	1.1	0.0	0.0	0.0	1.0	7.9	12.0	1.0	0.0	3.9
Mylonite	0.0	0.0	0.0	0.0	0.0	0.0	0.0	0.0	0.0	0.0	0.0	0.0	0.0
Volcanic	0.0	0.0	0.0	0.0	0.0	0.0	0.0	0.0	9.0	28.0	9.0	0.0	3.9
Sandstone	0.0	0.0	3.0	0.0	1.0	1.0	0.0	0.0	5.6	0.0	4.0	0.0	0.0
Conglomerate	0.0	0.0	1.0	0.0	0.0	0.0	0.0	0.0	1.1	0.0	0.0	0.0	0.0
Basin N2	A53	A58	A65	A71	A79	A502	A535	A539	A546	A549	A551	A552	A554
Plutonic	68	64	73	57	58	49	45	51	42	49	47	41	49
Foliated Plutonic	8	3	3	1	8	16	22	14	29	30	19	29	17
Gneiss	4	6	0	8	29	2	13	3	20	6	5	13	6
Marble	0	0	0	5	0	2	0	0	1	0	19	0	0
Schist	17	8	10	7	6	10	7	9	0	4	7	17	21
Quartzite	0	0	3	4	0	0	0	0	0	0	0	2	0
Mylonite	0	0	0	0	0	0	0	0	0	0	0	0	0

Volcanic	0	0	1	6	1	0	0	0	0	0	0	1	0
Sandstone	1	0	0	6	1	0	4	2	9	14	7	1	3
Conglomerate	1	11	10	8	3	0	0	0	0	0	0	0	0
Clast Totals	99	92	100	102	106	79	91	79	101	103	104	104	96
Percentages													
Plutonic	68.7	69.6	73.0	55.9	54.7	62.0	49.5	64.6	41.6	47.6	45.2	39.4	51.0
Foliated Plutonic	8.1	3.3	3.0	1.0	7.5	20.3	24.2	17.7	28.7	29.1	18.3	27.9	17.7
Gneiss	4.0	6.5	0.0	7.8	27.4	2.5	14.3	3.8	19.8	5.8	4.8	12.5	6.3
Marble	0.0	0.0	0.0	4.9	0.0	2.5	0.0	0.0	1.0	0.0	18.3	0.0	0.0
Schist	17.2	8.7	10.0	6.9	5.7	12.7	7.7	11.4	0.0	3.9	6.7	16.3	21.9
Quartzite	0.0	0.0	3.0	3.9	0.0	0.0	0.0	0.0	0.0	0.0	0.0	1.9	0.0
Mylonite	0.0	0.0	0.0	0.0	0.0	0.0	0.0	0.0	0.0	0.0	0.0	0.0	0.0
Volcanic	0.0	0.0	1.0	5.9	0.9	0.0	0.0	0.0	0.0	0.0	0.0	1.0	0.0
Sandstone	1.0	0.0	0.0	5.9	0.9	0.0	4.4	2.5	8.9	13.6	6.7	1.0	3.1
Conglomerate	1.0	12.0	10.0	7.8	2.8	0.0	0.0	0.0	0.0	0.0	0.0	0.0	0.0
Conglomerate													

Basin S3	**D1**	**D14**	**D26**	**D47**	**D50**	**D56**	**D65**	**D301**	**D306**	**D307b**	**D309**	**D331**	**D339**
Plutonic	73	67	53	91	55	70	76	68	82	84	36	85	70
Foliated Plutonic	7	20	9	5	8	0	13	0	15	6	0	6	5
Gneiss	0	6	4	0	0	3	5	0	9	15	8	14	14
Marble	10	0	2	0	3	0	0	10	0	0	12	3	10
Schist	8	3	3	1	0	8	4	0	0	1	2	4	1
Quartzite	0	0	0	0	14	1	1	3	0	2	1	1	0
Mylonite	0	0	0	0	0	0	0	0	0	0	0	0	0
Volcanic	0	0	5	0	1	0	0	1	0	0	0	1	0
Sandstone	1	3	6	3	0	5	2	7	0	0	0	0	0
Conglomerate	0	0	18	0	0	5	0	5	0	0	0	0	0
Clast Totals	99	99	100	100	81	92	101	94	106	108	59	114	100
Percentages													
Plutonic	73.737	67.677	53	91	67.9012	76.08696	75.2475	72.3404	77.35849	77.78	61	74.56	70
Foliated Plutonic	7.0707	20.202	9	5	9.87654	0	12.8713	0	14.15094	5.556	0	5.263	5

Gneiss	0	6.0606	4	0	0	3.26087	4.9505	0	8.490566	13.89	13.6	12.28	14
Marble	10.101	0	2	0	3.7037	0	0	10.6383	0	0	20.3	2.632	10
Schist	8.0808	3.0303	3	1	0	8.695652	3.9604	0	0	0.926	3.39	3.509	1
Quartzite	0	0	0	0	17.284	1.086957	0.9901	3.19149	0	1.852	1.69	0.877	0
Mylonite	0	0	0	0	0	0	0	0	0	0	0	0	0
Volcanic	0	0	5	0	1.23457	0	0	1.06383	0	0	0	0.877	0
Sandstone	1.0101	3.0303	6	3	0	5.434783	1.9802	7.44681	0	0	0	0	0
Conglomerate	0	0	18	0	0	5.434783	0	5.31915	0	0	0	0	0

Basin S3	**D506**	**Totals**
Plutonic	49	910
Foliated Plutonic	25	94
Gneiss	7	78
Marble	1	50
Schist	18	35
Quartzite	5	23
Mylonite	0	0
Volcanic	2	8
Sandstone	0	27
Conglomerate	0	28
Clast Totals	107	1253
Percentages		
Plutonic	45.794	72.626
Foliated Plutonic	23.364	7.502
Gneiss	6.5421	6.2251
Marble	0.9346	3.9904
Schist	16.822	2.7933
Quartzite	4.6729	1.8356
Mylonite	0	0
Volcanic	1.8692	0.6385
Sandstone	0	2.1548
Conglomerate	0	2.2346

Basin S1	02^3	00^3a	00^6a	00^10a	00^4b	Sectionb	Tape3a	Tape7a	Tape13a	Totals
Plutonic	20	4	16	10	23	43	30	31	32	209
Foliated Plutonic	14	2	2	27	11	27	8	7	13	111
Gneiss	4	0	0	3	3	3	4	8	12	37
Marble	31	57	44	7	36	90	25	44	27	361
Schist	11	0	0	0	0	0	2	0	0	13
Quartzite	4	15	12	0	0	6	8	3	5	53
Mylonite	0	0	0	32	1	14	1	0	1	49
Volcanic	10	1	2	5	2	12	9	33	2	76
Sandstone	0	20	20	17	16	15	7	6	12	113
Conglomerate	2	2	1	0	0	1	0	3	2	11
Clast Totals	96	101	97	101	92	211	94	135	106	1033
percentages										
Plutonic	20.8	4.0	16.5	9.9	25.0	20.4	31.9	23.0	30.2	20.2
Foliated Plutonic	14.6	2.0	2.1	26.7	12.0	12.8	8.5	5.2	12.3	10.7
Gneiss	4.2	0.0	0.0	3.0	3.3	1.4	4.3	5.9	11.3	3.6
Marble	32.3	56.4	45.4	6.9	39.1	42.7	26.6	32.6	25.5	34.9
Schist	11.5	0.0	0.0	0.0	0.0	0.0	2.1	0.0	0.0	1.3
Quartzite	4.2	14.9	12.4	0.0	0.0	2.8	8.5	2.2	4.7	5.1
Mylonite	0.0	0.0	0.0	31.7	1.1	6.6	1.1	0.0	0.9	4.7
Volcanic	10.4	1.0	2.1	5.0	2.2	5.7	9.6	24.4	1.9	7.4
Sandstone	0.0	19.8	20.6	16.8	17.4	7.1	7.4	4.4	11.3	10.9
Conglomerate	2.1	2.0	1.0	0.0	0.0	0.5	0.0	2.2	1.9	1.1

Basin S2	Tape 3	Tape 5	Tape 7	Tape 9	Tape 11	00^1	00^5	00^6	00^9	00^10	01^5	Totals
Plutonic	4	4	3	6	6	17	12	9	0	2	30	93
Foliated Plutonic	0	0	0	0	0	1	1	5	0	0	2	9
Gneiss	37	7	1	0	2	22	17	21	14	10	0	131
Marble	33	46	58	48	54	39	30	8	54	48	30	448
Schist	0	0	0	0	0	5	7	38	25	15	1	91
Quartzite	0	0	0	0	0	9	4	13	6	6	0	38
Mylonite	0	0	0	0	0	2	1	1	0	1	0	5
Volcanic	6	0	10	5	2	4	0	0	0	0	10	37

Sandstone	6	10	4	5	1	0	3	0	0	0	0	29
Conglomerate	0	0	0	0	0	0	1	0	0	0	0	1
Clast Totals	86	67	76	64	65	99	76	95	99	82	73	882
percentages												
Plutonic	4.7	6.0	3.9	9.4	9.2	17.2	15.8	9.5	0.0	2.4	41.1	10.5
Foliated Plutonic	0.0	0.0	0.0	0.0	0.0	1.0	1.3	5.3	0.0	0.0	2.7	1.0
Gneiss	43.0	10.4	1.3	0.0	3.1	22.2	22.4	22.1	14.1	12.2	0.0	14.9
Marble	38.4	68.7	76.3	75.0	83.1	39.4	39.5	8.4	54.5	58.5	41.1	50.8
Schist	0.0	0.0	0.0	0.0	0.0	5.1	9.2	40.0	25.3	18.3	1.4	10.3
Quartzite	0.0	0.0	0.0	0.0	0.0	9.1	5.3	13.7	6.1	7.3	0.0	4.3
Mylonite	0.0	0.0	0.0	0.0	0.0	2.0	1.3	1.1	0.0	1.2	0.0	0.6
Volcanic	7.0	0.0	13.2	7.8	3.1	4.0	0.0	0.0	0.0	0.0	13.7	4.2
Sandstone	7.0	14.9	5.3	7.8	1.5	0.0	3.9	0.0	0.0	0.0	0.0	3.3
Conglomerate	0.0	0.0	0.0	0.0	0.0	0.0	1.3	0.0	0.0	0.0	0.0	0.1

Basin S4	**Tape 1**	**Tape 4**	**Tape 6**	**Tape 10**	**Tape 14**	**Totals**
Plutonic	43	53	25	27	47	195
Foliated Plutonic	5	9	5	3	6	28
Gneiss	15	16	9	10	18	68
Marble	10	14	2	3	4	33
Schist	3	7	2	1	5	18
Quartzite	1	2	0	0	0	3
Mylonite	9	7	5	5	6	32
Volcanic	0	1	0	1	0	2
Sandstone	1	2	0	0	7	10
Conglomerate	0	0	0	0	1	1
Clast Totals	87	111	48	50	94	390
percentages						
Plutonic	49.4	47.7	52.1	54.0	50.0	50.0
Foliated Plutonic	5.7	8.1	10.4	6.0	6.4	7.2
Gneiss	17.2	14.4	18.8	20.0	19.1	17.4
Marble	11.5	12.6	4.2	6.0	4.3	8.5

Schist	3.4	6.3	4.2	2.0	5.3	4.6
Quartzite	1.1	1.8	0.0	0.0	0.0	0.8
Mylonite	10.3	6.3	10.4	10.0	6.4	8.2
Volcanic	0.0	0.9	0.0	2.0	0.0	0.5
Sandstone	1.1	1.8	0.0	0.0	7.4	2.6
Conglomerate	0.0	0.0	0.0	0.0	1.1	0.3
Basin N1	**10**	**17**	**47**	**10+17**		
Plutonic	31	90	72	121	314	
Foliated Plutonic	0	1	2	1	4	
Gneiss	1	0	1	1	3	
Marble	11	8	3	19	41	
Schist	1	0	0	1	2	
Quartzite	3	6	1	9	19	
Mylonite	0	0	0	0	0	
Volcanic	45	0	21	45	111	
Sandstone	6	0	0	6	12	
Conglomerate	1	0	0	1	2	
Clast Totals	99	105	100	204	508	
percentages						
Plutonic	31.3	85.7	72.0	59.3	61.8	
Foliated Plutonic	0.0	1.0	2.0	0.5	0.8	
Gneiss	1.0	0.0	1.0	0.5	0.6	
Marble	11.1	7.6	3.0	9.3	8.1	
Schist	1.0	0.0	0.0	0.5	0.4	
Quartzite	3.0	5.7	1.0	4.4	3.7	
Mylonite	0.0	0.0	0.0	0.0	0.0	
Volcanic	45.5	0.0	21.0	22.1	21.9	
Sandstone	6.1	0.0	0.0	2.9	2.4	
Conglomerate	1.0	0.0	0.0	0.5	0.4	
	100.0	100.0	100.0	100.0	100.0	